Stony Brook University

The Role of Dystroglycan in Differentiating Oligodendroglia and CNS Myelination

A Dissertation Presented

by

Christopher Edward Eyermann

to

The Graduate School

in Partial Fulfillment of the

Requirements

for the Degree of

Doctor of Philosophy

in

Molecular and Cellular Pharmacology

Stony Brook University

December 2012

Stony Brook University

The Graduate School

Christopher Edward Eyermann

We, the dissertation committee for the above candidate for the

Doctor of Philosophy degree, hereby recommend

acceptance of this dissertation.

Holly Colognato, Ph.D. – Dissertation Advisor
Associate Professor, Department of Pharmacological Sciences

Joel M. Levine, Ph.D. - Chairperson of Defense
Professor, Department of Neurobiology and Behavior

Joav Prives, Ph.D.
Professor, Department of Pharmacological Sciences

Carmen V. Melendez-Vasquez, Ph.D.
Assistant Professor, Department of Biological Sciences
Hunter College

This dissertation is accepted by the Graduate School

Charles Taber
Interim Dean of the Graduate School

Abstract of the Dissertation

The Role of Dystroglycan in Differentiating Oligodendroglia and CNS Myelination

by

Christopher Edward Eyermann

Doctor of Philosophy

in

Molecular and Cellular Pharmacology

Stony Brook University

2012

During central nervous system (CNS) development, individual oligodendrocytes myelinate multiple axons, thus requiring the outgrowth and extensive branching of oligodendroglial processes. Extrinsic cues including the extracellular matrix (ECM) molecule laminin regulate oligodendrocyte maturation; indeed, laminin-deficient mice have fewer myelinated axons, which may indicate a defect in the ability to properly extend and branch processes. It remains unclear, however, to what extent ECM receptors contribute to oligodendroglial process remodeling itself. Here I report that the ECM receptor dystroglycan is necessary for laminin enhancement of filopodial formation, process outgrowth, and process branching in differentiating oligodendroglia. During early oligodendroglial differentiation, the disruption of dystroglycan-laminin interactions, via blocking antibodies or dystroglycan siRNA, resulted in decreased filopodial number and length, decreased process length, and decreased numbers of primary and secondary processes. Later in oligodendrocyte differentiation, dystroglycan-deficient cells developed fewer branches, thus producing less complex networks of processes as determined by

Sholl analysis. In newly-differentiating oligodendroglia dystroglycan was localized in filopodial tips, while in more mature oligodendrocytes dystroglycan was enriched in FAK-positive focal adhesion structures. In addition to its role in promoting cytoskeletal reorganization, I have recently begun investigating a novel signaling role for dystroglycan in the nucleus. Our preliminary evidence suggests that dystroglycan localizes to the nucleus in oligodendrocyte progenitors (OPCs) and may play a role in dystroglycan-dependent modulation of oligodendroglial differentiation. β-dystroglycan expression in the nuclear fraction of proliferating OPCs is higher than in differentiating oligodendrocytes; furthermore, I have detected an increased proportion of a cleaved form of β-dystroglycan in the nucleus of OPCs relative to differentiated oligodendrocytes. Analysis of OPCs expressing a dystroglycan deletion construct reveal a preferential localization of the cytoplasmic domain of β-dystroglycan to the nucleus, redistribution of the dystroglycan-interacting protein dystrophin from the cytosol to the nucleus, and decreased proliferation in response to growth factor stimulation. Our results suggest that dystroglycan may contribute to the overall myelinogenic capacity of individual oligodendroglia by influencing oligodendroglial process dynamics through dystroglycan-laminin interactions, and potentially modulating differentiation by signaling in the nucleus of oligodendroglial progenitors.

Dedicated to my sister, Jennifer Lynn Trombino

I miss you.

Table of Contents

List of Figures

Chapter 1

GENERAL INTRODUCTION

Oligodendrocytes are the myelinating cells of the central nervous system (CNS) and enable the efficient transmission of signals along axons that are critical for normal nervous system function. Oligodendrocyte development, from oligodendrocyte lineage specification through myelination, occurs through a series of steps requiring the correct spatial-temporal regulation of intrinsic and extrinsic signals. The role of the extracellular matrix (ECM) during oligodendrocyte development has become increasingly recognized as an important regulator of oligodendrocyte development; however, the mechanisms by which ECM molecules transmit signals to affect oligodendrocyte development remain poorly understoood.

Laminin is an ECM molecule that recently has been shown to affect the generation of oligodendrocyte progenitors and the development of fully mature oligodendrocytes in laminin-deficient or knockout mouse models. The laminin receptor subunit, β1 integrin, is expressed in oligodendrocytes and has previously been shown to affect oligodendrocyte survival in cell culture experiments. However, several studies using conditional β1 integrin knockout mouse models have concluded that β1 integrin is not required for oligodendrocyte proliferation or differentiation. These experimental studies have suggested that another laminin receptor expressed in oligodendrocytes may contribute to the phenotype observed when laminin is either deficient or absent.

Dystroglycan is a second laminin receptor expressed in oligodendrocytes where it is has been reported to regulate oligodendrocyte differentiation (Colognato et al. 2007). In Schwann cells, the myelinating cells of the peripheral nervous system (PNS), dystroglycan has been reported to have a number of important roles during Schwann cell development. While the role of dystroglycan during oligodendrocyte development remains poorly understood, reports that dystroglycan may localize actin remodeling proteins suggests a possible role for dystroglycan in regulating cytoskeletal dynamics, possibly during early differentiation when oligodendrocytes begin to extend and branch processes. In addition, nuclear localized dystroglycan has been reported in several cell types. It is unknown whether dystroglycan localizes in the nucleus of oligodendrocytes; however, this suggests another possible mechanism by which dystroglycan may regulate oligodendroglial development.

The goal of the following thesis is to elucidate the functional role of the laminin receptor, dystroglycan, in the normal development and maturation of oligodendrocytes in the CNS. In order to clinically address diseases in which CNS myelin is compromised, it is important to fully investigate the mechanisms that regulate oligodendroglial maturation so that potential therapies to treat these disorders may be uncovered. The following chapter will provide broad overview of the functional implications of myelination, and describe the important steps during oligodendrocyte lineage specification, proliferation, and differentiation with particular emphasis on the role of the ECM. A potential role for dystroglycan in regulating oligodendrocyte development will be discussed in the following chapter.

Myelination

CNS myelination occurs postnally following neurogenesis in rodents (Richardson *et al.* 2006) and humans perinatally persisting from several weeks to years respectively (Welker and Patton 2012). The spatial-temporal regulation of the events both preceding and during myelination are thus critical to proper nervous system function. Myelin is a lipid-rich membraneous extension formed by oligodendrocytes in the central nervous system (CNS), and Schwann cells in the peripheral nervous system (PNS), that discontinuosly enwraps and insulates axons in a multilamellar sheath forming discrete functional domains that allow the efficient propagation of nerve impulses along axons. In both the CNS and PNS, myelinated segments of the axolemma (internodes) are separated by unmyelinated regions of the axolemma which are known as nodes of Ranvier (nodes). Compact myelin spans the length of the internode, while non-compact myelin forms the paranodal loops that contact the axolemma.

Residing within the nodes, along with associated para- and juxtapara- nodal domains, is the molecular machinery that enables the rapid conduction of action potentials along an axon. Voltage-gated Na^+ channels densely packed at the node, and voltage-gated K^+ channels at the juxtaparanode, facilitate depolarization of the axonal membrane and the subsequent initiation of an action potential which is propagated along the axon in a process known as saltatory conduction (McTigue and Tripathy 2008). Concentrating voltage-gated Na^+ channels at the node enables membrane depolarization and the initiation of an action potential to occur more rapidly with fewer voltage gated channels required. This is potentiated by the insulating capacity and composition of the myelin sheath which serves as a barrier to Na^+ diffusion (Chrast *et al.* 2011). Approximately 70% of the dry weight of myelin contains lipids (cholesterol, phospholipids, and glycosphingolipids), of which cholesterol and phospholipids contribute 27% and 31%

respectively (Jackman *et al.* 2009). Myelin basic protein (MBP) and proteolipid protein (PLP) are the two major constituents of the compact myelin sheath and account for 30% and 50% of the protein content respectively (Privat *et al.* 1979; Zeller *et al.* 1984; Griffiths *et al.* 1998).

Myelin Disorders

Normal brain development and cognitive function illustrates the importance of myelination in the CNS and is underscored by several aquired or inherited disorders in which myelin is compromised. The clinical pathologies of disorders affecting CNS myelin vary in their onset and severity, involving the dysfunction of several different cell types and proteins. Various degrees of hypomyelination, demyelination and/or dysmyelination may either accompany, or be exclusive to, conditions affecting myelin in both the CNS and PNS. Ultimately, myelin phenotypes associated with these disorders result in axonal damage and degeneration, which in turn, compromises the integrity of central and peripheral nervous system circuitry.

Multiple sclerosis (MS), for example, is an aquired demyelinating disorder affecting millions of people worldwide with devastating consequences for patients, particularly in the progressive stage of the disease. Clinical presentation can be in the form of an attack causing varied but common disturbances in both children and adults with symptoms such as optic neuritis, sensory, and motor disturbances. Lesions in presumably myelinated white matter revealed by magnetic resonance imaging (MRI), are often located within the ventricular and periventricular subcortical white matter (Barkhof *et al.* 1997; Dale *et al.* 2000).

Axonal degeneration in MS arises as result of an inflammatory autoimmune response targeting oligodendrocytes. The immune hypothesis proposes that differentiated Th17 cells that

are able to cross the blood brain barrier using a chemokine receptor, become activated by myelin epitopes, and secrete cytotoxic factors (TNF-α) that destroy oligodendrocytes (Eugster *et al.* 1999; Furtado *et al.* 2008; Reboldi *et al.* 2009). Inflammatory response includes the infiltration of T cells, macrophages, reactive microglia, and reactive astrocytes (Nakahara *et al.* 2010). However, reported lack of reactive gliosis and macrophage infiltration in some human MS lesions has suggested that immune response may be secondary to oligodendrocyte death (Barnett and Prineas 2004). In support of primary oligodendrogliopathy, oligodendrocytes deficient in the myelin component 2',3'-cyclic nucleotide phosphodiesterase (CNP) myelinate normally; however, later axon degeneration in CNP-deficient oligodendrocytes suggests intrisic oligodendrocyte properties support axon survival (Lappe-Siefke *et al.* 2003).

Normal myelination may also be compromised by inherited mutations in genes that affect central and peripheral nervous system development. For example, the hereditary congenital dystrophy MDC1A, caused by a mutation in the gene encoding the α2-subunit of the ECM protein laminin, is often associated with peripheral myopathy, white matter defects, and other CNS abnormalities (Renaud 2012). Mouse models of MDC1A have revealed that dysfunctional myelination may be caused by defects in the development of oligodendrocytes in the CNS, and Schwann cells in the PNS. While several abnormalities associated with Schwann cell development in MDC1A are currently known, whether or not CNS deficits are associated with dysregulated oligodendrocyte development remains poorly understood. However, recent *in vivo* studies have reported that laminin promotes oligodendrocyte suvival and maturation (Relucio *et al.* 2009, 2012).

Oligodendrocyte Progenitor Development

Oligodendrocyte development occurs in several distinct phases: lineage specification, proliferation, differentiation, and myelination. The progression through each of these stages can be characterized by the aquisition of specific cell surface markers including receptors, membrane proteins, and membrane lipids (Fig. 1-1). Developmental stage is also associated with the expression of transcription factors, adaptor proteins, and various epigenetic modifications. Additionally, developmental stage is also defined by dramatic morphological transformation which occurs as oligodendrocytes develop from proliferating precursor cells into fully mature myelinating oligodendrocytes. The lineage progression of oligodendrocytes from their initial specification, through their early development as a pool of proliferative and migratory precursors, is critical for normal CNS development. The following section will highlight some of the important steps and regulatory molecules that are necessary for oligodendrogenesis.

Neurons and glial cells are the major cell types in the vertebrate CNS (Peters *et al*. 1990). Glial cells include oligodendrocytes, astrocytes and microglia. Microglia are derived from the hematopoietic system during development and are macrophages of the CNS; neurons, oligodendrocytes and astrocytes are all derived from the neuroepithelium during development (Liu and Rao 2004). Oligodendrocytes arise from several discrete regions of the neuroepithelium during embryogenesis and postnatally from ventricular and subventricular zones. Oligodendrocyte lineage specification involves a number of factors including morphogenic proteins, membrane associated molecules, growth factors, and transcription factors. Evidence suggests that oligodendrocytes are specified from pool of progenitors that may give rise to neurons and oligodendrocytes. In the spinal cord, the motor neuron progenitor (pMN) domain gives rise first to neurons, and later to oligodendrocytes both expressing the basic helix-loop-

helix (bHLH) transcription factor *Olig2*. The homeodomain transcription factor, Nkx2.2, is also found co-expressed with *Olig* genes in oligodendrocyte progenitors (Lu *et al.* 2002; Zhou and Anderson 2002). Members of the transforming growth factor beta (TGFβ) superfamily, specifically bone morphgenic proteins (BMPs) 2 and 4, are dorsally derived factors that antagonize oligodendrocye precursor specification (Mabie *et al.* 1997; Mehler *et al.* 2000). Sonic hedgehog (Shh) is a ventrally derived morphogenic protein that promotes oligodendrocyte lineage specification (Orentas *et al.* 1999). The transmembrane glycoprotein Notch and basic fibroblast growth factor (FGF) have also been shown to provide instructive cues towards oligodendrocyte lineage specification (Bansal *et al.* 1996; Grandbarbe *et al.* 2003; Park and Appel 2003).

Oligodendrocyte and type-2 astrocyte precursors (O2A cells) are the best recognized glial intermediate cell types studied to date and are identified initially by the expression of cell surface antigens recognized by the monoclonal antibody A2B5, and later in more mature precursors by the monoclonal antibody O4 (Miller 2002). O2A cells are additionally identified by the expression of the platelet-derived growth factor receptor alpha (PDGF-αR), and mRNA for the myelin genes 2',3'-cyclic-nucleotide 3'-phosphodiesterase (CNP) and *DM20*, a proteolipid protein (PLP) isoform (Pringle *et al.* 1992; Miller 2002). *In vitro* experiments have shown that O2A cells can differentiate into type-2 astrocytes as well as oligodendrocytes, while *in vivo*, only oligodendrocytes have been shown to arise from these intermediate cells (Espinosa de los Monteros *et al.* 1993; Kondo and Raff 2000). Interestingly, O2A cells may revert into multipotent neural stem cells *in vitro* or remain in a dividing proliferative state indefinitely suggesting that these cells may have an instrinsic plasticity (Bogler and Nobel 1994; Kondo and Raff 2000). Oligodendrocyte progenitor cells are also identified by the cell surface marker

chondroitin sulfate proteoglycan NG2. NG2 expressing cells have been suggested to represent another resident glial cell in the CNS, polydendrocytes, that also retain lineage plasticity (Aguirre and Gallo 2004; Zhu *et al.* 2008; Nishiyama *et al.* 2009). While NG2+ polydendrocytes are found throughout the CNS after adulthood, some of which may ultimately differentiate into mature myelinating oligodendrocytes, the majority of these cells divide much slower than precursors derived much earlier in development (Polito and Reynolds 2005).

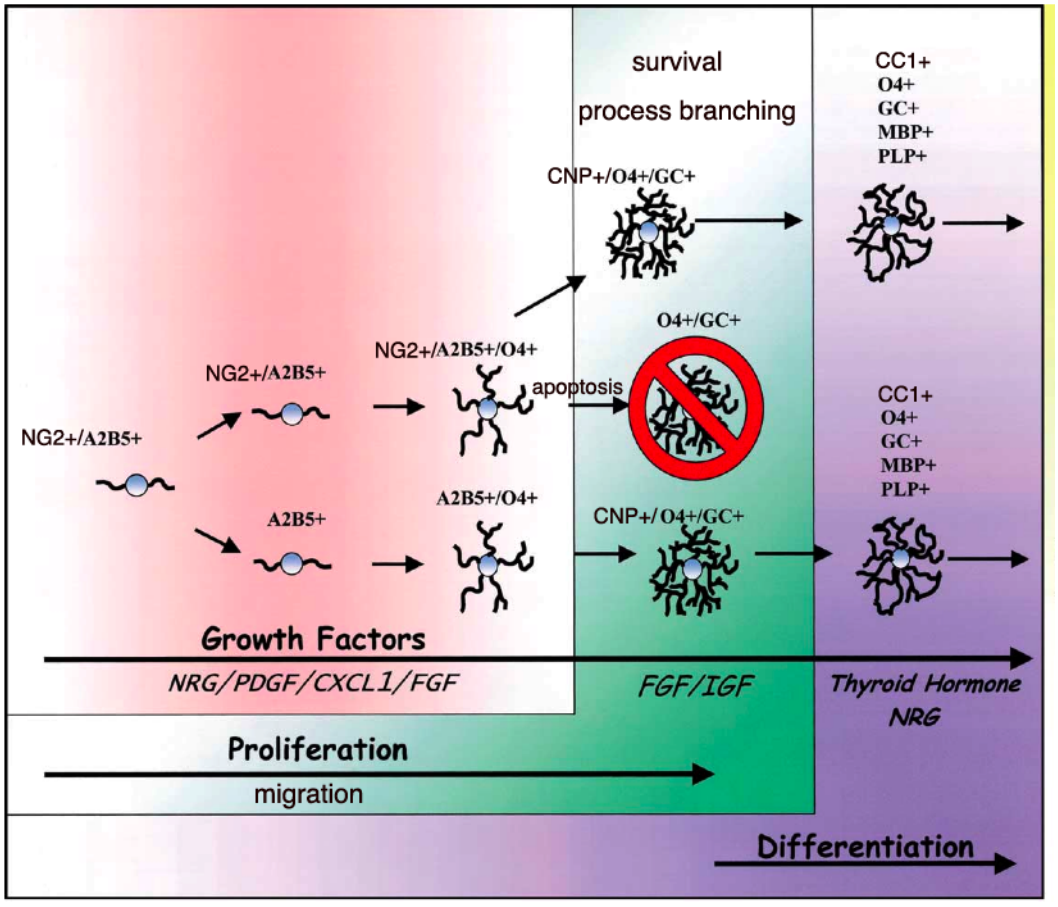

Figure 1-1. Oligodendrocyte Development

(Modified from: Robert H. Miller 2002)

From caudal locations in the developing spinal cord, ventrally derived oligodendrocyte precursors migrate towards more dorsal regions; while in more rostal regions, oligodendrocyte precursors populate the developing forebrain from their ventral origin in the lateral and medial ganglion eminence, and later the entire cerebral cortex from the subventricular zone (Lachapelle *et al.* 1984; Warrington *et al.* 1992; Gonye *et al.* 1994; Miller 2002). Several proteins have been shown to influence the migration of oligodendrocyte progenitors including platelet-derived growth factor A (PDGF), polysialic acid neuronal cell adhesion molecule (PSA-NCAM), the chemokine CXCL1, and netrin 1 (Trotter *et al.* 1988; Armstrong *et al.* 1990; Wang *et al.* 1994; Spassky *et al.* 2002; Tsai *et al.* 2002).

Proliferation of oligodendrocyte progenitors occurs primarily in the developing white matter upon specification and subsequent migration throughout the CNS (Miller *et al.* 1997). Among the most important and well studied mitogens for oligodendrocyte precursor cells is PDGF, which is distributed throughout the CNS by astrocytes and neurons (Yeh *et al.* 1991; Pringle *et al.* 1992). As noted previously, O2A cells express the PDGF-αR receptor through which both the enhancement of their proliferation and survival are promoted (Noble *et al.* 1988; Richardson *et al.* 1988; Barres *et al.* 1992). The effect of PDGF as a mitogen is also potentiated in response to basic fibroblast growth factor (FGF), having previously been shown to promote the up-regulation of PDGF-αRs in oligodendrocyte precursors (Bogler *et al.* 1990; McKinnon *et al.* 1991). The nerve growth factor (NGF) family member neurotrophin-3 (NT3), neuronal growth factor neuregulin-1 type III (NRG1), and insulin-like growth factor-1 (IGF-1) have have all been reported to have mitogenic effects on oligodendrocyte precursors as well (McMorris *et al.* 1986; Barres *et al.* 1992; Barres *et al.* 1994a; Vartanian *et al.* 1999; Jiang *et al.* 2001; Hsieh *et al.* 2004).

Oligodendrocyte Differentiation

Having reached their final destinations in the presumptive white matter regions of the CNS, oligodendrocyte progenitors receive input from a number of intrinsic and extrisic factors that drive their terminal differention allowing the transition to a mature myelinating oligodendrocyte. Developmentally, the transition from a newly-formed oligodendrocyte to a fully mature oligodendrocyte is characterized by the sequential expression of myelin proteins and lipids. Soon after oligodendrocytes become terminally differentiated, they begin to lose the expression of A2B5, PDGF-αR and NG2. Newly-formed oligodendrocytes can be identified by the expression of galactocerebroside (GalC), followed by the myelin component 2',3'-cyclic nucleotide phosphodiesterase (CNP), and finally by the expression of the major protein components of the myelin sheath, myelin basic protein (MBP) and proteolipid (PLP) (Fig. 1-1). Dramatic morphological transformation also characterizes the differentiation phase of oligodendrocyte development. From a multipolar newly-formed oligodendrocyte, maturing oligodendrocytes begin to extend dozens of highly branched processes toward target axons, and after making contact, elongate these processes along the axon before spirally enwrapping them with a compact myelin sheath. Finally, since the number of oligodendrocytes produced is in excess of the number required to myelinate axons in the CNS, the surviving oligodendrocyte population must be matched to the number of axons they are required to myelinate. In the developing optic nerve, for example, approximately 50% of the newly-formed oligodendrocytes undergo programmed cell death as a consequence of competition for a limiting amount of survival signals including PDGF (Barres *et al.* 1992). In the next few sections, I will address some of the intrinsic and extrinsic factors that regulate the transition from a proliferating progenitor, to a fully mature myelinating oligodendrocyte.

Intrinsic Regulation

Terminal differentiation of oligodendrocyte precursor cells involves the coordinated timing of a number of intrinsic and extrinsic factors. Intrinsic mechanisms including the expression of transcription factors, epigenetic modifications, and cell cycle regulators can influence the timing of both cell cycle exit, and the onset of differentiation. Myelin gene regulatory factor (MRF), for example, is a transcriptional activator expressed exclusively in post-mitotic oligodendendrocytes that functionally regulates myelin gene expression, including the major myelin proteins proteolipid protein (PLP) and myelin basic protein (MBP) (Emery *et al.* 2009). The Sox family transcription factor, Sox10, and the transcription factor, Olig1, are also expressed early, persist throughout the oligodendrocyte lineage, and induce the expression of myelin genes (Stolt *et al.* 2002; Lu *et al.* 2002; Liu *et al.* 2007). The transcription factor, Tcf4, a transcriptional activator in the Wnt signaling pathway, has been reported to both activate and repress myelin gene expression suggesting that Tcf4 may activate factors that repress myelin gene expression (He *et al.* 2007; Shimizu *et al.* 2005; Fancy *et al.* 2009; Rosenberg and Chan 2009). Evidence that Tcf4 is a transcriptional repressor was illustrated in a study that revealed the transcription factor Yin Yang 1 (YY1), binding to the Tcf4 promotor, could recruit a histone deacetylase (HDAC) and thereby inhibit Tcf4 expression allowing for the expression of myelin genes (He *et al.* 2007). Indeed, the global deacetylation of histone H3 and epigenetic modification to DNA, are also recognized as intial event that occurs between the transition from cell cycle exit to the onset of differentiation and the expression of myelin proteins (Shen *et al.* 2005).

The timing between cell cycle exit and differentiation is also determined by the accumulation of cell cycle regulators which balance both the proliferative capacity, as well as,

the differentiation potential of oligodendrocyte prescursors. The concept of an intrinsic timer was proposed some time ago in which oligodendrocyte precursors were suggested to divide a finite number of times prior to cell cycle exit and the onset of differentiation (Temple and Raff 1986). This was believed to result as a consequence of the accumulation of intrinsic factors that, over time, would increase the responsiveness to signals promoting differetiation. Subsequent studies showed that accumulation of the cyclin-dependent kinase inhibitor 1B ($p27^{Kip1}$), the cyclin-dependent kinase inhibitor 1 ($p21^{cip-1}$), and the cyclin-dependent kinase inhibitor 1C ($p21^{Kip2}$) in oligodendrocyte precursors is correlated with cell cycle exit and differentiation (Cassacia-Bonnefil *et al.* 1997; Zezula *et al.* 2001; Dugas *et al.* 2007).

Extrinsic Regulation

A number of extrinsic regulators of oligodendrocyte differentiation are known and include soluble factors, cell surface-associated molecules, and components of the extracellular matrix. The soluble factor thyroid hormone triiodothyronine (T3) contributes to the terminal differentiation of oligodendrocytes and is thought to act upon the intrisic timer by inhibiting the activator protein 1 (AP-1) transcription factor (Barres *et al.* 1994b; Hess *et al.* 2004). Insulin-like growth factor 1 (IGF-1) has also been reported to influence the numbers of mature oligodendrocytes, promote myelin protein expression, and increase myelin sheath thickness (Carson *et al.* 1993; Ye *et al.* 1995a,b; Mason *et al.* 2000; Ye *et al.* 2002). Fibroblast growth factor (FGF), in addition to its role in oligodendrocyte precursor specification and proliferation as described previously, is another soluble factor produced by neurons and astrocytes that has

recently been reported to regulate the later stages of oligodendrocyte differentiation (Furusho *et al.* 2012).

Cell-cell adhesion molecules also play a role in the initiation of differentiation, and in promoting survival and myelination. For example, removal of PSA from PSA-NCAM is required not only for normal CNS myelination, but also for strengthening the interactions between other membrane proteins including L1 cell adhesion molecule, N-cadherin, and integrins (Charles *et al.* 2000; Fujimoto *et al.* 2001; Johnson *et al.* 2005; Fewou *et al.* 2007). This coordination of adhesive properties may allow for alternate signaling complexes to form and thereby regulate the maturation of oligodendrocytes, although this has yet to be demonstrated experimentally. The induction of an oligodendroglial fate, as described previously, is regulated by the Notch receptor. However, γ-secretase-mediated cleavage of the Notch intracellular domain (NICD), NICD translocation to the nucleus, and upregulation of myelin-associated glycoprotein (MAG) has also been reported suggesting that Notch may have dual roles in promoting oligodendrocyte specification and differentiation (Givogri *et al.* 2002; Hu *et al.* 2003).

Studies over the last two decades have revealed that components of the extracellular matrix contribute signals that are important for regulating the development of myelinating glia in both the CNS and PNS. As described previously, merosin-deficient congenital muscular dystrophy type 1A (MDC1A) is caused by mutations in the gene encoding the α2-subunit of the ECM molecule laminin and is associated with both peripheral myopathy and white matter defects (Shorer *et al.* 1995; Caro *et al.* 1999; Philpot *et al.* 1999; Miyagoe-Suzuki *et al.* 2000; Di Muzio *et al.* 2003; Quijano-Roy *et al.* 2004). Laminins are secreted heterotrimers assembled from 3 subunits (αβγ) resembling a cruciform structure composed of 3 NH_2-terminal short arms and 1 COOH-terminal long arm (Colognato *et al.* 1999). Domains located within these arms

enable matrix assembly, interactions with other ECM molecules, and interactions with a number of cell-surface molecules. Laminin is widely distributed as a major component of basement membranes, which support a number of functions throughout development in many structures including muscle, peripheral nerve, and the brain (Miner and Yurchenco 2004).

Myelination defects associated with either laminin α2 deficiency or the complete absence of laminin α2 have been studied most extensively using the laminin α2-deficient dystrophic mouse (*dy/dy*), or the laminin α2 null mouse (LAMA2). In the PNS, Schwann cells are surrounded by a basal lamina containing the laminin α2 chain (Feltri and Wrabetz 2005). During development, Schwann cells migrate into the peripheral nerve and establish a 1:1 association with a single axon in a process known as radial sorting. Discontinuity of the basal lamina, defects in radial sorting, bundles of unmyelinated axons within the proximal spinal roots, and decreased numbers of proliferating Schwann cells have been reported in *dy/dy* mice (Bray *et al.* 1977; Feltri *et al.* 2002; Colognato *et al.* 2005).

Increasingly, the role of laminin α2 in regulating oligodendrocyte development and myelination in the CNS is becoming better understood. In contrast to Schwann cells, oligodendrocytes do not have an associated basal lamina and only encounter laminin transiently throughout development; however, laminin α2 is expressed along axons in myelinating tracts suggesting that target-dependent laminin-receptor interactions may regulate later stages of oligodendrocyte development and myelination (Colognato *et al.* 2002). Colognato *et al.* showed that such a target-mediated mechanism exists in the form of switch that promotes the survival of pre-myelinating oligodendrocytes, in which integrin α6β1-laminin α2 interactions change neuregulin-mediated dependence on the phosphatidylinositol-3-OH kinase (PI(3)K) signaling

pathway, toward activation of the mitogen-activated protein kinase (MAPK) pathway, and enhance oligodendrocyte survival by inhibiting the pro-apoptotic regulatory protein BAD. A subsequent study reported that the Src family kinase Fyn, downstream of laminin α2-β1 integrin, amplified the PDGF-mediated survival of newly-formed oligodendrocytes (Colognato *et al.* 2004). An earlier *in vitro* study had shown that when oligodendrocytes were difererentiated on laminin α2 substrate, they formed extensive myelin sheets suggesting that laminin α2-receptor interactions are important for stimulating the production of the myelin membrane required for wrapping axons (Buttery *et al.* 1999).

The significance of decreased laminin α2 expression on CNS myelination and oligodendrocyte development has been examined in dystrophic *dy/dy* mice. The results of these studies have shown an increase in oligodendrocyte progenitors, decreased numbers of mature oligodendrocytes, and dysmyelinated axons in the spinal cord and optic nerve suggesting that laminin α2-mediated signaling is necessary for normal oligodendrocyte differentiation (Chun *et al.* 2003; Relucio *et al.* 2009). Furthermore, Relucio *et al.* report the increased expression of inhibitory proteins that regulate Fyn activation, a Src family kinase necessary for normal CNS myelination (Sperber *et al.* 2001). A new report has lent further support for the role of laminin α2 during oligodendrocyte development, this time using the LAMA2 null mouse (Relucio *et al.* 2012). Relucio *et al.* reported an increase in oligodendrocyte precursor cell death in the germinal niche of the subventricular zone, delayed oligodendrocyte differentiation, and thinner myelin in the corpus callosum suggesting that laminin α2 promotes the survival of newly-formed oligodendrocyte progenitors, which in turn may contribute to delayed or altered myelination.

Oligodendrocytes express two laminin receptors: α6β1 integrin and dystroglycan (Milner and ffrench-Constant 1994; Buttery and ffrench-Constant 1999; Colognato *et al.* 2007). The contribution of β1 integrin upon oligodendrocyte development and myelination has been reported in two separate studies using two different conditional oligodendrocyte specific β1 integrin knockout mouse lines, and one CNS-specific β1 integrin knockout mouse line. In the first study, β1 integrin was excised via Cre recombinase under the 2',3'-cyclic nucleotide 3'-phosphodiesterase (CNP) promoter, active in pre-myelinating oligodendrocytes. In the second study, β1 integrin was excised 1) via Cre recombinase under the chondroitin sufate proteglycan 4 (NG2) promoter (active in oligodendrocyte progenitors), and 2) via Cre recombinase under the Nestin promoter (active in neural stem cells). CNP-β1-null mice exhibit increased apoptosis in the cerebellum, however, are myelinated normally in all regions (Benninger *et al.* 2006). NG2-β1-null and Nestin-β1-null mice contain thinner myelin; however, all three lines from the two studies exhibit normal oligodendroglial lineage progression (Barros *et al.* 2009). Since these two studies do not fully recapitulate the defects associated with either the laminin-deficient (*dy/dy*) mouse, or the laminin α2-null (LAMA2) mouse, it suggests that dystroglycan may also mediate the effects of laminin on normal oligodendrocyte development.

Chapter 2

INTRODUCTION TO DYSTROGLYCAN

Dystroglycan is most well known as an integral membrane component of the dystrophin glycoprotein complex (DGC) in skeletal muscle where it binds laminin in the extracellular matrix, linking to the actin cytoskeleton via dystrophin intracellularly, thereby forming a tether between the outside and inside of the cell. Originally, dystroglycan was discovered as a laminin-binding protein isolated in the brain and known for a time as cranin (Smalheiser and Schwartz 1987; Gee *et al.* 1993; Smalheiser and Kim 1995). Around the same time, a highly glycosylated component of the DGC in skeletal muscle was isolated and functionally shown to act as a transmembrane linker (Ervasti and Campbell 1991; Ibraghimov-Beskrovnaya *et al.* 1992; Ervasti and Campbell 1993). As this transmembrane linker was enriched in glycans and interacted with dystrophin in the DGC, the name dystroglycan was coined and is in common usage today. Since then, a great deal has been learned about the role of dystroglycan in a number cell types as a component of several different membrane complexes.

Dystroglycan is composed of two subunits (α/β) that are translated from a single transcript encoded by the *DAG1* gene (Fig. 2-1). Formed as a propeptide, dystroglycan is transported into the endoplasmic reticulum and cleaved within a full SEA (sea urchin, enterokinase, agrin) module via what is thought to be an autoproteolytic evolutionarily conserved mechanism (Akhavan *et al.* 2007). α/β-Dystroglycan are further post-translationally modified by

the addition of O- and N-linked glycans prior to being transported to the membrane. Located on the extracellular membrane surface, α-dystroglycan (120-156 kDa, depending on carbohydrate modifications) is a dumb-bell-shaped protein with globular N- and C-terminal domains separated by a highly glycosylated central mucin-like domain through which extracellular matrix (ECM) ligand-binding activities are mediated. The N-terminal domain of β-dystroglycan (43 kDa), a type 1 transmembrane protein, interacts with the C-terminus of α-dystroglycan at the cell surface via non-covalent interactions. The short 120 residue, unfolded, proline-rich intracellular C-terminal domain of β-dystroglycan contains a number of conensus motifs with over 40 predicted interaction sites (Moore and Winder 2010). The juxtamembrane domain of β-dystroglycan contains consensus motifs for a nuclear localization sequence (NLS), extracellular signal-regulated kinase (ERK), ezrin-radixin-moesin (ERM), and receptor-associated protein of the synapse (rapsyn). The extreme C-terminus of β-dystroglycan contains Src homology 2 (SH2) and Src homology 3 (SH3) consensus sequences, as well as, a WW (PPXY) domain that binds to a WW-like motif within the C-terminal domain of dystrophin (or its homologue utrophin) which binds to actin (Baressi and Campbell 2006). As a component of the dystrophin glycoprotein complex (DGC) in muscle, dystroglycan is closely associated with a number of other transmembrane proteins including sarcoglycans (SG-α, SGβ, SGγ, SGδ), and sarcospan which are thought to stabilize the DGC in the membrane (Baressi and Campbell 2006).

The central mucin domain of α-dystroglycan binds several ECM molecules that contain laminin globular (LG) modules including laminin (Ervasti and Campbell 1993; Gee *et al.* 1993; Yamada *et al.* 1994; Smalheiser and Kim 1995; Montanaro *et al.* 1999), agrin (Gee *et al.* 1994; Yamada *et al.* 1996), perlecan (Peng *et al.* 1998; Talts *et al.* 1999), neurexin (Sugita *et al.* 2001), and pikachurin (Sato *et al.* 2008). LG 4/5 domains of laminin α2 bind with high affinity to the

mucin domain of α-dystroglycan. Perturbations of the O-linked carbohydrate modifications to α-dystroglycan can significantly reduce, or completely abbrogate, its interactions with laminin (Michele *et al.* 2002). The consequences of disturbed laminin-dystroglycan interactions results in phenotypes that resemble CNS abnormalities occurring in congential muscular dystrophies (CMDs). Diseases associated with dysfunctional (or absent) dystroglycan are collectively referred to as dystroglycanopathies.

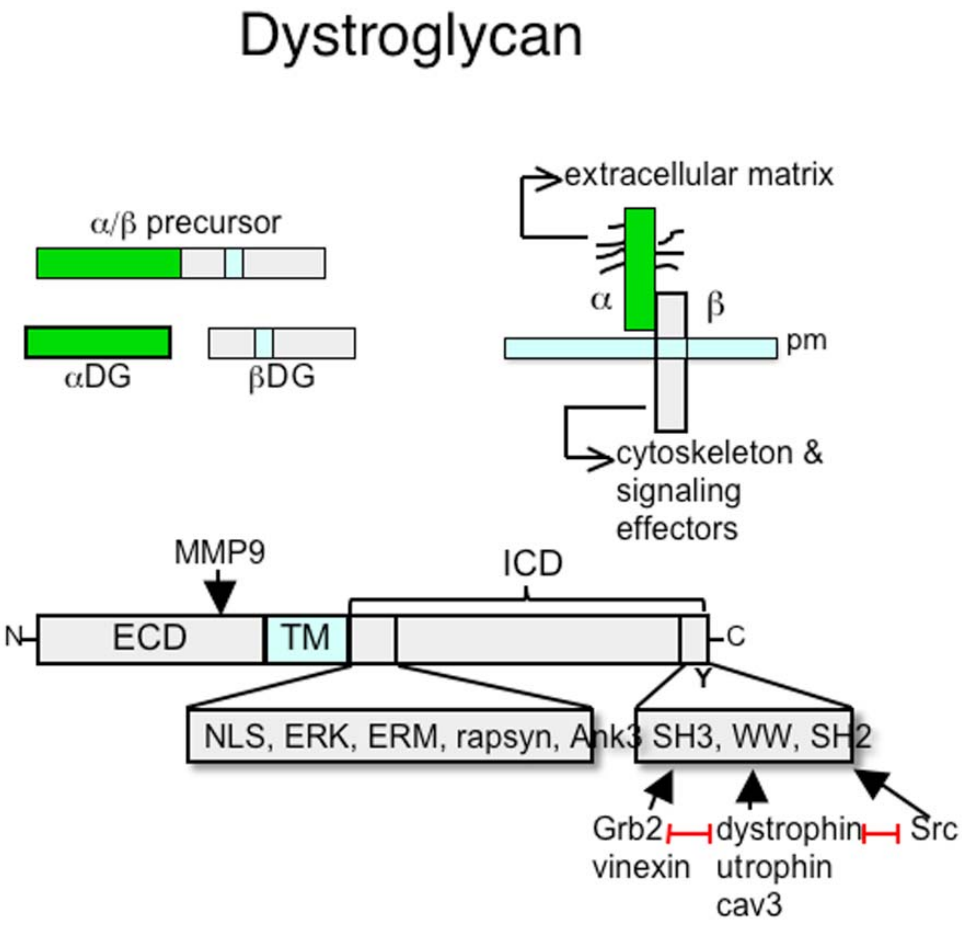

Figure 2-1. Dystroglycan Domains

(Courtesy of Holly Colognato)

Dystroglycanopathies

Mutations in genes encoding known or putative glycosyltransferase enzymes that directly or indirectly post-translationally modifiy of α-dystroglycan with carbohydrate chains necessary for binding to its extracellular ligands, e.g. laminin, are collectively known as secondary dystroglycanopathies. To date, only two known cases with a mutation in *DAG1* itself have been reported; these are referred to as primary dystroglycanopathies (Frost *et al.* 2010; Hara *et al.* 2011). The clinical severity of dystroglycanopathies ranges from mild to severe peripheral myopathy with significant brain and eye involvement (Cormand *et al.* 2001; Clement *et al.* 2008; Guglieri *et al.* 2008). Brain abnormalities include white matter defects, agenesis of the corpus callosum, transient dysmyelination, cobblestone lissencephaly, polymicrogyria, cerebellar cysts, cerebellar hypolasia, ventricular enlargement, and occaisional hemispheric fusion (Kondo-Iita *et al.* 1999; Cormand *et al.* 2001; Clement *et al.* 2008). Late-onset limb-girdle muscular dystrophy (LGMD) lies at the mild end of the clinical spectrum in severity, while the congenital muscular dystrophies 1C and 1D (MDC1C, MDC1D) are moderate, followed by significant impairment in the disorders Fukuyama congenital muscular dystrophy (FCMD), muscle-eye-brain disease (MEB), and Walker-Warburg syndrome (WWS) (Barresi and Campbell 2006; Clement *et al.* 2008; Frost *et al.* 2010). To date, a variety of genetic anomalies including deletions, insertions, frameshifts, splice variants, and missense mutations have been reported in these disorders affecting the following six known or putative glycosyltranferase genes: *Protein-O-mannosyl transferase* 1 (*POMT1*), *Protein-O-mannosyl transferase* 2 (*POMT1*), *Protein-O-mannose 1,2-N-acetylglucoaminyltransferase 1* (*POMGnT1*), *fukutin*, *Fukutin-related protein* (*FKRP*), and *like-acetylglucosaminyltransferase* (*LARGE*) (Godfrey *et al.* 2007).

Mentioned above, there are only two known cases of primary dystroglycanopathy. The first described case is of a girl followed from age 5 years to 11 years with severe learning disabilities resulting from a 2-Mb heterozygous deletion of chromosome 3 that includes *DAG1* (Frost *et al.* 2010). Frost *et al.* report cortical abnomalities based on MRI examination including ventricular enlargement and patchy white matter abnormalities. The second case was reported in a woman with LGMD whose brain was structually normal, however, had severe mental retardation and was later found to have a missense (Thr192→Met) mutation in *DAG1* (Dincer *et al.* 2003; Hara *et al.* 2011). Hara *et al.* show that this mutation reduced the capacity of laminin to bind α-dystroglycan both in the patient, and, in vivo using a T192→M mouse, which further analysis suggested was a direct result of inhibiting modification of phosphorylated O-mannosyl glycans on α-dystroglycan via *LARGE*.

Dystroglycan In The Brain: Lessons From Animal Models

This section highlights some of the known roles of dystroglycan during normal brain development following the lessons learned from studies on conditional DAG1 knockout mice, and mice lacking the putative glycosyltransferases that modify dystroglycan. The *Dag1* null mouse is embryonic lethal (E6.5) due to a breach in an extraembryonic membrane (Reichert's membrane) that has been suggested to separate maternal and embryonic circulations (Williamson *et al.* 1997). A brain-specific conditional dystroglycan null mouse was later generated (GFAP-Cre/DG-null) using Cre-*loxP* technology to drive Cre recombinase expression under the glial fibrillary acid (GFAP) promoter and excise the floxed *Dag1* allele at embryonic day 13.5, producing viable and fertile mice. (Moore *et al.* 2002). GFAP-Cre/DG-null mice have cortical

and cerebellar abnormalities resembling those found in congenital muscular dystrophies including intrahemispheric fusion, abnormal neural migration, breaches of the pial basement membrane, and neuronal heterotopias. Basement membrane disruptions found in the GFAP-Cre/DG-null mice have been suggested to reflect dysfunctional laminin-receptor interactions which have previously been shown to facilitate laminin polymerization and basement membrane formation (Colognato *et al.* 1999; Miner and Yurchenco 2004). Deletion of dystroglycan earlier in the epiblast (E7.5) was subsequently accomplished using a Mox-2-Cre transgenic mouse line to generate the MORE-DG null mouse (Satz *et al.* 2008). MORE-DG null mice exhibit severe brain and eye abnormalities that phenotypically resemble severe cases of WWS. In addition to the brain defects noted in the GFAP-Cre/DG-null mouse above, the MORE-DG null mice have overall smaller brain size, cerebellar hypoplasia, reduced laminin expression, cortical dysplasia and ventricular enlargement.

In order to distinguish the function of dystroglycan between neurons and glia in the brain, the following study excised dystroglycan at E10.5 using a *NEX*-Cre transgenic mouse line to create the NEX-Cre/DG-null mouse with *NEX* expression restriced to neurons of the telencephalon, cortical neurons, and hippocampal neurons (Satz *et al.* 2010). Concurrently, Satz *et al.* also generated a *Nestin*-Cre transgenic line producing (Nestin-Cre/DG-null mice) that excised dystroglycan earlier (E10.5) than the GFAP-Cre/DG-null mouse, and restricted expression of *Nestin*-cre more broadly to include all neurons and glia derived from neural stem cells (NSCs). Brain-specific deletion of dystroglycan in the Nestin-Cre/DG-null mouse resulted in abnormal cortical and cerebellar migration, glial/neuronal heterotopias, megalencephaly, hydrocephalus, and cortical malformations resembling cobblestone lissencephaly. Compared to GFAP-Cre/DG-null mice, with dystroglycan excision occuring later in development, brain

defects were generally more severe and suggested a temporal requirement for dystroglycan during normal brain development. Interestingly, the neuronal-specific Nex-Cre/DG-null mice did not have similar brain defects suggesting that dystroglycan has distinct functions in neurons and glia during normal brain development.

The function of dystroglycan has also been examined in mouse models of secondary dystroglycanopathy including mice lacking the glycosyltransferase *LARGE* (*Large*^{myd}, myodystrophy). *LARGE* post-translationally modifies dystroglycan by the addition of glycans to its mucin domain thereby increasing the affinity of α-dystroglycan to bind extracellular ligands including laminin. *Large*^{myd} mice are a model of MDC1D and phenocopy many of the abnormalities described for the dystroglycan knockout mice noted above (Holzfeind *et al.* 2002; Michele *et al.* 2002; Satz *et al.* 2010). Intriguingly, overexpression of *LARGE* in *Large*^{myd} mice was shown to ameliorate the functional deficits of dystroglycan and restore its ability to bind laminin creating the possibility that a similar therapeutic intervention might someday be applied to patients with various dystroglycanopathies (Barresi *et al.* 2004).

Myelination In The PNS: A Role For Dystroglycan

Because of the nature of its role in the DGC, and in disorders including congenital muscular dystrophy, dystroglycan has been studied intensely in the peripheral nervous system where a role for dystroglycan has been identified in Schwann cell development and myelination. Two important distinctions between Schwann cells and oligodendrocytes have been stated previously, but are worthwhile to mention again. The first is the association with laminin and a basal lamina. Schwann cells are in intimate contact with a laminin-rich basal lamina that

surrounds their outer membrane. Oligodendrocytes do not have a similar association with a basal lamina and only contact laminin transiently during development. The second important distinction is in the number of axons that Schwann cells and oligodendrocytes myelinate. During their early development, Schwann cells undergo a process called radial sorting in which a 1:1 relationship between a Schwann cell and the axon it will myelinate is formed. In contrast, an oligodendrocyte may extend dozens of highly branched processes toward target axons and myelinate up to 50 or more axons (Chong *et al.* 2012). Thus, while their ultimate function is the same, the interactions with ECM and cytoskeletal rearrangements that need to take place for successful myelination are clearly different, and this important point should be kept in mind.

As described previously, merosin-deficient congenital muscular dystrophy type 1A (MDC1A) is caused by mutations in the gene encoding the α2-subunit of the ECM molecule laminin and is associated with both peripheral myopathy and white matter defects (Shorer *et al.* 1995; Caro *et al.*, 1999; Philpot *et al.* 1999; Miyagoe-Suzuki *et al.* 2000; Di Muzio *et al.* 2003; Quijano-Roy *et al.* 2004). PNS defects associated with laminin α2 deficiency have been studied most extensively using the laminin α2-deficient dystrophic mouse (*dy/dy*). Discontinuity of the basal lamina, defects in radial sorting, bundles of unmyelinated axons within the proximal spinal roots, and decreased numbers of proliferating Schwann cells have been reported in *dy/dy* mice (Matsumura *et al.* 1996). Sequential deletion of Schwann cell laminin receptors (α6β1 integrin, α6β4 integrin, dystroglycan) was subsequently undertaken in order to determine laminin receptor involvement in the defects associated with *dy/dy* mice.

In the first study, conditional Schwann cell-specific deletion of β1 integrin resulted in impaired axonal sorting and severe peripheral neuropathy (Feltri et al 2002). A subset of

Schwann cells were able to myelinate normally, however, suggesting that an additional laminin receptor was likely involved. Regional differences were discovered after a further comparison of the β1 integrin conditional knockout and *dy/dy* mouse revealing that bundles of unmyelinated axons were prominent in the proximal spinal roots and distal nerve of *dy/dy* and β1 integrin mice respectively (Previtali *et al.* 2003). Since α6β4 integrin and dystroglycan are expressed after birth at the onset of myelination, Previtali *et al.* suggested that specific laminin-receptor interactions, before and after birth explained the regional differences in axonal sorting and myelination. However, when α6β4 integrin was conditionally knocked out, Schwann cells myelinated normally with the defects arising after myelination due to abnormal myelin folding and myelin maintenance (Nodari *et al.* 2008). Conditional deletion of both α6β4 integrin and dystroglycan, however, induces major myelin folding abnormalities and regional demyelination suggesting that α6β4 integrin is only required for myelin stability. Not until the α6β1 integrin/dystroglycan double knockout was generated, were the *dy/dy* and β1 integrin myelination defects phenocopied (Berti *et al.* 2011). These results showed that the requirement for laminin-receptor engagement was not redundant, but relied on the sequential engagement of β1 integrin and dystroglycan during normal Schwann cell development.

To assess the role of dystroglycan during normal Schwann cell development, conditional Schwann cell-specific dystroglycan knockout mice (P0-DG-null) were generated. P0-DG-null exhibit abnormal myelin outfoldings in sciatic nerve, disorganized microvilli at Nodes of Ranvier, and a reduction in voltage-gated Na^+ channel clustering at the nodes (Saito *et al.* 2003). Additionally, P0-DG-null lysates were found to contain only the DGC components utrophin, α1-syntrophin, DRP2, and periaxin; WT mice, on the other hand, contain all of the known DGC components. A subsequent study compared the *dy/dy* to the P0-DG-null and characterized

remarkably similar phenotypes, although the P0-DG-null defects were slightly more severe (Occhi *et al.* 2005). Taken together, these studies revealed functional roles for dystroglycan in nodal organization, myelin sheath elongation and myelin folding. Additionally, the more severe phenotype seen in P0-DG-null mice, in comparison to the *dy/dy* and *LARGE*^{myd} mice, suggests that cytoplasmic dystroglycan interactions play an important role in normal Schwann cell development and myelination.

Dystroglycan Function: Beyond the DGC

Numerous additional functions have been uncovered for dystroglycan apart from its discovery as a component of the DGC in recent years including roles in signaling, cytoskeletal reorganization, adhesion, cytokinesis, and cell division. The ability of dystroglycan to participate in these varied processes is reflected by the number of consensus motifs in the cytoplasmic domain of β-dystroglycan that have been shown either directly, or indirectly, to scaffold proteins that mediate these functions. Proteolytic processing of β-dystroglycan has also been observed in a variety of tissues, and although the significance is still poorly understood, the cleavage product is elevated in some pathological diseases including cancer (Sgambato and Brancaccio 2005). In addition, while β-dystroglycan contains a nuclear localization sequence (NLS), it has only recently been found to localize there in several cell types while its function there remains obscure. The following section will describe some of these alternative functions for dystroglycan.

A role for dystroglycan in signaling was not expected given its structural function in skeletal muscle. Interestingly, several reports surfaced that β-dystroglycan could be

phosphorylated in an adhesion-dependent manner and, in response to laminin, influence the interaction of dystroglycan with dystrophin (Russo et al 2000; Ilsley *et al.* 2001). Tyrosine phosphorylation of β-dystroglycan at its extreme C-terminus was found to inhibit the interaction of dystrophin/utrophin with β-dystroglycan's C-terminal WW domain, which suggested that this phosphorylation could regulate dystroglycan function (Russo et al 2000; Ilsley *et al.* 2001). It was later shown that this tyrosine phosphorylation of β-dystroglycan was mediated by SH2 domain containing proteins including Fyn, c-Src, Csk, NCK, and SHC (Sotgia *et al.* 2001). Sotgia *et al.* also show that these SH2 domain containing proteins interact with β-dystroglycan suggesting the possibility that tyrosine phosphorylation of dystroglycan might act as a switch to promote the recruitment of other SH2 domain containing proteins. This possibility, however, is still unresolved. Growth factor receptor-bound protein 2 (Grb2), an SH2/SH3 domain containing adaptor molecule involved in mitogen activated protein kinase (MAPK) / extracellular signal-regulated kinase (ERK) signaling, has also been reported to interact with dystroglycan in muscle and brain (Cavaldesi *et al.* 1999; Russo *et al.* 2000). This interaction is mediated through an SH3 domain in the extreme C-terminal domain of β-dystroglycan which overlaps the dystrophin binding WW domain and suggests that competitive interactions influence binding to dystroglycan (Yang *et al.* 1995). While the functional significance of these competitive interactions is unknown, a recent study from our lab identified a ternary complex containing dystroglycan, Grb2, and insulin receptor substrate 1 (IRS-1) (involved in IGF-1 mediated MAPK signaling) in differentiating oligodendrocytes (Galvin *et al.* 2010). Galvin *et al.* found that maximal MAPK activation in response to IGF-1, downstream of dystroglycan-laminin interaction, was dependent on dystroglycan and necessary for IGF-1 to promote oligodendrocyte

differentiation. Thus, dystroglycan-laminin interactions may recruit complexes to dystroglycan that potentiate signaling by other receptors.

One of the first indications that dystroglycan, instead of merely existing as a static constituent to link the actin cytoskeleton to the ECM, could modulate cytoskeletal dynamics was the discovery that β-dystroglycan could bind directly to F-actin, independently of the dystrophin homologue utrophin, and bundle actin filaments (Chen *et al.* 2003). Overexpression of dystroglycan in REF52 fibroblasts induced an apparent dissolution of stress fiber formation throughout the cell and tightly reorganized actin toward the periphery of the cell body; furthermore, Chen *et al.* reported that overexpression also induced the formation of microvilli with enriched dystroglycan expression. The ezrin-radixin-moesin (ERM) cytoskeletal adapter protein, ezrin, was later found to interact directly with β-dystroglycan in the juxtamembrane C-terminal domain and mediate the ability of dystroglycan to form these microvilli structures (Spence *et al.* 2004). A following study revealed that a ternary complex consisting of β-dystroglycan, ezrin and the Rho GDP/GTP exchange factor (RhoGEF), Dbl, was sufficient to induce filopodia formation (Batchelor *et al.* 2007). By recruiting ezrin and Dbl (a RhoGEF for the Rho GTPase, Cdc42) to the cell membrane, Batchelor *et al.* showed that β-dystroglycan localized Cdc42 activation resulting in the formation of filopodia.

It is unclear whether dystroglycan can modulate the oligodendroglial actin cytoskeleton; however, considering the functional role of dystroglycan in recruiting molecules that modify actin, it is intriguing possibility that dystroglycan may regulate the morphological transformation of newly-differentiated oligodendrocytes during initial process outgrowth and process branching. Indeed, actin reorganization is required during early oligodendrocyte differentiation as F-actin

assembly precedes the invasion of microtubules into processes which is required for process extension (Song *et al.* 2001). Process formation is generally thought to start by the initial formation of thin filopodia containing bundles of F-actin that protrude from the oligodendrocyte cell membrane. These filopodia then coalesce forming a wider lamellopdia containing a branching network of microfilaments, followed closely behind by invading microtubules (Bauer *et al.* 2009). Evidence that dystroglycan can drive filopodia formation suggests a potential mechanism by which oligodendrocytes can initiate process extension and branching (Batchelor *et al.* 2007). Failure to properly extend and branch processes would drastically reduce survival, decrease the number of internodes formed, and compromise the ability of oligodendrocytes to myelinate properly.

Dystroglycan has also been previously implicated in regulating cell cycle progression. An increased accumulation of cells in S-phase has been reported in dystroglycan-depleted mammary mouse epithelial cells (Sgambato *et al.* 2006). A possible role for dystroglycan during cell division was later proposed after the observation that dystroglycan localized in the cleavage furrow and midbody during cytokinesis in REF52, 3T3, and Hela cells (Higginson *et al.* 2007). Higginson *et al.* showed that the cytoplasmic tail of β-dystroglycan is required for localization to the cleavage furrow, and that dystroglycan depleted cells were delayed in the S-phase to G2/M-phase transition consistent with the previous report. Dystroglycan, Dp71, and the nuclear envelope protein lamin B1 were also found to co-localize in the cleavage furrow, mitotic spindle, and midbody of neuronal PC12 cells during cell division (Villarreal-Silva *et al.* 2011). Dp71 is a 71 kDa dystrophin isoform generated by alternative splicing and is the most abundant dystrophin isoform present throughout the brain (Waite *et al.* 2009). Dp71 lacks an actin binding domain; however, dystroglycan retains the ability to interact with Dp71. Villarreal-Silva *et al.* report that

PC12 cells depleted of Dp71 were stalled in the G0/G1 phase with marked growth arrest coinciding with a decrease in proliferation, and decreased expression of dystroglycan and lamin B1 in the cleavage furrow, mitotic spindle, and midbody. From these studies one can conclude that both dystroglycan and Dp71 localize with machinery necessary for progression through the cell cycle; however, it remains unclear how Dp71 regulates dystroglycan expression, and, whether or not the cell cycle delay is a consequence of redistribution of these or other proteins involved in cell division. Interestingly, a role for β-dystroglycan in oligodendrocyte precursor proliferation or cell cycle dynamics has not been investigated.

One of the more intriguing developments over the last few years concerning alternative roles for dystroglycan have been reports finding dystroglycan and components of the DGC in the nucleus of several cell types. The characterization of the specific components of the DGC and nuclear binding partners have been the the initial focus of these investigations. The first putative nuclear DGC complex was identified in Hela cells and included β-dystroglycan, Dp71, β-sarcoglycan, α- and β- syntrophin, α1- and β- dystrobrevin and neuronal nitric oxide sythase (nNOS) (Fuentes-Mera *et al.* 2006). All of the aforementioned DGC members were observed in the nuclear matrix of Hela cells via confocal microscopy, cell fractionation and coimmunopreciptiation experiments. β-dystroglycan, Dp71 and β-dystrobrevin were additionally shown to interact with lamin B1 and actin. With the exception of β-syntrophin and β-dystrobrevin, the same DGC components were identified together in the nuclear envelope of C_2C_{12} muscle cells and showed particular enrichment of β-dystroglycan and α-sarcoglycan (Gonzalez-Ramirez *et al.* 2008). In agreement with the previous study mentioned above showing that cells depleted of Dp71 showed a marked decrease in the expression of β-dystroglycan in the cleavage furrow, mitotic spindle, and midbody during cell division; PC12 cells depleted of Dp71

also show a decrease in the expression of β-dystroglycan and other DGC components expressed in the nuclear matrix (Villarreal-Silva *et al.* 2010). Interestingly, Silva *et al.* noted increased expression of the dystrophin homologue utrophin; however, immunoprecipitations failed to show increased interaction with β-dystroglycan or any other DGC member suggesting that utrophin could not compensate for the depletion of Dp71.

Trafficking of the DGC into the nucleus remained an unresolved question and was assumed to be mediated by β-dystroglycan since of the DGC components mentioned, dystroglycan contained the only predicted NLS sequence. This question was finally answered in two separate studies. A functional bipartite NLS was identified in the C-terminal domain of β-dystroglycan that mediated the nuclear import of constructs containing full length dystroglycan, β-dystroglycan, or a full length monomeric uncleavable precursor designed to mimic the propeptide prior to SEA autoproteolysis (Oppizzi *et al.* 2008; Lara-Chacon *et al.* 2010). In a screen of several cancer cell lines, Oppizzi *et al.* found that nuclear β-dystroglycan expression levels are highly variable, and furthermore, suggested that nuclear import seems to be independent of extracellular ligand binding as there is no correlation between nuclear localization of β-dystroglycan and α-dystroglycan glycosylation. Using an *in vitro* reconstituted nuclear transport assay, Lara-Chacon *et al.* report that the nuclear transport molecules importin-α and importin-β bound with high affinity to the dystroglycan NLS and were required for dystroglycan transport into the nucleus. Lara-Chacon *et al.* also suggest that tyrosine phosphorylated β-dystroglycan is sequestered in the nucleus. Together these studies have identified common DGC components including β-dystroglycan which form a putative complex in the nuclear matrix of three different cell lines. The functional significance of nuclear localized

dystroglycan is currently unknown, but the consensus based on each of these studies suggests that dystroglycan, together with elements of the DGC, may function to anchor and/or organize the nuclear matrix facilitating cell division, intranuclear sorting, and, possibly, transcriptional regulation. Whether or not oligodendrocytes or their precursors contain nuclear localized β-dystroglycan is not currently known.

Finally, post-translational processing of dystroglycan has been reported to include not only glycosylation of α-dystroglycan, but the enzymatic cleavage of β-dystroglycan as well. A truncated 30 kDa β-dystroglycan form has been reported in a number of breast cancers cell lines and squamous carcinoma cells (Loasso *et al.* 2000). This truncated form of β-dystroglycan was shown to be the result of proteolytic processing of β-dystroglycan, and was followed by detachment of α-dystroglycan from the cell surface (Loasso *et al.* 2000; Singh *et al.* 2004). The membrane-associated matrix metalloproteinases (MMPs) -2 and -9 were implicated in mediating the cleavage of β-dystroglycan in the extracellular N-terminal domain near the cell surface (Yamada *et al.* 2001; Zhong *et al.* 2006). Furthermore, aberrant accumulation of the trucated 30 kDa β-dystroglycan form in several oral squamous cell carcinomas have been noted; in contrast, full length α/β-dystroglycan expression is largely gone in these cells (Shang *et al.* 2008). In the context of cancer, dysregulation of ECM-cell interactions are thought to perturb cell behaviors and promote tumor growth and invasiveness (Sgambato and Brancaccio 2005). It should be noted that the retention of the truncated β-dystroglycan and its significance are not understood. Instead, the focus has been primarily on α-dystroglycan and its detachment from basement membrane structures as a mechanism to potentiate cancer growth and invasiveness.

While the role of the truncated form of β-dystroglycan remains unclear, in the dystrophin-null model of Duchenne muscular dystrophy (the *mdx* mouse), MMP -2 and -9 are more active in Schwann cell peripheral nerve, and the 30 kDa β-dystroglycan form accumulates in Schwann cell membranes (Hnia *et al.* 2006). Interestingly, a later study showed that the conditional deletion MMP-2 and -9 in Schwann cells resulted in decreased β-dystroglycan cleavage and the formation of abnormal Schwann cell compartments during development (Court *et al.* 2011). Importantly, Court *et al.* show that β-dystroglycan and α-dystroglycan may have functions independent of each other since each may polarize to different Schwann cell abaxonal domains and interact with alternate DGC components. To illustrate, a complex between dystroglycan (α/β), dystrophin-related protein 2 (Drp2) and periaxin in the outer cell membrane is stabilized by periaxin in appositions (Sherman *et al.* 2001). MMP-2 and -9 cleave β-dystroglycan where it remains in the outer membrane in Cajal Bands and exchanges its interactors to include utrophin or Dp116 (Court *et al.* 2011). MMP-2/9 $^{-/-}$ mice have larger appositions and smaller Cajal Bands suggesting that regulated β-dystroglycan cleavage is required for normal Schwann cell myelination (Court *et al.* 2011). In the CNS, myelination deficits in the corpus callosum and decreased numbers of mature oligodendrocytes have been reported in the MMP-9 and -12 null mouse, although it should be noted that the myelination delay was transient (Larsen *et al.* 2006). Since the myelination deficit was transient, there are likely mechanisms to compensate for the loss of MMP-9 and -12. However, that does not preclude the spatial-temporal requirement for MMP activity during normal oligodendrocyte development, and whether or not a cleaved form of dystroglycan is present in oligodendrocytes is still an open question.

A Role For Dystroglycan In Oligodendrocyte Development

Perturbing dystroglycan function in differentiating oligodendrocytes, either by disturbing laminin-dystroglycan interactions with blocking antibodies or depleting dystroglycan via siRNA, has been reported to reduce the number of myelinating segments in DRG co-cultures and cause a delay in differentiation (Colognato *et al.* 2007). However, the delay in differentiation was not attributable to a defect in survival, as only β1 integrin was was necessary to enhance oligodendrocyte survival in response to the survival factor PDGF (Colognato *et al.* 2007). This finding suggests that dystroglycan and β1 integrin may act either in concert, or sequentially to promote different stages of oligodendrocyte development.

Interestingly, laminin has been previously shown to potentiate the formation of myelin sheets by oligodendrocytes differentiated *in vitro* (Buttery and ffrench-Constant 1999). The ability to elaborate myelin membrane requires the extensive formation and arborization of numerous oligodendrocyte processes that support the myelin membrane in a physical sense, as well as, by facilitating the transport of myelin proteins into growing myelin. Previous work in our lab has demonstrated that dystroglycan-deficient oligodendrocytes grown in culture produce less myelin basic protein (MBP), a major protein component of myelin (Colognato *et al.* 2007). The myelination defects associated with the *dy/dy* mouse may, therefore, partially reflect the inability of oligodendrocytes to properly extend and branch processes, which are necessary for both making contact with target axons, and supporting the polarized transport of myelin proteins from the cell body out towards the myelin membrane.

The recent findings that β-dystroglycan localizes to the nucleus in some cell types raises another possible mechanism by which dystroglycan may regulate oligodendrocyte development

(Oppizzi *et al.* 2008; Lara-Chacon *et al.* 2010). Together with the dystrophin isoform Dp71, β-dystroglycan has been found to localize in both the nuclear envelope and at the cleavage furrow during cytokinesis (Higginson *et al.* 2008; Villareal-Silva *et al.* 2011). As it is currently unknown whether β-dystroglycan localizes to the nucleus or cleavage furrow in oligodendrocytes, it is tempting to speculate whether a similar localization may contribute to normal oligodendrocyte development as well. I have begun to investigate these possibilities, the results of which are shown in Chapter 4.

Together, these studies suggest that dystroglycan may have several important roles during normal oligodendrocyte development. For instance, it was unknown whether dystroglycan regulates processes formation and branching in newly-formed oligodendrocytes, or, whether dystroglycan localizes to the nucleus in oligodendrocytes or their progenitors. The goal of the following dissertation research was to investigate the role of dystroglycan in normal oligodendrocyte development, and to test the hypothesis that **dystroglycan regulates process outgrowth and branching, localizes to the nucleus, and contributes to the to the overall myelinogenic capacity of of individual oligodendroglia.**

Chapter 3

DYSTROGLYCAN PROMOTES FILOPODIAL FORMATION AND BRANCHING IN DIFFERENTIATING OLIGODENDROGLIA

INTRODUCTION

The correct regulation of oligodendroglial morphology is critical to enable the efficient and timely myelination of central nervous system (CNS) axons. Differentiating oligodendrocytes undergo extensive cytoskeletal remodeling to enable multiple cell processes to extend toward, contact, and wrap around dozens of axons (Richter-Landsberg *et al.* 2008). While several intrinsic mechanisms e.g. the cytoskeletal regulator, WAVE1, have been shown to be critical for oligodendroglial process outgrowth (Kim *et al.* 2006), the role of extrinsic factors such as the extracellular matrix (ECM) in regulating oligodendrocyte morphology remains poorly understood.

Deficiencies in the ECM protein laminin, however, have revealed that laminin is necessary for normal oligodendroglial development. Mutations in the gene encoding the α2 subunit of laminin-2, *LAMA2*, cause a subtype of congenital muscular dystrophy (CMD) known as merosin-deficient congenital muscular dystrophy or MDC1A (Miyagoe-Suzuki *et al.* 2000), which presents with varying degrees of white matter abnormalities and severe cognitive deficits (Jones *et al.* 2001). The dystrophic *dy/dy* mouse, a laminin-α2 deficient model of MDC1A, has

regional myelin abnormalities that include inappropriately unmyelinated axons as well as thinner myelin (Chun *et al.* 2003; Relucio *et al.* 2009). Oligodendrocytes express two laminin receptors: integrin α6β1 and dystroglycan (Buttery and ffrench-Constant 1999; Colognato *et al.* 2007; Milner and ffrench-Constant 1994). Oligodendrocytes that lack integrin β1-subunits extend shorter processes than do control oligodendrocytes (Barros *et al.* 2009). However, conditional deletion of the integrin β1-subunit in oligodendrocytes leads to normal myelin (Benninger *et al.* 2006), or thinner myelin (Barros *et al.* 2009), depending on the Cre driver used, yet in both cases, appropriate numbers of axons are myelinated. These data suggest that an additional laminin receptor, possibly dystroglycan, may contribute to the inability of oligodendroglia in laminin-deficient mice to myelinate the correct number of axons.

As a component of the dystrophin glycoprotein complex (DGC), dystroglycan is known for its mechanical role in linking the ECM with the actin cytoskeleton to stabilize the sarcolemma during muscle contraction (Barresi *et al.* 2006; Moore *et al.* 2010). However, recent studies have implicated dystroglycan as a cytoskeletal modulator, where, for example, dystroglycan has been found to associate indirectly with FAK in fibrillar adhesions to regulate myoblast cell spreading (Thompson *et al.* 2009). In addition, dystroglycan helps mediate the assembly of myoblast podosomes - transient adhesion structures found in many migrating cell types - by localizing Tks5 and Src (Thompson *et al.* 2008). And, in both Swiss 3T3 and REF52 cells, dystroglycan was shown to recruit the Rho GTPase Cdc42 to the cell membrane thereby helping drive filopodia formation (Batchelor *et al.* 2007). Our previous work demonstrated that disrupting oligodendroglial dystroglycan interactions led to smaller MBP-positive myelin sheets, as well as fewer myelin segments in co-culture with DRG neurons (Colognato *et al.* 2007), suggesting that dystroglycan may indeed regulate oligodendroglial process dynamics.

In the current study I investigated whether dystroglycan-laminin interactions regulate filopodia formation, process outgrowth and branching in pre-myelinating oligodendrocytes. I report that laminin positively-regulates filopodia formation, and confirmed that laminin regulates process outgrowth and process branching (Eyermann *et al.* 2012). This in agreement with previous reports that have shown that culturing on laminin enhances the cell area of differentiating oligodendrocytes (Buttery and ffrench-Constant 1999; Lafrenaye and Fuss *et al.* 2010). I found that dystroglycan localizes within filopodia and in processes at leading edges and at branch points, and, that dystroglycan partially co-localizes with FAK in oligodendroglial focal adhesions (Eyermann *et al.* 2012). In addition, I found that disrupting dystroglycan-laminin interactions, either with blocking antibodies or via dystroglycan-specific siRNA, reduced filopodia formation, process outgrowth and branching (Eyermann *et al.* 2012). These data suggest that dystroglycan modulates cytokeletal remodeling during oligodendrocyte development, and may contribute towards the ability of oligodendrocytes to myelinate large numbers of axons in the CNS.

RESULTS

Process outgrowth and filopodia formation are increased in response to laminin

Filopodia are small filamentous projections extending from the cell membrane and have been proposed to contribute to oligodendrocyte process outgrowth (Bauer *et al.* 2009; Mattila *et al.* 2008). To examine a potential role for laminins in regulating filopodia formation in newly differentiated oligodendrocytes, cells were grown for 12 hours on PDL or laminin-2 (Lm) substrates, after which filopodia were seen to be forming along the length and near the leading

distal edge of processes (Fig. 3-1A). The mean number of filopodia formed was increased when oligodendrocytes were differentiated on laminin for 12 hours (Fig. 3-1B: 49.4 ± 3.3 on Lm, vs. 26.8 ± 1.4 on PDL, n = 3, P = < 0.001). To control for differences in the number of filopodia formed as a function of the surface area covered by the cells, I normalized the number of filopodia to the cell perimeter, and again found that the relative number of filopodia formed was increased when oligodendrocytes were differentiated on laminin (Fig. 3-1C: 0.24 ± 0.016 filopodia per micron on Lm, vs. 0.15 ± 0.013 on PDL, n = 3, P = < 0.001). Additionally, mean filopodia length was also increased slightly when oligodendrocytes were differentiated on laminin (Fig. 3-1D: 2.67 μm ± 0.053 μm on Lm, vs. 2.46 μm ± 0.062 μm on PDL, n = 3, P = < 0.001).

To evaluate whether laminin can positively regulate process outgrowth during early stages of oligodendrocyte maturation, I differentiated cells for 4, 12, 24, or 72 hours on PDL or laminin and measured process length. Representative images of F-actin in oligodendrocytes differentiated for the previously mentioned time points on PDL or Lm are shown (Fig. 3-1E). Mean process length was not significantly increased on laminin 4 hours into differentiation (Fig. 3-1F: 25.5 μm ± 0.6 μm on Lm, vs. 24.7 μm ± 0.6 μm on PDL, n =3, P = 0.367); however, process length was significantly increased on laminin at 12, 24 and 72 hours into differentiation (Fig. 3-1F: 12h, 39.6 μm ± 1.3 μm on Lm, vs. 34.5 μm ± 1.3 μm on PDL, P = < 0.001; 24h, 58.3 μm ± 1.8 μm on Lm, vs. 50.4 μm ± 1.6 μm on PDL, P = 0.002; 72h, 64.4 μm ± 1.8 μm on Lm, vs. 56.9 μm ± 1.5 μm on PDL, P = 0.001; n = 3). It should be noted that for all morphometric experiments I only evaluated oligodendrocytes, which were identified as such by performing immunocytochemistry with appropriate antibodies to oligodendroglial lineage stage-specific

proteins e.g. CNP (Fig. 3-1G). Taken together, these data suggest that laminin positively regulates filopodia formation and process outgrowth in pre-myelinating oligodendrocytes.

Primary process formation and process branching by newly-formed oligodendrocytes is increased in response to laminin

I next sought to determine whether laminin potentiated process formation and branching in differentiating oligodendrocytes. Oligodendrocyte processes were classified according to the order by which they form initial protrusions from the cell body, and subsequently, by the order in which they branch off from primary processes (illustrated in Fig. 3-2A). I first sought to determine whether laminin promoted primary process formation and branching to form secondary processes by immature oligodendrocytes differentiated for 4 or 12 hours on PDL or laminin (Fig. 3-2B). The mean number of primary processes per cell was slightly increased in cells differentiated 4 hours on laminin (Fig. 3-2C: 2.2 ± 0.1 on Lm vs. 1.9 ± 0.1 on PDL, n = 3, P = 0.001); however, there was no significant difference in the mean number of secondary processes in cells differentiated 4 hours on PDL or laminin (Fig. 3-2D: 2.3 ± 0.1 on Lm vs. 2.3 ± 0.1 on PDL, n = 3, P = 0.815). In cells differentiated on laminin for 12 hours, however, both the mean number of primary processes (Fig. 3-2E: 2.7 ± 0.1 on Lm vs. 2.2 ± 0.1 on PDL, n = 3, P = < 0.001) and secondary processes (Fig. 3-2F: 4.3 ± 0.2 on Lm vs. 3.5 ± 0.2 on PDL, n = 3, P = 0.008) were increased. These data suggest that process outgrowth and branching by newly differentiated oligodendrocytes is potentiated in response to laminin.

Process branching complexity is increased in response to laminin

Efficient myelination requires that an oligodendrocyte contacts and ensheathes as many as 50 axons, which is dependent on higher-order process branching (Richter-Landsberg 2008). Laminin has previously been shown to increase MBP positive membrane area *in vitro* (Buttery and ffrench-Constant 1999), which involves the elaboration of numerous process branches in order to support the extensive myelin membrane. I therefore investigated whether laminin potentiated higher-order process branching complexity in pre-myelinating oligodendrocytes. Sholl analysis, illustrated in Fig. 3-3A, was used to evaluate process branching complexity. Oligodendrocytes were differentiated for 24 hours on PDL or laminin (Fig. 3-3B), and the mean number of intersections made at a distance of 10 microns from the origin was similar (Fig. 3-3C: 5.8 ± 0.4 on Lm, vs. 4.9 ± 0.4 on PDL, n = 3, P = 0.107). However, the mean number of intersections made at distances of 20, 30 and 40 microns from the origin was significantly increased when cells were differentiated on laminin for 24 hours (Fig. 3-3C; at 20 μm: 8.2 ± 0.7 on Lm, vs. 6.3 ± 0.8 on PDL, P = 0.013; at 30 μm: 8.0 ± 0.8 on Lm, vs. 5.9 ± 0.7 on PDL, P = 0.009; at 40 μm: 6.5 ± 0.8 on Lm vs. 4.6 ± 0.6 on PDL, P = 0.014; n = 3). Differences in the intersections made at the furthest distance evaluated, 50 microns, however, were variable and therefore not statistically significant, when cells were differentiated for 24 hours on PDL or laminin (Fig. 3-3C: 5.5 ± 0.8 on Lm, vs. 3.8 ± 0.6 on PDL, P = 0.106, n = 3).

Additionally, I evaluated process branching in more mature oligodendrocytes in F-actin positive processes and associated branches of cells differentiated for 72 hours on PDL or laminin (Fig. 3-3D). Here, the mean number of intersections made at a distance of 10 microns from the origin was significantly increased when cells were differentiated on laminin for 72 hours (Fig. 3-3E: 11.8 ± 0.8 on Lm, vs. 9.3 ± 0.7 on PDL, P = 0.014, n = 3). However, while there was a

modest increase in the intersections made at distances of 20, 30, 40 and 50 microns from the origin in response to laminin, the differences were not statistically significant when cells were differentiated on either laminin or PDL (Fig. 3-3E; at 20 μm: 24.7 ± 2.0 on Lm vs. 21.2 ± 1.5 on PDL, P = 0.231; at 30 μm: 25.5 ± 2.5 on Lm vs. 21.7 ± 1.8 on PDL, P = 0.318; at 40 μm: 20.7 ± 2.0 on Lm vs. 17.6 ± 2.2 on PDL, P = 0.183; at 50 μm: 14.1 ± 1.7 on Lm vs. 12.3 ± 1.6 on PDL, P = 0.362; n = 3). Together, these data suggest that laminin positively regulates process branching complexity in pre-myelinating oligodendrocytes; however, at later time points branching complexity begins to "catch up" on non-laminin substrates.

Dystroglycan is localized in processes, process branch points, and in focal adhesions

Dystroglycan has previously been shown by our group to be expressed by differentiating oligodendrocytes both *in vitro* and *in vivo* (Colognato *et al.* 2007); however, dystroglycan localization in oligodendroglial processes has not been fully evaluated. Therefore, I used a live-labeling technique to visualize dystroglycan immunoreactivity in newly-formed oligodendrocytes differentiated for 4 or 12 hours, and in more mature pre-myelinating oligodendrocytes differentiated for 24 or 72 hours; oligodendrocytes were co-stained to visualize F-actin. In newly-formed oligodendrocytes differentiated for 4 hours, dystroglycan was expressed cortically around cell bodies, as well as at the leading edge of extending processes (Fig. 3-4A). Dystroglycan expression was also observed at branch points in pre-myelinating oligodendrocytes differentiated for 24 or 72 hours (Fig. 3-4A, lower insets). These observations suggest that dystroglycan is positioned at sites where it may contribute to cytoskeletal reorganization including primary process formation, outgrowth, and branching.

Focal adhesion kinase (FAK) has been shown to regulate process outgrowth and branching, and has been found to coprecipitate with dystroglycan in brain synaptosomes (Cavaldesi *et al.* 1999; Hoshina *et al.*2007; Lafrenaye *et al.* 2010). Therefore, I next asked whether dystroglycan associated with FAK in oligodendrocytes. First, via immunostaining I found that dystroglycan and FAK partially overlap in punctate structures resembling focal adhesion sites (Fig. 3-4B). To further investigate potential dystroglycan-FAK associations, I performed coimmunoprecipitation assays and found that β-dystroglycan antibodies coprecipitate FAK in lysates obtained from oligodendrocytes differentiated for two days (Fig. 3-4C). Conversely, I also found that antibodies directed against FAK coprecipitate β-dystroglycan (Fig. 3-4C). I therefore conclude that dystroglycan is located in processes and at branch points, often in focal adhesion type structures, thus is well placed to mediate cytoskeletal reorganization during process outgrowth and branching.

Dystroglycan blocking antibody decreases filopodia formation and length

Dystroglycan has previously been reported to localize Rho GTPase activation near the cell membrane in Swiss 3T3 and REF52 cell lines, and thereby promote filopodia formation (Batchelor *et al.* 2007). I therefore sought to determine whether dystroglycan localizes in filopodia formed in newly-differentiated oligodendrocytes (12 hours in differentiation medium). Using dystroglycan immunocytochemistry in combination with F-actin labeling, I found that dystroglycan was located in punctate structures at the tips of filopodia, as well as near the base of some filopodia forming near the leading edges of secondary branch points (Fig. 3-5A: *Dystroglycan Live Label*, inset). Additionally, I used a dystroglycan-expressing lentiviral construct (DAG1-GFP) to further evaluate and confirm dystroglycan localization in filopodia. I

observed DAG1-GFP expression at the tips of filopodia, in filopodia at the leading edge of processes, and in filopodia protruding from the cell body of oligodendrocytes differentiated for 48 hours (Fig. 3-5A: *Dystroglycan GFP Lentivirus*, insets i-iv).

I next asked whether using dystroglycan blocking antibodies (IIH6) to disrupt dystroglycan-laminin interactions in differentiating oligodendrocytes would decrease filopodia formation and length. Filopodia in oligodendrocytes differentiated for 12 hours on laminin in the presence of dystroglycan blocking or control antibodies were visualized by F-actin labeling (Fig. 3-5B). The mean number of filopodia was decreased when oligodendrocytes were differentiated in the presence of dystroglycan blocking antibody (Fig. 3-5C: 53.1 ± 2.4 in control, versus 29.6 ± 1.5 with IIH6, n = 3, P = < 0.001). To control for differences in the number of filopodia formed as a function of the cell area, I normalized the mean number of filopodia to the cell perimeter measured in microns, and found that this relative number of filopodia was also decreased when oligodendrocytes were differentiated with dystroglycan blocking antibody (Fig. 3-5D: 0.225 ± 0.01 in control, versus 0.12 ± 0.01 with IIH6, n=3, P = < 0.001). Additionally, mean filopodia length was significantly decreased when oligodendrocytes were differentiated with dystroglycan blocking antibody (Fig. 3-5E: 2.65 μm ± 0.05 μm in control, versus 2.00 μm ± 0.04 μm with IIH6, n=3, P = < 0.001). Taken together, these data suggest that dystroglycan-laminin interactions promote filopodia formation by newly-formed oligodendrocytes.

Dystroglycan blocking antibody decreases process outgrowth and process branching

I next asked whether disrupting dystroglycan-laminin interactions would attenuate process outgrowth and branching in differentiating oligodendrocytes. Oligodendrocytes were differentiated for 24 or 72 hours on laminin, in the presence of dystroglycan blocking antibody

(IIH6) or control antibody (Fig. 3-6A). In the presence of IIH6 for 24 hours, mean process length was significantly decreased (Fig. 3-6B: 46.3 μm ± 1.2 μm with IIH6, vs. 58.7 μm ± 1.7 μm in control, P = < 0.001, n = 3). Mean process length was also decreased in more mature oligodendrocytes differentiated with IIH6 for 72 hours (Fig. 3-6C: 59.0 μm ± 1.5 μm with IIH6, vs. 71.3 μm ± 2.0 μm in control, P = < 0.001, n = 3).

I also tested whether blocking dystroglycan-laminin interactions with IIH6 decreased primary process formation (Fig. 3-6D). Here, I observed a significant decrease in the mean number of primary processes formed by oligodendrocytes differentiated for 24 hours in the presence of IIH6 (Fig. 3-6E: 4.3 ± 0.1 with IIH6, vs. 5.3 ± 0.2 in control, P = < 0.001, n = 3). Next, I asked whether process branching complexity was affected by blocking dystroglycan receptor interactions. Using Sholl analysis, I observed no substantial differences in the mean numbers of intersections made by oligodendrocytes differentiated on laminin for 24 hours in the presence of IIH6 at 10 and 50 microns from the origin (Fig. 3-6F; at 10 μm: 5.7 ± 0.4 with IIH6 vs. 6.0 ± 0.5 in control, P = 0.964; at 50 μm: 4.3 ± 0.7 with IIH6 vs. 5.2 ± 0.9 in control, P = 0.454; n = 3). I did, however, observe a significant decrease in the mean numbers of intersections made by oligodendrocytes differentiated on laminin for 24 hours in the presence of IIH6 at distances 20, 30 and 40 microns from the origin (Fig. 3-6F; at 20 μm: 7.1 ± 0.6 with IIH6 vs. 10.2 ± 1.0 in control, P = 0.006; at 30 μm: 5.7 ± 0.6 with IIH6 vs. 10.0 ± 1.5 in control, P = 0.008; at 40 μm: 4.8 ± 0.8 with IIH6 vs. 7.0 ± 0.9 in control, P = 0.046; n = 3).

Finally, I asked whether in more mature oligodendrocytes, primary process formation and process branching complexity were affected by blocking dystroglycan-laminin interactions (Fig. 3-6G). The mean number of primary processes was decreased in oligodendrocytes differentiated on laminin for 72 hours in the presence of IIH6 (Fig. 3-6H: 5.2 ± 0.2 with IIH6, vs. 6.3 ± 0.2 in

control, P = < 0.001, n = 3). Again, process branching complexity was not significantly decreased by dystroglycan blocking antibody at a distance of 10 microns from the origin (Fig. 6I: 9.5 ± 0.7 with IIH6 vs. 11.1 ± 0.7 in control, P = 0.070, n = 3). At distances of 20, 30, 40 and 50 microns from the origin, however, I observed a significant decrease in the mean numbers of intersections made by oligodendrocytes differentiated in the presence of IIH6 (Fig. 3-6I: at 20 μm, 14.3 ± 1.0 with IIH6 vs. 22.3 ± 1.7 in control; at 30 μm, 15.4 ± 1.2 with IIH6 vs. 26.1 ± 2.5 in control; at 40 μm, 11.0 ± 1.0 with IIH6 vs. 22.6 ± 2.6 in control; at 50 μm, 7.7 ± 0.8 in with IIH6 vs. 14.0 ± 1.3 in control; P = < 0.001; n = 3). These data suggest that dystroglycan-laminin interactions positively regulate primary process formation and branching complexity in pre-myelinating oligodendrocytes. It should be noted that no changes in oligodendroglial death were observed in the presence of IIH6 (Colognato *et al.*, 2007).

Dystroglycan and β1 integrin blocking antibodies decrease process outgrowth and process branching

I next asked whether dystroglycan and β1-containing integrins (i.e. α6β1 for laminin interactions) cooperate to facilitate process extension during pre-myelinating stages of oligodendrocyte maturation. Oligodendrocytes were therefore differentiated in the presence of dystroglycan (IIH6) and β1 integrin (HA2/5) blocking antibodies, or control antibodies, for 24 and 72 hours (Fig. 3-7A). When differentiated on laminin for 24 hours in the presence of both IIH6 and HA2/5, mean process length was significantly decreased (Fig. 3-7B: 45.7 μm ± 0.9 μm with IIH6 and HA2/5, vs. 59.1 μm ± 1.3 μm in control, P = < 0.001, n=3). Mean process length was also significantly decreased in mature oligodendrocytes differentiated for 72 hours on laminin in the presence of IIH6 and HA2/5 (Fig. 3-7C: 55.5 μm ± 1.2 μm with IIH6 and HA2/5,

vs. 77.6 μm ± 1.6 μm in control, P = < 0.001, n=3). I next asked whether blocking dystroglycan and β1 integrin receptor interactions affected process branching complexity. Oligodendrocytes were differentiated on laminin in the presence of IIH6 and HA2/5 or control antibodies for 24h (Fig. 3-7D) and 72h (Fig. 3-7F). Using Sholl analysis, I observed significant decreases in the mean numbers of intersections made at each radius from the origin measured (Fig. 3-7E; at 10 μm: 6.0 ± 0.3 with IIH6 and HA2/5 vs. 8.7 ± 0.5 in control, P = < 0.001; at 20 μm: 10.0 ± 0.7 with IIH6 and HA2/5 vs. 13.7 ± 1.2 in control, P = 0.021; at 30 μm: 10.0 ± 0.7 with IIH6 and HA2/5 vs. 15.8 ± 1.4 in control, P = < 0.001; at 40 μm: 7.5 ± 0.5 with IIH6 and HA2/5 vs. 12.1 ± 1.4 in control, P = 0.010; at 50 μm: 5.3 ± 0.5 with IIH6 and HA2/5 vs. 8.9 ± 1.2 in control, P = 0.040; n=3). When oligodendrocytes were differentiated for 72 hours in the presence of IIH6 and HA2/5, I also observed significant decreases in the mean numbers of intersections made at 30, 40 and 50 microns from the origin (Fig. 3-7G; at 30 μm: 17.8 ± 1.8 with IIH6 and HA2/5 vs. 30.2 ± 2.7 in control, P = < 0.001; at 40 μm: 13.0 ± 1.4 with IIH6 and HA2/5 vs. 26.6 ± 2.4 in control, P = < 0.001; at 50 μm: 7.7 ± 0.8 with IIH6 and HA2/5 vs. 17.2 ± 1.4 in control, P = < 0.001; n=3). I did not, however, observe substantial decreases in the mean numbers of intersections made at 10 or 20 microns from the origin (Fig. 3-7G; at 10 μm: 9.6 ± 0.6 with IIH6 and HA2/5 vs. 10.2 ± 0.6 in control, P = 0.552; at 20 μm: 17.6 ± 1.4 with IIH6 and HA2/5 vs. 21.1 ± 1.5 in control, P = 0.093; n=3). Given that blockade of both receptor types (Fig. 3-7) has a more pronounced effect than the sole blockade of dystroglycan (Figs. 3-5,3-6), this suggests that dystroglycan-laminin and β1 integrin-laminin interactions both positively regulate process outgrowth and branching complexity, and are not functionally redundant.

Dystroglycan siRNA decreases process outgrowth, process formation and process branching

In order to more fully assess the requirement for dystroglycan in the regulation of process dynamics, I determined whether the absence of dystroglycan affected process formation, outgrowth, and branching during early oligodendrocyte maturation. Oligodendrocyte progenitor cells (OPCs) transfected with either siRNA directed against dystroglycan (DG siRNA) or control siRNA (Ctrl siRNA), were maintained for 48 hours as OPCs (to allow sufficient time for knockdown), followed by trypsinization and replating on laminin-coated wells in differentiation medium. To ensure adequate depletion of dystroglycan protein, lysates from oligodendrocytes differentiated for 24 or 72 hours were resolved by SDS PAGE and immunoblotted with antibodies against β-dystroglycan (β-DG) (Fig. 3-8A). Oligodendrocytes were transfected with either DG siRNA or Ctrl siRNA and differentiated for 24 or 72 hours on laminin, followed by F-actin labeling to visualize processes (Fig. 3-8B). Depletion of dystroglycan significantly decreased process length in oligodendrocytes differentiated on laminin for 24 hours (Fig. 3-8C: 41.3 μm ± 1.1 μm with DG siRNA, vs. 55.6 μm ± 1.5 μm with ctrl siRNA, P = < 0.001, n = 3); and, in mature oligodendrocytes differentiated for 72 hours (Fig. 3-8D: 69.7 μm ± 2.3 μm with DG siRNA vs. 89.0 μm ± 2.3 μm with ctrl siRNA, P = < 0.001, n = 3). I next evaluated primary process formation and branching in oligodendrocytes with reduced dystroglycan expression (Fig. 3-8E). After 24 hours of differentiation on laminin, the mean numbers of both primary and secondary processes was significantly decreased in oligodendrocytes transfected with siRNA targeting dystroglycan (Fig. 3-8F: 4.0 ± 0.2 with DG siRNA vs. 5.4 ± 0.2 with ctrl siRNA, P = < 0.001, n = 3; Fig. 3-8G: 4.6 ± 0.3 with DG siRNA vs. 8.7 ± 0.4 with ctrl siRNA, P = < 0.001, n =3). In more mature oligodendrocytes differentiated for 72 hours on laminin, the mean number

of primary processes was significantly decreased in oligodendrocytes transfected with dystroglycan siRNA (Fig. 3-8H: 4.7 ± 0.2 with DG siRNA vs. 6.1 ± 0.2 with ctrl siRNA, P = < 0.001, n = 3).

Finally, Sholl analysis was performed to address whether dystroglycan influences process complexity. In oligodendrocytes that were depleted of dystroglycan, the mean numbers of intersections at all distances measured (10, 20, 30, 40 and 50 microns from the origin) were significantly decreased following differentiation on laminin for 72 hours (Fig. 3-8I; at 10 μm: 5.2 ± 0.3 with DG siRNA vs. 7.0 ± 0.4 with ctrl siRNA, P = 0.002; at 20 μm: 7.2 ± 0.5 with DG siRNA vs. 12.5 ± 0.9 with ctrl siRNA, P = < 0.001; at 30 μm: 7.3 ± 0.4 with DG siRNA vs. 14.4 ± 1.0 with ctrl siRNA, P = < 0.001; at 40 μm: 4.5 ± 0.4 with DG siRNA vs. 13.1 ± 1.0 with ctrl siRNA, P = < 0.001; at 50 μm: 3.1 ± 0.4 with DG siRNA vs. 9.7 ± 0.8 with ctrl siRNA, P = < 0.001; n = 3). In summary, these data suggest that dystroglycan normally regulates the cytoskeletal dynamics associated with oligodendroglial process formation, extension, and, particularly, process branching.

DISCUSSION

The morphological transformation of oligodendrocytes requires coordinated reorganization of the cytoskeleton, in turn involving numerous intracellular proteins that affect the sequential polymerization of actin and microtubules in order to extend and branch processes toward multiple target axons (Lunn *et al.* 1997; Song *et al.* 2001; Rumsby *et al.* 2003). Here I report that in addition to promoting the expansion of myelin membrane (Buttery and ffrench-

Constant 1999), laminin promotes the formation and extension of oligodendroglial filopodia; and, that the ECM receptor, dystroglycan, is necessary for laminin's ability to enhance oligodendroglial filopodia formation, processes extension, and process branching (Eyermann *et al.* 2012).

Transcribed from a single gene, *DAG1*, dystroglycan is translated as a propeptide and proteolytically processed into α/β subunits. α-Dystroglycan is an extracellular glycoprotein, but remains non-covalently associated with transmembrane β-dystroglycan. α-Dystroglycan contains a glycosylated central mucin domain, which binds with high affinity to LG 4/5 globular domains of laminin and other LG-containing ECM proteins e.g. agrin, neurexin. As a component of the dystrophin glycoprotein complex (DGC), muscle dystroglycan provides a structural bridge between the actin cytoskeleton, via dystrophin binding to the C-terminus of β-dystroglycan, and the ECM, via laminin binding to α-dystroglycan (Barresi *et al.* 2006). Mutations in dystroglycan itself (primary dystroglycanopathy; Hara *et al.* 2011), or in known or putative glycosyltransferases that modify α-dystroglycan (secondary dystroglycanopathies) show many similarities to MDC1A (Clement *et al.* 2008). In mice, brain-specific deletion of dystroglycan recapitulates many of the same abnormalities associated with congenital muscular dystrophy and dystroglycanopathies. For example, aberrant neuronal ectopias, discontinuities of the pial basement membrane, and blunted hippocampal long-term potentiation - also noted in *Large*^{myd} mice with a mutation of *Large* - have been reported in dystroglycan mutant mice (Moore *et al.* 2002; Satz, *et al.* 2008; Satz *et al.* 2010). To date it remains unclear if oligodendroglial dysfunction is associated with dystroglycanopathies, however, preliminary evidence suggests that brain- or oligodendrocyte-specific loss of dystroglycan in mice delays CNS myelination (F.M., C.E., and H.C., unpublished observations).

Interactions between laminins and laminin receptors have long been implicated in PNS myelination. Loss of laminin-2 from the Schwann cell basal lamina leads to peripheral dysmyelination (Matsumura *et al.* 1997), while α6β1 integrin and α6β4 integrin inactivation results in impaired axonal sorting, or long-term destabilization of the myelin sheath, respectively (Feltri *et al.* 2002; Nodari *et al.* 2008). The combined deletion of α6β4 integrin and dystroglycan results in major myelin folding abnormalities (Nodari *et al.* 2008); and interestingly, a new report shows that combined α6β1 integrin and dystroglycan deletion not only phenocopies the loss of laminin-2, but that each receptor has distinct sequential functions during radial sorting (Berti *et al.* 2011). Schwann cell dystroglycan has been further shown to affect sodium channel clustering at Nodes of Ranvier, Schwann cell process outgrowth, and nodal structure including microvilli organization and elongation of internodes (Saito *et al.* 2003; Occhi *et al.* 2005; Court *et al.* 2009). Thus, many of the phenotypes in dystroglycan-null Schwann cells suggest that dystroglycan may regulate Schwann cell cytoskeletal remodeling during myelination.

Filopodia have been suggested to function primarily as 'antennae' in a variety of cell types that sense and respond to cues in the local microenvironment (Mattila *et al.* 2008), and are thought to have a role in the morphological differentiation of oligodendrocytes by forming the initial protrusions from the cell body which coalesce into a lamellipodium at the leading edge of a growing process (Bauer *et al.* 2009). Process outgrowth by oligodendrocytes has often been compared to neurite outgrowth, which in the case of cortical neurons, is dependent on filopodia formation and promoted in a directed orientation by laminin (Dent *et al.* 2007; Jang *et al.* 2010). Here I have shown for the first time that both filopodia formation and filopodia length are increased in newly-formed oligodendrocytes differentiated on laminin substrate (Fig. 3-1:A-D) (Eyermann *et al.* 2012). Laminin is expressed in pre-myelinated axon tracts of the CNS

(Colognato *et al.* 2002), thus it is possible that filopodia formation by oligodendrocytes in response to laminin may serve as a permissive guidance cue promoting process outgrowth along target axons. I found that dystroglycan is expressed in filopodia at the leading edge of processes and near emerging process branch points (Fig. 3-5A); and, dystroglycan blocking antibodies decrease both filopodia formation and filopodia length in cells grown on laminin (Fig. 3-5:B-E) (Eyermann *et al.* 2012). Dystroglycan blocking antibodies did not, however, cause a significant difference in filopodia formation or length when oligodendrocytes were differentiated on PDL. These data suggest that dystroglycan's ability to interact with ECM proteins may help to promote, or stabilize, filopodial extension, perhaps, due to the existence of an oligodendroglial dystroglycan complex that is recruited in the presence of laminin (Eyermann *et al.* 2012). Indeed, β-dystroglycan can interact directly with F-actin, while dystroglycan over-expression promotes actin re-organization and filopodia formation (Chen *et al.* 2003). Ezrin, an ezrin-radixin-moesin (ERM) family protein that functions as a scaffold linking actin to the cell membrane, has been shown to interact with the juxtamembrane domain of β-dystroglycan, and thus recruit Dbl, a guanine exchange factor (GEF) for the Rho GTPase Cdc42, into a complex near the cell membrane to stimulate filopodia formation (Batchelor *et al.* 2007; Spence *et al.* 2004). Thus, by blocking dystroglycan receptor interactions, the recruitment of cytoskeletal-associated proteins to dystroglycan may be decreased.

I found that dystroglycan was expressed in puncta along the length of extending processes, at the leading edge, and in branch points, suggesting that dystroglycan may be positioned to affect process outgrowth and branching (Fig. 3-4A) (Eyermann *et al.* 2012). Process length, process number, and process branching complexity were significantly decreased when laminin-dystroglycan interactions were perturbed with dystroglycan blocking antibodies

(Fig. 3-6:A-I) (Eyermann *et al.* 2012). Since oligodendrocytes derived from mice in which β1 integrins had been deleted from the CNS also exhibit decreased process outgrowth (Barros *et al.* 2009), I assessed the contribution of β1 integrin during pre-myelinating stages of process outgrowth in double-blocking experiments with antibodies to perturb laminin interactions with both dystroglycan and a6β1 integrin (Fig. 3-7:A-G). I was surprised to find that branching complexity and process length was, while somewhat more affected, not substantially more affected (with the exception of a more drastic decrease in length at 72 hours), when oligodendrocytes were differentiated in the presence of both blocking antibodies in contrast to dystroglycan blocking antibodies alone (Fig. 3-7:A-G) (Eyermann *et al.* 2012). It should be noted that for continuity throughout our Sholl experiments, only cells with at least one process 50μm in length were analyzed for branching complexity, and only a small proportion of oligodendrocytes met these requirements in the presence of both blocking antibodies (data not shown). Out data may, therefore, reflect the ability to a small subset of oligodendrocytes to overcome the disruption of all laminin-receptor interactions. Along these lines, it has been suggested that dystroglycan and β1 integrin competition for binding with laminin reflects some of the differences observed when β1 integrin function has been compromised in vivo (O'Meara *et al.* 2010).

Finally, I also found that process length, process formation, and process branching complexity were significantly decreased when oligodendrocytes were depleted of dystroglycan via siRNA (Fig. 3-8:A-I), with process branching being particularly affected (Fig. 3-8:G,I) (Eyermann *et al.* 2012). When oligodendrocytes were differentiated on PDL, dystroglycan blocking or depletion did not result in significant changes in process formation, outgrowth, or branching (data not shown) (Eyermann *et al.* 2012). The more pronounced reduction in process

complexity that was observed in the presence of dystroglycan siRNA, compared to the reduction seen with dystroglycan blocking antibodies, may reflect the fact that dystroglycan loss interferes with integrin association with signaling adaptors, thus enabling a more complete shut down of adhesion-based signals (as compared to using blocking antibodies that solely perturb extracellular interactions). In epithelial cells for example, disruption of endogenous laminin-dystroglycan interactions can disrupt α6β1 integrin-mediated activation of ERK (Ferletta *et al.* 2003), and, laminin engagement by dystroglycan can decrease the interaction between β1 integrin and laminin (Driss *et al.* 2006).

Focal adhesion kinase (FAK), a common interacting signaling molecule for both β1 integrin and dystroglycan, is found in ECM-cell adhesion sites and integrates signals downstream of integrins and growth factors affecting cell shape, adhesion, and motility (Mitra *et al.* 2005). Dystroglycan has been reported to interact with FAK in brain synaptosomes (Cavaldesi *et al.* 1999), and, more recently it was demonstrated for the first time that β-dystroglycan localizes in focal adhesions (Thompson *et al.* 2010). Here I report that dystroglycan partially co-localizes with FAK in oligodendroglial processes (Fig. 3-4B), and can be coimmunoprecipitated together (Fig. 3-4C), indicating that dystroglycan and FAK may be associated in focal adhesions (Eyermann *et al.* 2012). A role for FAK in regulating process outgrowth has been shown to occur in a Fyn-dependent manner in the CG4 oligodendrocyte-like cell line (Hoshina *et al.* 2007). More recently it was reported that network expansion (a measure of process branching complexity) was decreased in oligodendrocytes depleted of FAK via siRNA, specifically in cells in contact with laminin but not fibronectin (Lafrenaye and Fuss 2010). Interestingly, it has been reported that mice with conditional loss of FAK have cortical abnormalities resembling those associated with dystroglycanopathies (Beggs *et al.* 2003). In

addition, decreased numbers of myelinated fibers and primary processes have been observed via ultrastructural analysis of optic nerve in an inducible oligodendrocyte-specific $FAK^{-/-}$ mouse at the onset of myelination (Forrest *et al.* 2009), while CNP-Cre mediated deletion of FAK prior to myelination resulted in increased threshold for myelination favoring larger diameter axons in optic nerve (Camara *et al.* 2009). The failure to extend multiple processes that might target more small caliber axons was proposed in a model by Camara *et al.* to explain these results, and it is tempting to speculate whether loss of dystroglycan-FAK interactions in focal adhesions contributes to this.

Based on the findings in this study, I propose a model in which laminin can potentiate filopodia formation, process outgrowth, and branching at least in part by interacting with dystroglycan during several stages of oligodendrocyte differentiation (Fig. 3-9) (Eyermann *et al.* 2012). During initial myelination events, therefore, it may be that oligodendrocyte processes that make contacts with laminin-associated axon tracts have a selective advantage in terms of process growth and branching. Given that oligodendrocyte progenitor cells express relatively low levels of dystroglycan (Colognato *et al.* 2007), it may be that increased dystroglycan expression in differentiating oligodendrocytes helps to "jump start" the ability of oligodendroglia to begin the myelination process itself. Future studies to address these and other questions would further expand our knowledge regarding the potential molecular mechanisms that underlie the myelination defects associated with laminin deficits.

Figure 3-1

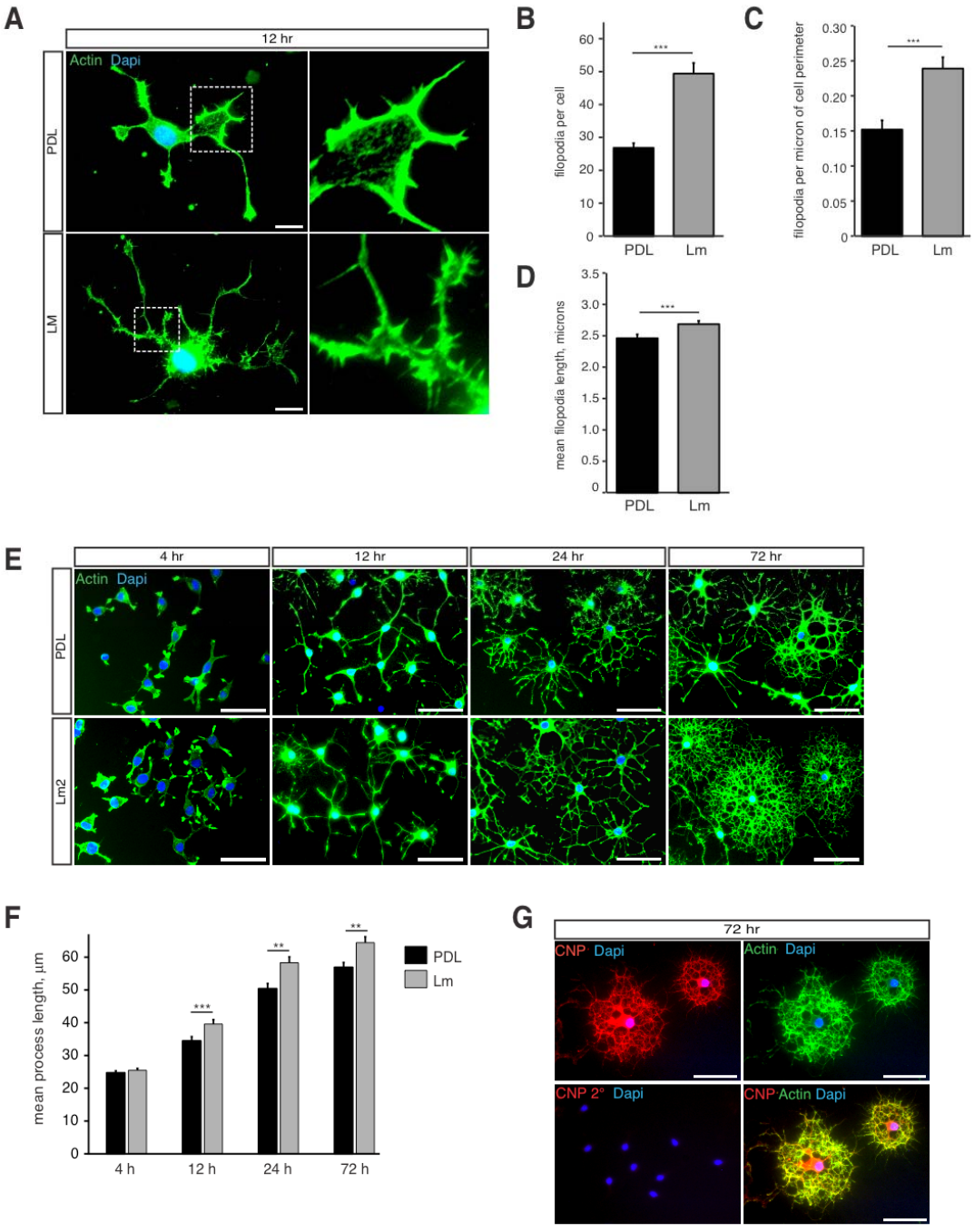
A
12 hr
Actin Dapi
PDL
LM
B
filopodia per cell
***
PDL
Lm
C
filopodia per micron of cell perimeter
***
PDL
Lm
D
mean filopodia length, microns
***
PDL
Lm
E
4 hr
12 hr
24 hr
72 hr
Actin Dapi
PDL
Lm2
F
mean process length, µm
PDL
Lm
4 h
12 h
24 h
72 h
G
72 hr
CNP Dapi
Actin Dapi
CNP 2° Dapi
CNP Actin Dapi

Figure 3-1. Process outgrowth and filopodia formation are increased in response to laminin. Oligodendrocyte progenitor cells (OPCs) were differentiated for 4, 12, 24 or 72 hours on poly-D-lysine (PDL) or laminin (Lm) substrates. **A)** Representative micrographs of newly-formed oligodendrocytes (OLs) differentiated for 12 hours depict F-actin (green) and DAPI for nuclei (blue). Scale bars = 10 μm. Insets show an increase in the number of filopodia formed in an OL when differentiated on Lm in comparison to PDL. **B)** Bar graph depicting the mean (± SEM) number of filopodia formed by OLs differentiated for 12 hours on either PDL or Lm. **C)** Bar graph depicting the relative number of filopodia formed by OLs differentiated for 12 hours on either PDL or Lm and normalized against the perimeter (μm) of each cell. Bars represent the mean (± SEM) filopodia formed per micron of cell perimeter. **D)** Bar graph depicting the mean (± SEM) filopodia length (μm) of OLs differentiated for 12 hours on PDL or Lm. **E)** Representative micrographs of OLs differentiated for 4, 12, 24, and 72 hours on PDL or Lm substrates depict F-actin (green) and DAPI (blue). Process length is increased when OLs are differentiated on Lm relative to OLs differentiated on PDL. Scale bars = 50 μm. **F)** Bar graph depicting the mean (± SEM) process length of OLs differentiated for 4, 12, 24 and 72 hours on PDL and Lm substrates. **G)** Differentiated OLs were analyzed throughout all experiments using OL lineage specific markers co-stained with phalloidin to visualize actin in filopodia and processes. A representative micrograph in which CNP immunoreactivity (red) in combination with phalloidin (green) is shown in an OL differentiated for 72 hours. Scale bars = 50 μm, **P< 0.01; ***P < 0.001.

Figure 3-2

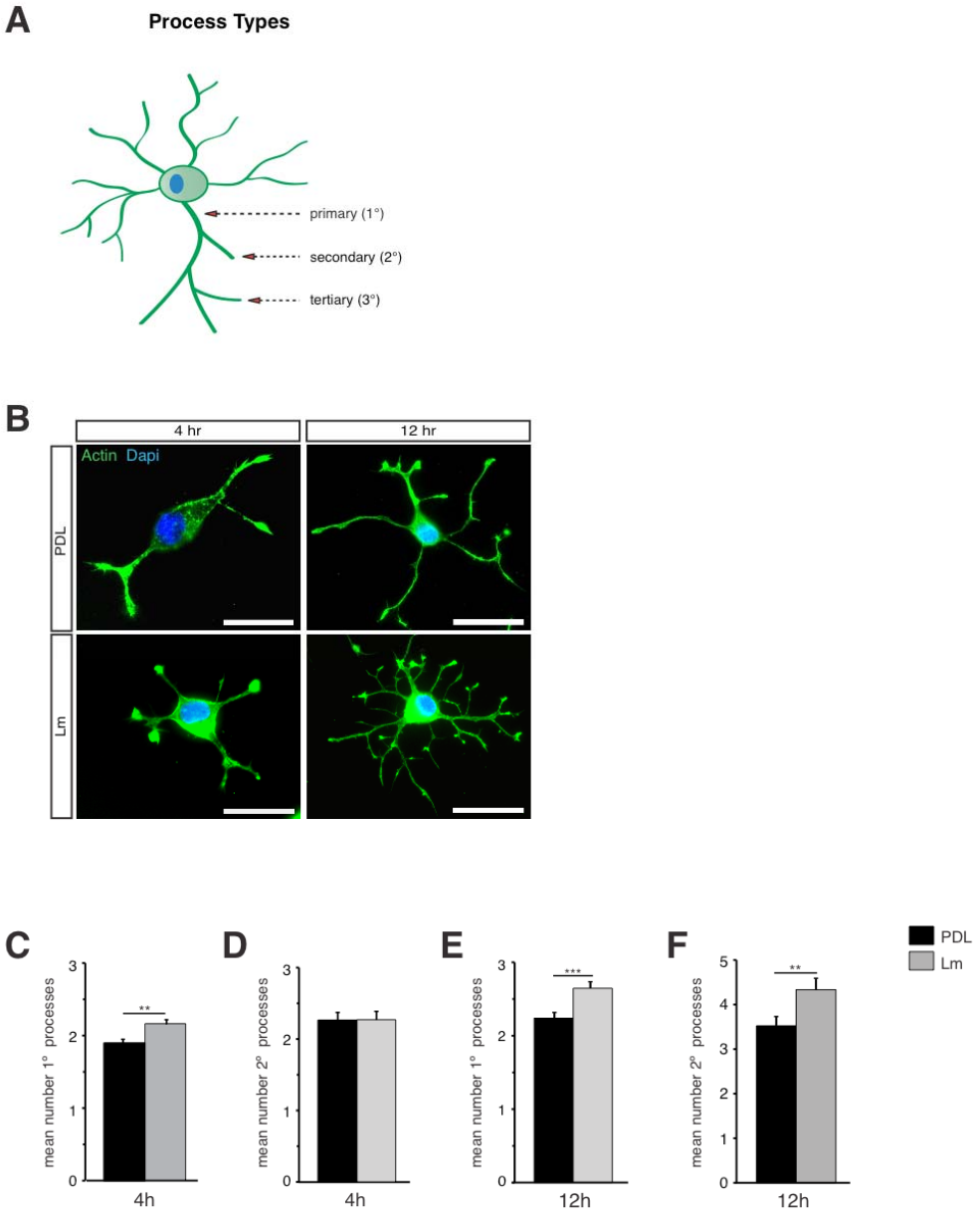
A
Process Types
primary (1°)
secondary (2°)
tertiary (3°)
B
4 hr
12 hr
Actin Dapi
PDL
Lm
C
D
E
F
mean number 1° processes
mean number 2° processes
4h
12h
PDL
Lm

Figure 3-2. Primary process formation and process branching are increased in response to laminin. A) Cartoon depicting the types of processes analyzed in the following experiments. Primary (1°) processes extend from the OL cell body; secondary (2°) processes are extensions from branch points in primary processes; and finally, although not evaluated here, tertiary (3°) processes are formed by extensions beyond 2° process branch points. **B)** Representative micrographs of newly formed OLs differentiated 4 or 12 hours on PDL or Lm substrates depict F-actin (green) and DAPI for nuclei (blue). When compared to OLs differentiated on PDL, OLs differentiated 4 or 12 hours on Lm show increased formation of 1°processes; however, the number of 2° processes formed is increased when OLs are differentiated on Lm for 12 hours, but not 4 hours. Scale bars = 25 μm. **C,E)** Bar graphs depicting the mean (± SEM) number of 1° processes formed by OLs differentiated 4 **(C)** or 12 **(E)** hours on PDL or Lm. **D,F)** Bar graphs depicting the mean (± SEM) number of 2° processes formed by OLs differentiated 4 **(D)** or 12 **(F)** hours on PDL or Lm (**P < 0.01; ***P<0.001).

Figure 3-3

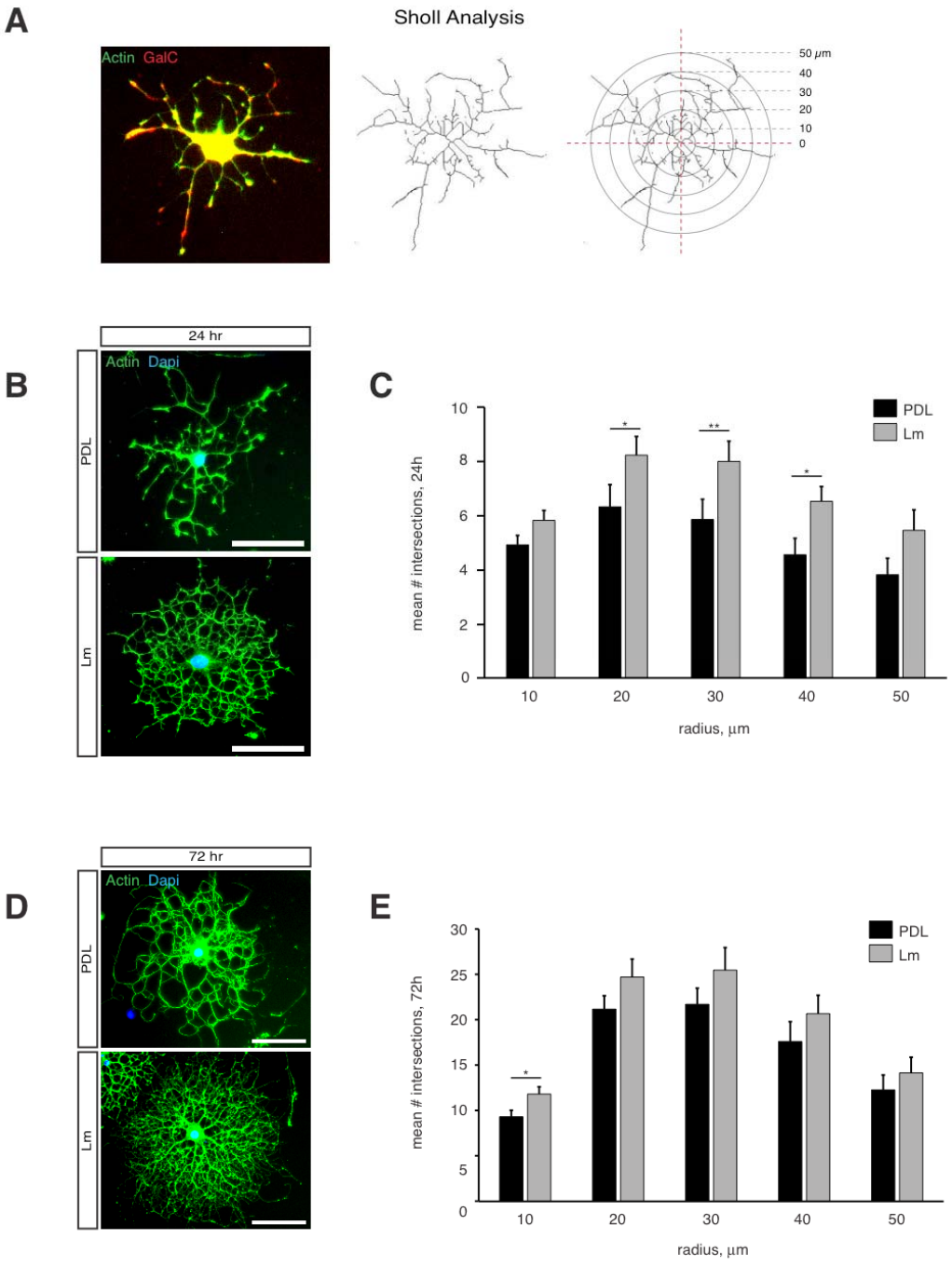
A
Sholl Analysis
Actin GalC
50 μm
40
30
20
10
0
B
24 hr
Actin Dapi
PDL
Lm
C
mean # intersections, 24h
radius, μm
PDL
Lm
D
72 hr
Actin Dapi
PDL
Lm
E
mean # intersections, 72h
radius, μm
PDL
Lm

Figure 3-3. Process branching complexity is increased in response to laminin. A) Cartoon description of Sholl analysis as a measure of OL process branching complexity. *Left panel:* A representative micrograph of a newly-formed OL differentiated 24 hours and visualized using GalC immunoreactivity (red) and phalloidin labeling of F-actin (green). *Middle panel*: Using a Sholl analysis plugin for Image J software, the RGB image is converted to an 8-bit black and white skeletonized image. *Right panel*: A series of concentric circles is superimposed around the center of the cell (origin) and the average number of intersections the skeletonized OL makes at each radius is determined. The following parameters were used: 10 μm starting radius, 50 μm ending radius, 10 μm step size, and 0.1 μm span. **B,D)** Representative micrographs of OLs differentiated for 24 **(B)** or 72 **(D)** hours on PDL or Lm substrates depict F-actin (green) and DAPI for nuclei (blue). OLs differentiated on Lm typically exhibit more complex branching in comparison to OLs differentiated on PDL, particularly at an earlier stage of differentiation (24 hrs). Scale bars = 50 μm. **C,E)** Bar graph depicting the mean (± SEM) number of intersections made by oligodendrocytes differentiated for 24 **(C)** or 72 **(E)** hours on PDL or Lm substrates as evaluated using Sholl analysis (*P <0.05; **P <0.01).

Figure 3-4

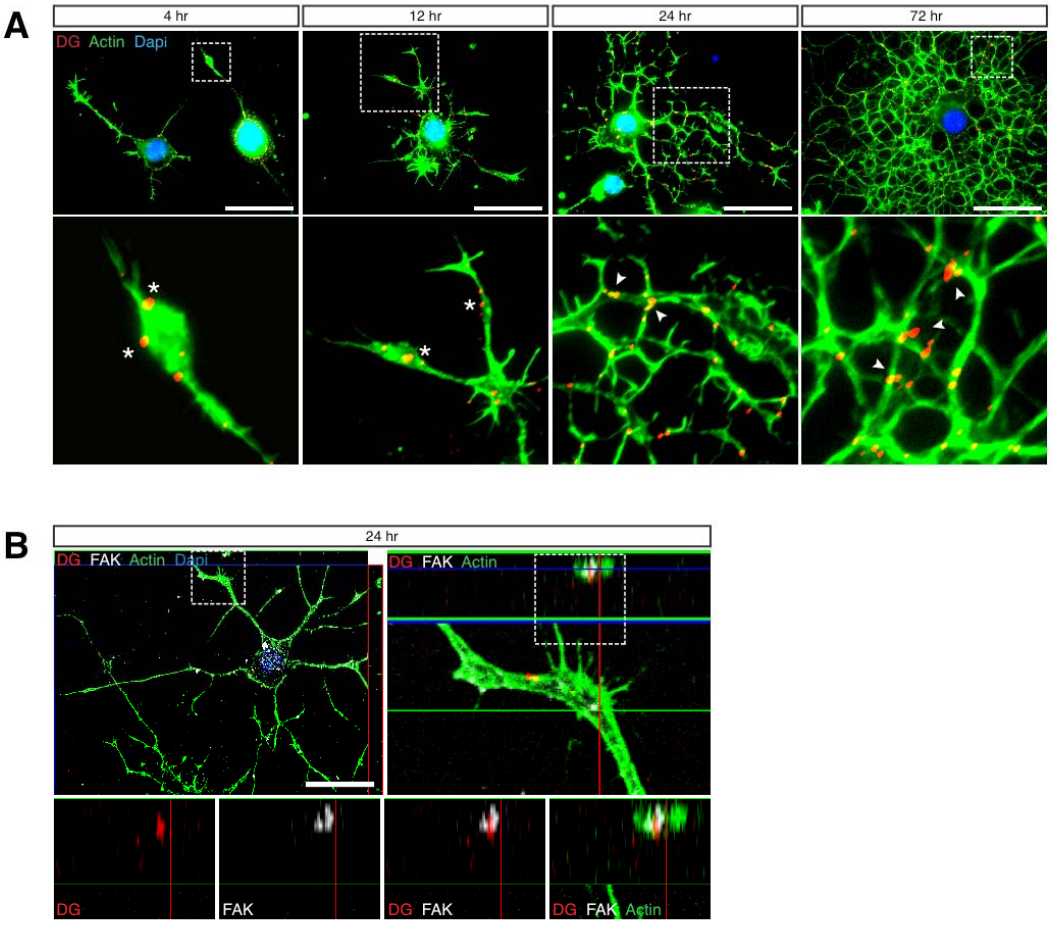
A
4 hr
12 hr
24 hr
72 hr
DG Actin Dapi
B
24 hr
DG FAK Actin Dapi
DG FAK Actin
DG
FAK
DG FAK
DG FAK Actin
C
IP: ß-DG IgG Input
ß-DG 42 kDa
FAK 125 kDa
IP: FAK IgG Input
FAK 125 kDa
ß-DG 42 kDa

Figure 3-4. Dystroglycan is localized in processes, process branch points, and in focal adhesions. A) Representative micrographs of differentiated OLs showing α-dystroglycan (DG) (red) immunoreactivity in combination F-actin labeling (green) and DAPI for nuclei (blue). In newly-formed OLs differentiated for either 4 or 12 hours, DG immunoreactivity is localized at the cortical cell body and in the leading edge of processes (asterisks) as shown in the insets. As OLs differentiate, processes begin to branch and DG immunoreactivity can frequently be found enriched at process branch points (See arrowheads in insets for OLs differentiated 24 or 72 hours). Scale bars = 25 μm**. B)** Representative orthogonal view confocal images showing α-dystroglycan (DG) (red) and FAK phosphotyrosine 397 (FAK) (white) immunoreactivity, in combination with F-actin labeling (green). Inset from the top left panel is shown in the top right panel, and illustrates DG co-localization with FAK in a focal adhesion near the leading edge of a process. Bottom panels show individual channels in the z plane corresponding to the inset in the top right panel. Scale bar = 20 μm. **C)** Lysates obtained from OLs grown for 96 hours on PDL yield immunoprecipitation complexes containing dystroglycan and FAK. Antibodies directed against β-DG coimmunopreciptated FAK (top panel), while in reverse, antibodies directed against FAK coimmunoprecipitated β-DG (bottom panel).

Figure 3-5

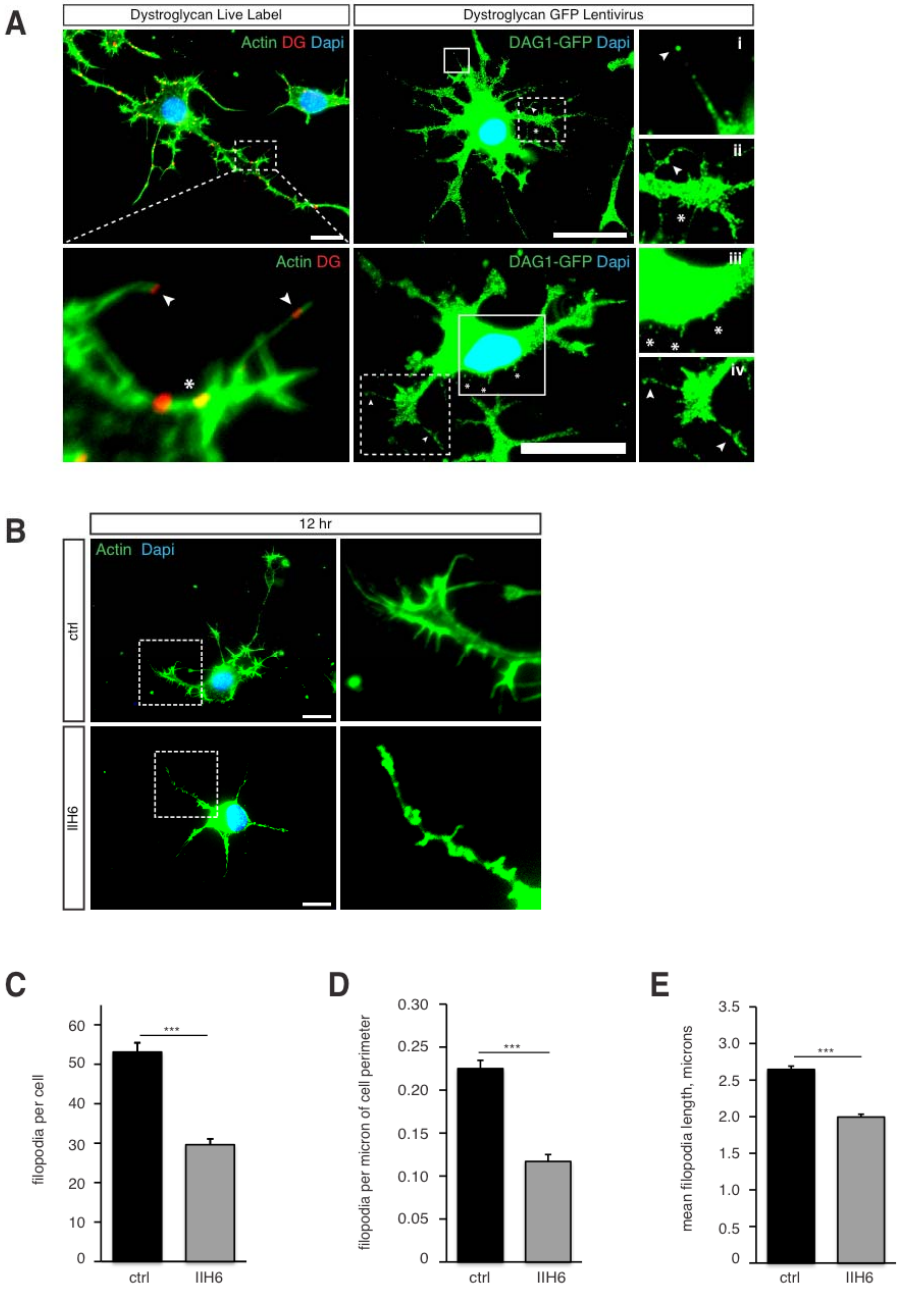
A
Dystroglycan Live Label
Dystroglycan GFP Lentivirus
Actin DG Dapi
DAG1-GFP Dapi
i
ii
Actin DG
DAG1-GFP Dapi
iii
iv
B
12 hr
Actin Dapi
ctrl
IIH6
C
filopodia per cell
***
ctrl
IIH6
D
filopodia per micron of cell perimeter
***
ctrl
IIH6
E
mean filopodia length, microns
***
ctrl
IIH6

Figure 3-5. Dystroglycan blocking antibody decreases filopodia formation and length. A) *Dystroglycan Live Label:* Representative micrograph of an OL differentiated for 12 hours showing α-dystroglycan (αDG) (red) immunoreactivity using a live labeling technique, in combination with F-actin labeling (green) and DAPI for nuclei (blue). Inset below shows αDG immunoreactivity at the tip (arrowheads) and near the base (asterisk) of filopodia. Scale bar = 10 μm. *Dystroglycan GFP Lentivirus:* OPCs were infected with a full length DAG1-GFP lentiviral construct and subsequently differentiated for 48 hours. Representative micrographs depict DAG1-GFP (green) and DAPI (blue). Top Panel: inset **(i)** shows DAG1-GFP localization at the tip of a filopodium (arrowhead), while inset **(ii)** shows DAG1-GFP localization in both longer (arrowhead) and shorter (asterisk) filopodia along a process. Bottom Panel: inset **(iii)** shows DAG1-GFP in filopodia along the cell body (asterisks), while inset **(iv)** shows DAG1-GFP localization in filopodia at the leading edge of a process (arrowheads). Scale bars = 25 μm. **B)** Representative micrographs of an OL differentiated for 12 hours on Lm in the presence of dystroglycan blocking antibody (IIH6) or control antibody (ctrl), visualized using F-actin labeling (green) and DAPI (blue). Both the number of filopodia and filopodia length were decreased when OLs are differentiated in the presence of IIH6. Scale bars = 10 μm. **C)** Bar graph depicting the mean (± SEM) number of filopodia formed by OLs differentiated for 12 hours on Lm in the presence or absence of IIH6. **D)** Bar graph depicting the relative number of filopodia formed by OLs differentiated for 12 hours on Lm in the presence of IIH6 or control antibody and normalized to the perimeter (μm) of each cell. Bars represent the mean (± SEM) filopodia formed per micron of cell perimeter. **E)** Bar graph depicting the mean (± SEM) filopodia length (μm) of OLs differentiated for 12 hours on Lm in the presence of IIH6 or control antibody (*** $P < 0.001$).

Figure 3-6

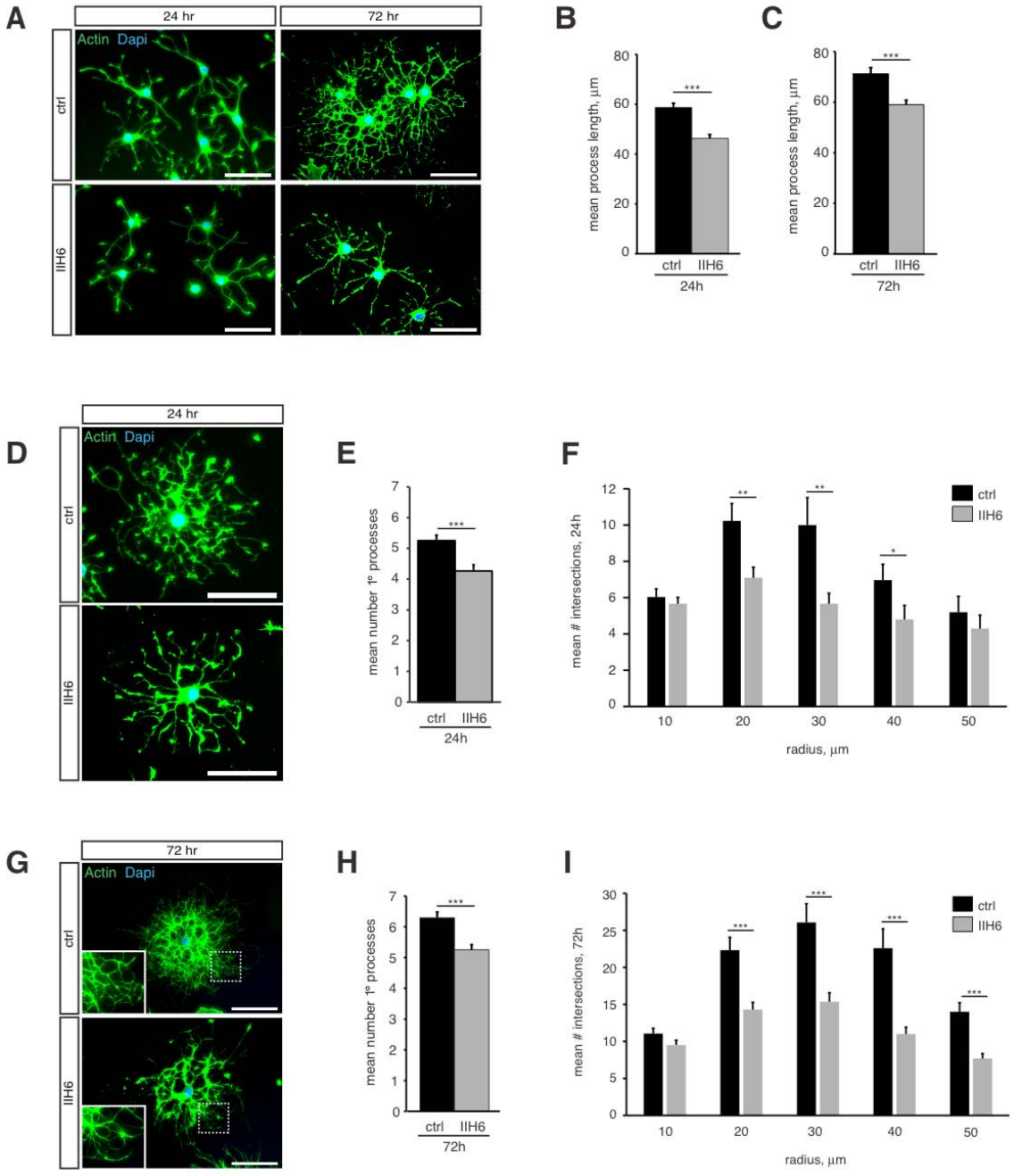
A
24 hr
72 hr
Actin Dapi
ctrl
IIH6
B
mean process length, µm
ctrl IIH6
24h
C
mean process length, µm
ctrl IIH6
72h
D
24 hr
Actin Dapi
ctrl
IIH6
E
mean number 1° processes
ctrl IIH6
24h
F
mean # intersections, 24h
ctrl
IIH6
radius, µm
G
72 hr
Actin Dapi
ctrl
IIH6
H
mean number 1° processes
ctrl IIH6
72h
I
mean # intersections, 72h
ctrl
IIH6
radius, µm

Figure 3-6. Dystroglycan blocking antibody decreases process outgrowth and process branching. A) Representative micrographs of OLs differentiated for 24 and 72 hours on Lm depict F-actin labeling (green) and DAPI for nuclei (blue). At both 24 and 72 hours of differentiation, OL process lengths are decreased in the presence of dystroglycan blocking antibody (IIH6). Scale bars = 50 μm. **B,C)** Bar graphs depicting the mean (± SEM) process length of OLs differentiated on Lm for 24 hours (**B)** or 72 hours (**C)** in the presence of IIH6 or control antibody (ctrl). **D,G)** Representative micrographs of OLs differentiated for 24 **(D)** or 72 **(G)** hours on Lm in the presence of IIH6 or control antibody and visualized with phalloidin (green) and DAPI (blue). Process branching was less complex when OLs were differentiated in the presence of IIH6. Scale bars = 50 μm. **E,H)** Bar graph depicting the mean (± SEM) number of 1° processes formed by OLs differentiated for 24 **(E)** or 72 **(H)** hours on Lm in the presence of IIH6 or control antibody. **F,I)** Bar graph depicting the mean (± SEM) number of intersections made by OLs differentiated for 24 **(F)** or 72 **(I)** hours on Lm in the presence of IIH6 or control antibody as evaluated using Sholl analysis (*P <0.05; **P < 0.01; ***P < 0.001).

Figure 3-7

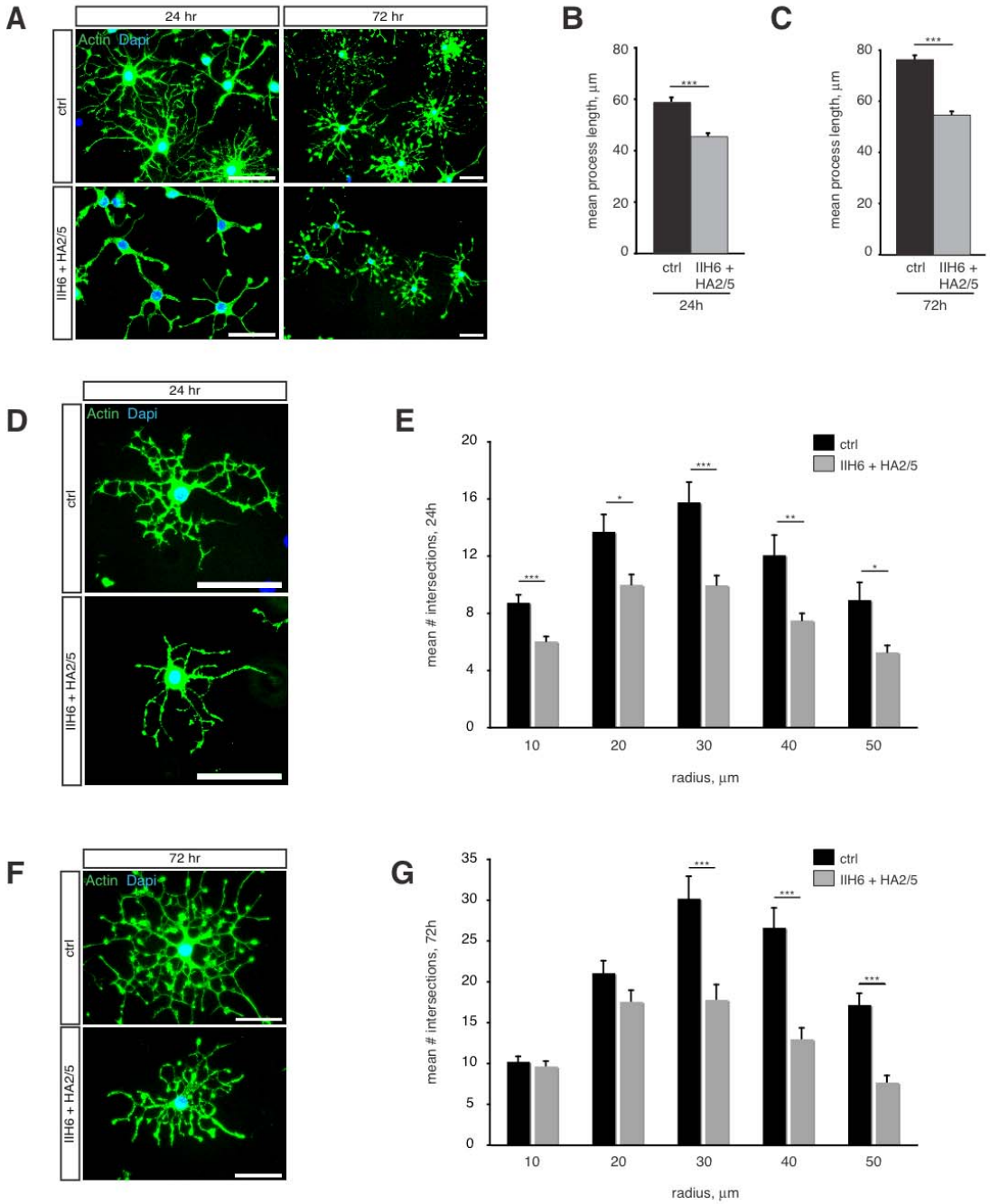
A
24 hr
72 hr
Actin Dapi
ctrl
IIH6 + HA2/5
B
mean process length, µm
***
ctrl
IIH6 + HA2/5
24h
C
mean process length, µm
***
ctrl
IIH6 + HA2/5
72h
D
24 hr
Actin Dapi
ctrl
IIH6 + HA2/5
E
mean # intersections, 24h
ctrl
IIH6 + HA2/5
radius, µm
F
72 hr
Actin Dapi
ctrl
IIH6 + HA2/5
G
mean # intersections, 72h
ctrl
IIH6 + HA2/5
radius, µm

Figure 3-7. Dystroglycan and β1 integrin blocking antibodies decrease process outgrowth and process branching. A) Representative micrographs of OLs differentiated in the presence of dystroglycan (IIH6) and β1 integrin (HA2/5) blocking antibodies, or control antibodies (ctrl), for 24 and 72 hours on Lm depict F-actin labeling (green) and DAPI for nuclei (blue). In the presence of IIH6 and HA2/5, process length is significantly decreased compared to controls at both 24 and 72 hours. Scale bars = 50 μm. **B,C)** Bar graphs depicting the mean (± SEM) process length at 24 **(B)** and 72 **(C)** hours in the presence of IIH6 and HA2/5 or control antibodies. **D,F)** Representative micrographs illustrating process branching complexity of OLs differentiated for 24 **(D)** or 72 **(F)** hours in the presence of IIH6 and HA2/5, or control antibodies, depict F-actin labeling (green) and DAPI (blue). In the presence IIH6 and HA2/5, process branching complexity is significantly decreased at both 24 and 72 hours compared to controls. Scale bars = 50 μm. **E,G)** Bar graph depicting the mean (± SEM) number of intersections made by OLs differentiated for 24h **(E)** or 72h **(G)** in the presence of IIH6 and HA2/5, or control antibodies, as evaluated using Sholl analysis (*P <0.05; **P =0.01; ***P <0.001).

Figure 3-8

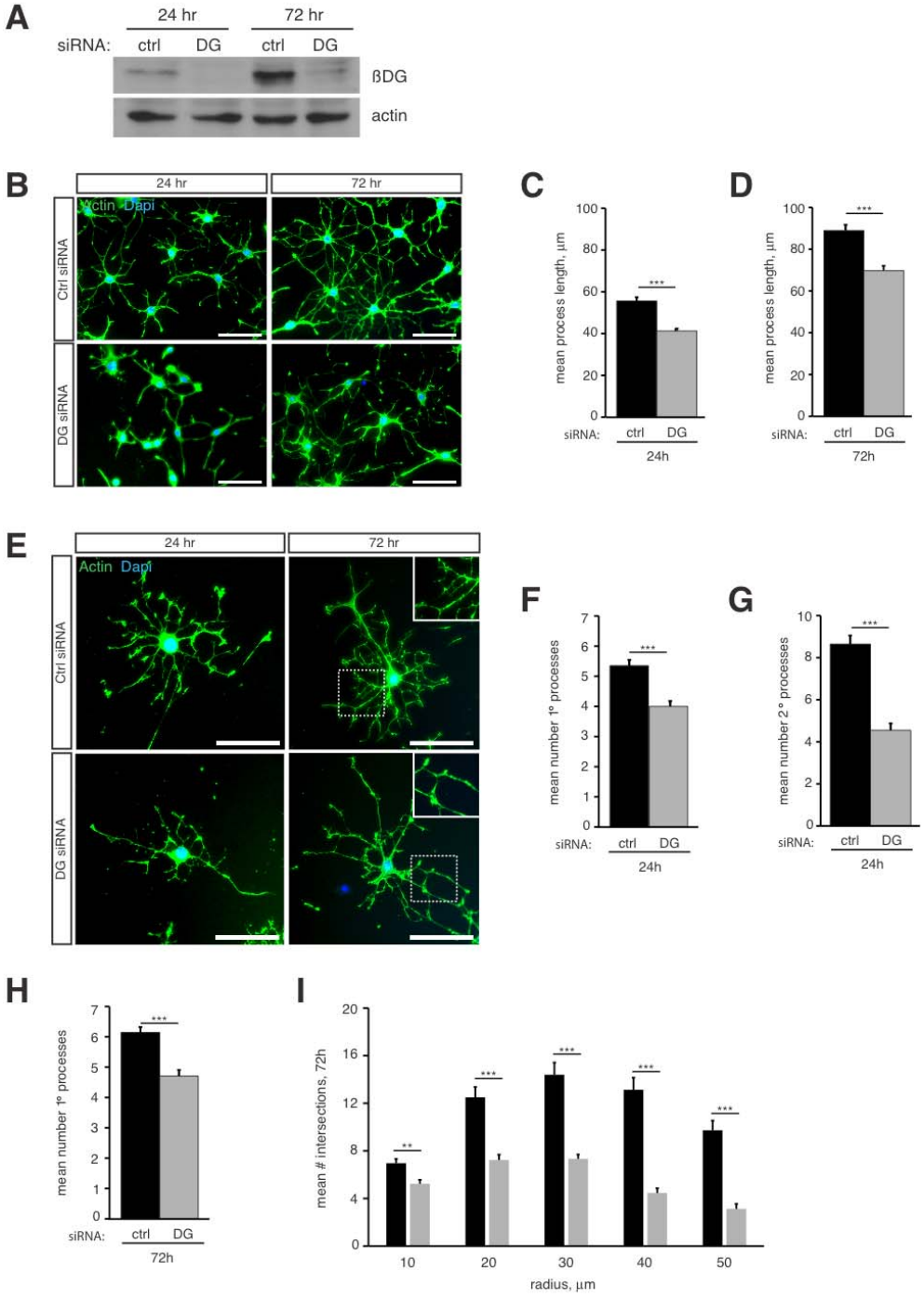
A
24 hr
72 hr
siRNA:
ctrl
DG
ctrl
DG
ßDG
actin
B
24 hr
72 hr
Actin Dapi
Ctrl siRNA
DG siRNA
C
mean process length, µm
siRNA:
ctrl
DG
24h
D
mean process length, µm
siRNA:
ctrl
DG
72h
E
24 hr
72 hr
Actin Dapi
Ctrl siRNA
DG siRNA
F
mean number 1° processes
siRNA:
ctrl
DG
24h
G
mean number 2° processes
siRNA:
ctrl
DG
24h
H
mean number 1° processes
siRNA:
ctrl
DG
72h
I
mean # intersections, 72h
radius, µm

Figure 3-8. Dystroglycan siRNA decreases process outgrowth, process formation and process branching. A) Immunoblot analysis showing β-dystroglycan (βDG) and actin (loading control) in cell lysates of OLs transfected with either control siRNA (ctrl) or dystroglycan siRNA (DG) and differentiated for 24 or 72 hours. **B)** Representative micrographs of OLs transfected with ctrl or DG siRNA and differentiated for 24 or 72 hours on Lm; F-actin labeling (green) and DAPI for nuclei (blue). OLs transfected with DG siRNA exhibited a decrease in process length. Scale bars = 50 μm. **C,D)** Bar graphs depicting the mean (± SEM) process length of OLs transfected with ctrl siRNA or DG siRNA and differentiated on Lm for 24 hours (**C)** or 72 hours (**D**). **E)** Representative micrographs of OLs transfected with ctrl siRNA or DG siRNA and differentiated for 24 or 72 hours on Lm; F-actin labeling (green) and DAPI (blue). DG siRNA resulted in decreased primary process formation and process branching complexity. Insets in images of OLs differentiated for 72 hours illustrate the reduction in process branching. Scale bars = 50 μm. **F,H)** Bar graph depicting the mean (± SEM) number of 1° processes formed by OLs transfected with ctrl siRNA or DG siRNA and differentiated for 24 **(F)** or 72 **(H)** hours on Lm. **G)** Bar graph depicting the mean (± SEM) number of 2° processes formed by OLs transfected with ctrl siRNA or DG siRNA and differentiated for 24 hours on Lm. **I)** Bar graph depicting the mean (± SEM) number of intersections made by OLs transfected with ctrl siRNA or DG siRNA and differentiated on Lm for 72 hours as evaluated using Sholl analysis (**P <0.01 , ***P < 0.001).

Figure 3-9

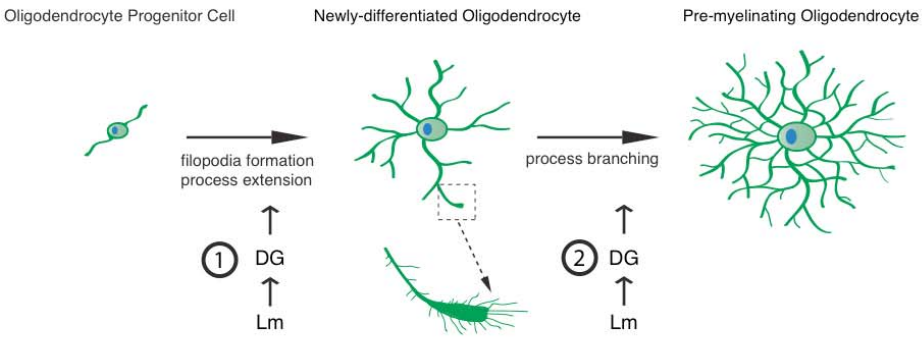
Oligodendrocyte Progenitor Cell
Newly-differentiated Oligodendrocyte
Pre-myelinating Oligodendrocyte
filopodia formation
process extension
process branching
1
DG
Lm
2
DG
Lm

Figure 3-9. Dystroglycan-Lm interactions promote filopodia formation, process outgrowth, and process branching in differentiating oligodendrocytes. (1) Upon cell cycle exit, oligodendrocyte progenitor cells (OPCs) differentiate into newly-formed oligodendrocytes and undergo a dramatic morphological transformation. These immature oligodendrocytes extend numerous processes containing thin filopodial projections found near the leading edge of processes; membrane proteins localized in or near these projections respond to cues within the local extracellular microenvironment. **(2)** Secondary and higher order process branching, associated with more mature pre-myelinating oligodendrocytes, increases the capacity of an oligodendrocyte to contact multiple target axons. Laminin, found within pre-myelinating axon tracts, binds to the oligodendroglial receptor, dystroglycan, and promotes process extension, filopodia formation, and branching by newly-formed oligodendrocytes. Overall, laminin-dystroglycan interactions may help to ensure that individual oligodendrocytes obtain their maximal myelinogenic capacity.

Chapter 4

β-DYSTROGLYCAN LOCALIZES TO THE NUCLEUS IN OLIGODENDROGLIAL CELLS: FUNCTIONAL IMPLICATIONS

INTRODUCTION

Dystroglycan is best known for it central role in skeletal muscle, where as a component of the dystrophin glycoprotein complex (DGC), it forms a structural link between the extracellular matrix and the actin cytoskeleton. Transcribed from a single gene, *DAG1*, dystroglycan is translated as a propetide and cleaved into two subunits (α/β). α-Dystroglycan is an extracellular membrane protein, modified by the addition of O- and N-linked carbohydrates, which facilitate binding to several ECM molecules including laminin and perlecan. α-Dystroglycan remains tightly associated with its transmembrane subunit, β-dystroglycan, through non-covalent interactions at the extracellular surface. The intracellular domain of β-dystroglycan contains binding sites for several proteins including dystrophin, an actin-binding adaptor protein that forms a crucial bridge between the actin cytoskeleton and dystroglycan. Mutations in the gene that encode dystrophin, *DMD*, result in the absence of dystrophin,

disruption of the link between the ECM and the cytoskeleton, and cause the degenerative muscle disease Duchenne muscular dystrophy (DMD).

For many years, much emphasis has been placed on understanding the complex post-translational pathways that modify α-dystroglycan. Mutations in known or putative glycosyltransferases that modify α-dystroglycan result in a decreased affinity for laminin binding. As is the case in DMD with a disturbed linkage between the DGC and the cytoskeleton, the reduced ability of α-dystroglycan to bind laminin in the ECM also disrupts the integrity of the DGC, thus causing several congenital muscular dystrophies including Walker-Warburg syndrome (WWS), muscle-eye-brain disease (MEB), and Fukuyama CMD (FCMD). Together, the disorders associated with dysfunctional dystroglycan are referred to as dystroglycanopathies. However, dystroglycan function is also crucial for normal central nervous system (CNS) development. In addition to peripheral myopathy associated with dystroglycanopathy, brain abnormalities, white matter defects, and severe cognitive disabilities have also been linked to dysregulated dystroglycan function in humans. Cobblestone lissencephaly, neuronal ectopias, cerebellar dysplasia, and ventricular enlargement are often found in patients with these disorders, and are recapitulated in transgenic mouse models with either deleted or dysfunctional dystroglycan. The conditional deletion of deletion of dystroglycan in the entire CNS has severe consequences for normal brain development (Satz *et al.* 2008). Conditional deletion in neurons or astrocytes does not, however, fully recapitulate the phenotype associated with the entire CNS knockout of dystroglycan (Moore *et al.* 2002; Satz *et al.* 2010). White matter defects associated with dystroglycanopathies have not been investigated in mouse models, nor has the oligodendrocyte-specific deletion of dystroglycan been reported to date, although work in our lab is currently underway to address this.

More recently, the view of dystroglycan has begun to shift in which the cytosolic domain of β-dystroglycan has gained more attention as a potential signaling platform, or quite possibly as a signaling molecule in its own right. For example, the discovery that β-dystroglycan could be tyrosine phosphorylated in an adhesion-dependent manner and recruit SH2 domain containing proteins including the Src family kinase Fyn, first opened the door to the idea of dystroglycan as a signaling platform (Russo *et al.* 2000; Isley *et al.* 2001; Sotgia *et al.* 2001). Mitogen activated protein kinase (MAPK) and extracellular signal-regulated protein kinase (ERK) were later reported to interact directly with the juxtamembrane domain of dystroglycan (Spence *et al.* 2004). Finally, cytoskeletal adaptor protein interactions with β-dystroglycan have been shown to recruit Rho GDP/GTP exchange factors (GEFs) for the Rho GTPase Cdc42 and localize Cdc42 activation resulting in cytoskeletal modifications (Batchelor *et al.* 2007).

Recently, it was found that β-dystroglycan could function *independently* from α-dystroglycan forming an alternate complex with modified components of the DGC in the outer membrane of Schwann cells (Court *et al.* 2011). Interestingly, formation of this complex is precipitated by matrix metalloproteinase-2 and -9 cleavage of dystroglycan, forming a truncated 30 kDa isoform of β-dystroglycan, which accumulates in the nerves of dystrophin-deficient (*mdx*) mice (Hnia *et al.* 2006; Court *et al.* 2011). β-dystroglycan has also been found to co-localize with the short dystrophin isoform Dp71 in the cleavage furrow of dividing REF52 and PC12 cells; furthermore, deletion of either β-dystroglycan or Dp71 also attenuates cell cycle progression in REF52, PC12, Hela and Swiss 3T3 cells (Higginson *et al.* 2008; Villarreal-Silva *et al.* 2011). An association between β-dystroglycan and Dp71 has additionally been observed in the nuclear membrane of a number of different cell types including C2C12 muscle, Hela, and PC12 neural cells, where it has been proposed to form a complex in the nuclear lamina and

stabilize the nuclear matrix (Fuentes-Mera *et al.* 2006; Gonzalez-Ramirez *et al.* 2008; Villarreal-Silva *et al.* 2010). Intriguingly, a functional nuclear localization sequence (NLS) has also been identified in β-dystroglycan within the last few years prompting suggestions that dystroglycan may have a signaling role within the nucleus (Oppizzi *et al.* 2008; Lara-Chacon *et al.* 2010). Whether or not this is the case, is currently unknown.

Oligodendrocytes were recently found to express dystroglycan (Colognato *et al.* 2007). Dystroglycan depletion causes delayed oligodendrocyte differentiation and decreases maximal activation of MAPK in response to IGF-1, an important neurotrophic factor in oligodendrocyte development (Colognato *et al.* 2007; Galvin *et al.* 2010). Together, these findings suggest that dystroglycan is an important regulator of oligodendroglia development. However, the specific functional contribution of β-dystroglycan during oligodendrocyte development has not been explored in detail. Considering the evidence that β-dystroglycan can localize to the nucleus in a number of cell types, it would be interesting to ascertain whether β-dystroglycan is similarly localized in the nucleus of oligodendrodroglia.

There are currently two unknowns concerning β-dystroglycan in oligodendroglia: 1) the subcellular distribution of β-dystroglycan, and 2) whether the cytosolic domain of β-dystroglycan has a role in normal oligodendrocyte development, independent of α-dystroglycan. I have examined the first question by using subcellular fractionation and immunocytochemistry in order to demonstrate the presence of endogenous β-dystroglycan in various cellular fractions in oligodendrocyte progenitor cells and differentiated oligodendrocytes. To address the second question, I have overexpressed the cytosolic domain of β-dystroglycan in oligodendrocyte progenitor cells, and examined a functional role in regulating the cell cycle and in localizing

components of the DGC. The experiments presented in the following chapter therefore make an initial foray into addressing both of these questions.

RESULTS

Subcellular distribution of β-dystroglycan in oligodendrocytes and progenitor cells

The subcellular localization of β-dystroglycan in nuclear fractions has been reported in A549 human lung, Hela, Hepa-1 mouse hepatic, C2C12 mouse muscle, and mammary epithelial cell lines (Fuentes-Mera *et al.* 2006; Oppizzi *et al.* 2008; Lara-Chacon *et al.* 2010). Oligodendrocytes express dystroglycan, however, the subcellular distribution of β-dystroglycan is currently unknown. In order to assess the subcellular distribution of oligodendroglial β-dystroglycan, I performed subcellular fractionation experiments using lysates obtained from oligodendrocyte progenitors (OPCs) or immature oligodendrocyes. OPCs isolated from rat mixed glial cultures were expanded for 3 days on poly-D-lysine (PDL) coated plates in proliferation media (Sato's medium supplemented with 20 ng/ml PDGF and 20 ng/ml FGF). Alternatively, purified OPCs were grown on PDL coated plates for 3 days in differentiation media (Sato's medium supplemented with 0.5%FCS). After 3 days, the cells were lysed and separated into cytosolic, nuclear, and total protein fractions. Lysates were then subjected to immunoblot analysis using anti-β-dystroglycan antibody, anti-lamin B1 antibody for the nuclear loading control, and anti-α-tubulin antibody for the cytosolic loading control (Fig. 4-1A).

I found very little contamination between cytosolic and nuclear fractions with α-tubulin (55 kDa) expression being restricted to the cytosolic fraction, and lamin B1 (68 kDa) expression

restricted to the nuclear fraction, as expected. I found two forms of β-dystroglycan in the total, cytosolic, and nuclear fractions corresponding to full length (43 kDa) and cleaved (30 kDa) β-dystroglycan; these forms were found in both OPCs and in differentiated oligodendrocytes (DIFF) (Fig. 4-1A). Cleaved β-dystroglycan has been reported to be elevated in a number of breast cancer cell lines and is also found independently of α-dystroglycan in Schwann cell compartments (Sgambato and Brancaccio 2005; Court *et al.* 2011). The relative percent distribution of total β-dystroglycan (full length + cleaved) in the nuclear fraction of OPCs and differentiated oligodendrocytes (DIFF) was evaluated by densitometry as shown in Figure 4-1B. While there was a twofold increase in total β-dystroglycan levels in the nuclear fraction of OPCs compared to the nuclear fraction of differentiated oligodendrocytes, this difference was not significant (Fig. 4-1B; 8.4% ± 3.2% in the nuclear fraction of OPCs vs. 4% ± 1.6% in the nuclear fraction of differentiated oligodendrocytes, n=3, P = 0.285).

I next asked whether there was a difference in the relative distribution of the full length versus the cleaved form of β-dystroglycan in the nuclear fractions of OPCs and oligodendrocytes. To my surprise, I found that the cleaved β-dystroglycan was the predominant form found in the nuclear fractions of both OPCs and oligodendrocytes (Fig. 4-1C; 98.7% ± 1.3% cleaved β-dystroglycan vs. 1.3% ± 1.3% full length β-dystroglycan in OPCs, n=3, ***P<0.001; and, 85% ± 9.3% cleaved β-dystroglycan vs. 15% ± 9.3% full length β-dystroglycan in oligodendrocytes, n=3, **P=0.006). However, there was no significant difference in relative distribution of either cleaved or full length β-dystroglycan in the nuclear fractions of OPCs compared to oligodendrocytes (Fig. 4-1C; 98.7% ± 1.3% cleaved β-dystroglycan in OPCs vs. 85% ± 9.3% cleaved β-dystroglycan in oligodendrocytes, n=3,

P=0.219); 1.3% ± 1.3% full length β-dystroglycan in OPCs vs. 15% ± 9.3% full length β-dystroglycan in oligodendrocytes, n=3, P=0.219).

Additionally, I asked whether there was a difference in the relative distribution of the full length versus the cleaved form of β-dystroglycan in the cytosolic fractions of OPCs and oligodendrocytes. In this case, I encountered the opposite result. While cleaved β-dystroglycan is the predominant form in the nucleus of both OPCs and oligodendrocytes, full length β-dystroglycan is predominantly found in the cytosolic fraction of both OPCs and oligodendrocytes (Fig. 4-1D; 100% full length β-dystroglycan vs. 0% cleaved β-dystroglycan in the cytosolic fraction of OPCs; and 98% ± 2% full length β-dystroglycan vs. 2% ± 2% cleaved β-dystroglycan in the cytosol of oligodendrocytes, n=3, ***P<0.001). Not surprisingly, there is no significant difference between levels of either full length or cleaved length β-dystroglycan in the cytosolic fraction of OPCs in comparison to oligodendrocytes (Fig. 4-1D; 100% full length β-dystroglycan in OPCs vs. 98% ± 2% full length β-dystroglycan in the cytosol of oligodendrocytes, n=3, P=0.374; and 0% cleaved β-dystroglycan in OPCs vs. 2% ± 2% cleaved β-dystroglycan in the cytosol of oligodendrocytes, n=3, P=0.374).

Finally, I asked whether or not β-dystroglycan was localized in the nucleus of other glial cells in the CNS. I performed subcellular fractionation on astrocytes as described above and found that β-dystroglycan is expressed in both the cytosol and nucleus (Fig. 4-1E). Interestingly, full length β-dystroglycan is expressed predominately in the cytosol of astrocytes similarly to OPCs and oligodendrocytes; in contrast, the full length also seems to be the predominant form of β-dystroglycan in the nucleus while cleaved β-dystroglycan seems to be more weakly expressed. This may illustrate different functional roles for β-dystroglycan in oligodendrocytes and their

precursors versus astrocytes. Taken together, these findings show that β-dystroglycan is found in the nuclear fractions of both OPCs and oligodendrocytes, suggesting that β-dystroglycan may potentially play role in regulating oligodendroglial functions via interactions in the nucleus.

Endogenous β-dystroglycan expression in oligodendrocytes and progenitor cells

Next I asked whether β-dystroglycan can be detected via immunocytochemistry in oligodendrocyte progenitor cells (OPCs) and immature oligodendrocytes. Oligodendrocytes have previously been shown to express dystroglycan using α-dystroglycan antibodies; however, the antibodies used to detect dystroglycan (IIH6) recognized carbohydrate epitopes on α-dystroglycan at the extracellular surface of the cell (Colognato *et al.* 2007; Galvin *et al.* 2010). Since α/β-dystroglycan have been viewed primarily as an obligate pair, β-dystroglycan expression has been assumed to coincide with α-dystroglycan immunoreactivity. While this is certainly most likely true in most cases, β-dystroglycan expression has been reported in the outer membane of Schwann cells in the absence of α-dystroglycan (Court *et al.* 2011). Using antibodies directed against β-dystroglycan, I was able to visualize expression in OPCs and oligodendrocytes differentiated for 3 days *in vitro* (Fig. 4-2). In OPCs, β-dystroglycan expression is distributed throughout the cell body extending into the processes (Fig. 4-2A). The pattern of staining is alternately diffuse and punctate with occasional strong localization either in or near the nucleus. The punctate pattern is consistent with α-dystroglycan immunoreactivity (Colognato *et al.* 2007; Galvin *et al.* 2010), however, β-dystroglycan levels seem particularly prominent in the cell body and the nucleus. The pattern of β-dystroglycan location is similar in immature oligodendrocytes with β-dystroglycan expression extending out into processes and into

process branches (Fig. 4-2B). Immunoreactivity is also very strong in the cell body and shows occaisional prominent staining associated with the nucleus.

Overexpression of cytosolic β-dystroglycan shows preferential localization in the nucleus of oligodendrocyte progenitor cells

In order to visualize the expression pattern of the cleaved (30 kDa) form of β-dystroglycan, I transfected oligodendrocyte progenitor cells (OPCs) with a truncated construct containing the entire cytosolic domain of β-dystroglycan fused to green fluorescent protein (GFP) (Cyto-BDG-GFP). A schematic of this construct in relation to full length dystroglycan is found in Figure 4-3A. Transfected OPCs were seeded onto PDL coated glass coverslips and kept in proliferation media (Sato's medium supplemented with 20ng/ml PDGF and 20 ng/ml FGF) overnight. 12-24 hours later, transfection efficiency was confirmed visually by fluorescence microscopy, the cells were fixed, and immunolabeling was performed with antibodies to detect GFP and dystrophin. To provide additional confirmation of transfection efficiency, I obtained lysates from transfected cells, separated protein extracts via SDS-PAGE, and detected GFP via immunoblot. The Cyto-BDG-GFP construct migrates at ~55 kDa in a 10% gel, while the vector control (Ctl-GFP) migrates at ~25 kDa (Fig. 4-3B). GFP immunoreactivity in OPCs transfected with the Cyto-BDG-GFP construct or Ctl-GFP construct was visualized via confocal microscopy (Fig. 4-3C). GFP expression is preferentially localized in the nucleus of Cyto-BDG-GFP transfected cells. GFP staining is also apparent in the cytosol, but is less concentrated than the nucleus. OPCs expressing Ctl-GFP show weak staining within the nucleus and prominent staining in the cytosol. Interestingly, when co-labeling with antibodies to detect dystrophin, I noted a marked redistribution of dystrophin out of the cytosol and into the nucleus of OPCs

transfected with the Cyto-BDG-GFP construct. A similar redistribution of dystrophin was not apparent in Ctl-GFP transfected cells. These data suggest that β-dystroglycan and dystrophin may form a complex in the nucleus of OPCs.

Cytosolic β-dystroglycan is redistributed out of the nucleus following microtubule disruption

It is currently unknown how β-dystroglycan is shuttled to the nucleus, and, whether it is trafficked from the plasma membrane in response to a signal, or if it is sent directly from the Golgi. Interestingly, tyrosine phosphorylation of β-dystroglycan in response to laminin causes internalization of β-dystroglycan within vesicles where it colocalizes with the endosomal marker transferrin in Cos-7 cells (Sotgia *et al.* 2003). Sotgia *et al.* further speculate that β-dystroglycan internalization may function as an intracellular signaling platform. Many proteins are trafficked via motor proteins along microtubules throughout the cell, which suggests a potential mechanism by which β-dystroglycan can be trafficked to the nucleus. I've noted that GFP immunoreactivity strongly co-localizes with what appears to be microtubules in some oligodendrocytes transfected with a full length α/β-dystroglycan-GFP construct (data not shown). This led me to ask 1) whether dystroglycan may be trafficked along microtubules, and 2) whether or not disrupting microtubules would affect localization of the cytosolic β-dystroglycan construct (Cyto-BDG-GFP) which shows particularly strong nuclear localization. In order to address the first question, I first sought to answer the second. Microtubule depolymerization can be induced in the presence of nocodazole. Oligodendrocytes cultured in the presence of nocodazole exhibit marked process retraction following the collapse of the microtubule network (Song *et al.* 2001). I transfected oligodendrocyte progenitor cells (OPCs) with either Cyto-BDG-GFP or vector control (Ctl-GFP)

constructs and treated them with either 10 μg/ml nocodazole or vehicle control, DMSO (CTL), for 2 hours after which they were subsequently fixed. Anti-GFP antibodies were used to detect GFP, while anti-α-tubulin was used to visualize microtubules and confirm depolymerization. In the absence of nocodazole, Cyto-BDG-GFP and Ctl-GFP transfected OPCs exhibit normal microtubule distribution in a mesh like pattern throughout the cell body, extending in parallel bundles into the processes (Fig. 4-4:A,G,J). Nocodazole treated cells exhibited a retraction of processes and the collapse of microtubules resulting in punctate α-tubulin staining throughout the cell body (Fig. 4-4:D,M,P). GFP expression in Ctl-GFP transfected cells was evenly distributed throughout the cytosol in both nocodazole treated and untreated cells (Fig. 4-4:B,E,C,F). As expected, Cyto-BDG-GFP transfected cells treated with vehicle control exhibited strong nuclear localization of GFP (Fig. 4-4:H,K,I,L). However, in the presence of nocodazole, GFP was redistributed out of the nucleus and into the cytosol of Cyto-BDG-GFP transfected cells (Fig. 4-4:N,O,Q,R). These results show that microtuble disruption does affect the localization of Cyto-BDG-GFP; furthermore, they suggest that it is possible that dystroglycan may be actively trafficked along microtubules in oligodendrocyte progenitor cells.

Delayed cell cycle exit in oligodendrocyte progenitor cells overexpressing cytosolic β-dystroglycan

I've shown thus far that the cleaved form of β-dystroglycan is enriched in the nuclear fraction of oligodendrocyte progenitors. Overexpression of a construct containing the cytosolic domain of β-dystroglycan localizes preferentially in the nucleus of oligodendrocyte progenitors, and coincides with a redistribution of dystrophin from the cytosol to the nucleus. The functional significance of nuclear localized β-dystroglycan is still unknown; however, several recent studies

have implicated β-dystroglycan in regulating the cell cycle (Higginson *et al.* 2008; Villarreal-Silva *et al.* 2011). In order to address the functional significance of nuclear localized β-dystroglycan in oligodendrocyte progenitor cells (OPCs), I next asked whether proliferation would be affected in OPCs expressing the cytosolic β-dystroglycan construct (Cyto-BDG-GFP). To answer this question, I transfected oligodendrocyte progenitor cells (OPCs) with either Cyto-BDG-GFP or vector control (Ctl-GFP) constructs and treated them with increasing amounts of the soluble growth factor PDGF. Proliferation was evaluated by BrdU incorporation. 12-14 hours post-transfection, I washed the cells twice in serum free Dulbecco's modified Eagle's medium (DMEM), prior to adding PDGF (in Sato's modified medium), and cultured them for 8 hours after which they were subsequently fixed. Anti-GFP antibodies were used to detect GFP, while anti-BrdU was used to visualize BrdU incorporation into replicating DNA. Nuclei were stained with DAPI. Representative micrographs of Cyto-BDG-GFP, Ctl-GFP and BrdU immunoreactivity in untreated and treated (10 ng/ml) OPCs are shown in Figure 4-5A. Proliferation was assessed by counting the number of BrdU-positive cells in the GFP-positive cell population. The percent BrdU and GFP double-positive population was evaluated in 3 independent experiments counting a minimum of 100 GFP-positive cells per condition. BrdU incorporation in response to high levels of growth factor (10 ng/ml and 20 ng/ml) was not significantly different between OPCs expressing Cyto-BDG-GFP or Ctl-GFP (Fig. 4-5B: at 10 ng/ml: 49.6% ± 1.9% in Cyto-BDG-GFP vs. 50.7% ± 1.4% in Ctl-GFP, P=0.668; at 20 ng/ml: 56.6% ± 1.7% in Cyto-BDG-GFP vs. 52.7% ± 1.2% in Ctl-GFP, P=0.130; n=3). However, there was a small, but significant difference in BrdU incorporation in conditions without PDGF or with limiting amounts of growth factor (Fig. 4-5B: at 0 ng/ml PDGF: 36.2% ± 1.7% in Cyto-BDG-GFP vs. 26.4% ± 2.1% in Ctl-GFP, *P=0.023; at 1 ng/ml: PDGF: 52.8% ± 1.3% in Cyto-

BDG-GFP vs. 44.7% ± 2.2% in Ctl-GFP, *P=0.032; n=3). These results show that in conditions that promote cell cycle exit (i.e. 0 ng/ml PDGF), OPCs expressing Cyto-BDG-GFP are delayed in exiting the cell cycle. Thus, nuclear localized β-dystroglycan may indeed play a role in regulating the cell cycle in oligodendrocyte progenitor cells.

DISCUSSION

β-dystroglycan subcellular distribution and expression in oligodendroglia

In the first two figures of this chapter, I demonstrated the subcellular distribution of β-dystroglycan (Fig. 4-1), and the location of endogenous β-dystroglycan in oligodendroglial cells (Fig. 4-2). Using subcellular fractionation, I reported that β-dystroglycan is present in the cytosol and nucleus of both oligodendrocyte progenitor cells (OPCs) and immature oligodendrocytes (iOLs). I also found that two distinct forms of β-dystroglycan are found in the cytosolic, nuclear, and total cell lysates of OPCs and iOLs. The first is the full length (43 kDa) isoform of β-dystroglycan, and the second is a cleaved (30 kDa) isoform of β-dystroglycan. I was initially surprised to find that the subcellular distribution of total β-dystroglycan (full length + cleaved) was twofold higher in the nuclear fraction of OPCs compared to the nuclear fraction of differentiated oligodendrocytes. While this difference was not significant, these results are consistent with my previous observations (data not shown) that increased total β-dystroglycan levels are found in the nucleus of OPCs compared to differentiated oligodendrocytes. I further found that within the nuclear compartment, the cleaved form of β-dystroglycan is almost exclusively present in both OPCs and iOLs. Furthermore, within the cytosolic compartment, the

full length form of β-dystroglycan is almost exclusively present. In contrast to previous studies that examined β-dystroglycan in nuclear fractions of several cell types, to the best of my knowledge, this is the first time that the cleaved form of β-dystroglycan has been shown as the most prevalent form within the nuclear fraction of any cell type. I can only find one report that shows that the cleaved form of dystroglycan is found in the nuclear fraction, in C2C12 muscle cells in an immunoblot; however, the full length form of β-dystroglycan was still the most prevalent in the C2C12 nuclear fraction, and the potential significance of the cleaved isoform in the nuclear fraction was not elaborated upon (Lara-Chacon *et al.* 2010).

An important point must be mentioned regarding the distribution of the full length and cleaved forms of β-dystroglycan, and their distribution within the cytosolic and nuclear compartment of OPCs and iOLs. The first, is the discrepancy between the total β-dystroglycan distribution in the nuclear fraction of OPCs versus iOLs. I've shown that there is more total β-dystroglycan in the nucleus of OPCs than in the nucleus of iOLs, and that in both OPCs and iOLs, the most prevalent forms in the cytosolic and nuclear fractions are the full length and cleaved form of β-dystroglycan, respectively. One way to explain the difference in the amount of β-dystroglycan in the nuclear fraction is to consider the increased association of β-dystroglycan with the actin cytoskeleton in differentiating oligodendrocytes. The morphological differentiation of oligodendrocytes involves cytoskeletal remodeling and growth in order to extend and branch processes. In simple terms, oligodendrocytes are larger cells, have a more complex actin cytoskeleton, and thus, more β-dystroglycan interactions with the cytoskeleton are likely to occur. β-dystroglycan can bind to F-actin directly, or via dystrophin (Chen *et al.* 2003; Baressi and Winder, 2006). Although the cell fractionation method I used in these experiments should not have solubilized the cytoskeleton or the cell membrane (with the exception of the total cell

fraction), I cannot rule out the possiblity that β-dystroglycan in these compartments contributes to the cytosolic fraction of iOLs. Therefore, the difference between total β-dystroglycan in the nucleus of OPCs and iOLs, may simply reflect more actin associated β-dystroglycan in the cytosolic fraction of iOLs.

Another important point to mention is the slight increase in the cleaved form of β-dystroglycan in the nuclear fraction of OPCs in comparison to iOLs. While I did not observe any significant difference in the levels of cleaved β-dystroglycan between OPCs and iOLs in these experiments, I have previously observed that that the cleaved form of β-dystroglycan is often significantly higher in OPCs versus iOLs. One way to explain this is the finding that dystroglycan expression fluctuates during the cell cycle and peaks during S-phase (Hosokawa *et al.* 2002). Dystroglycan levels may also fluctuate in OPCs, and depending on when I lysed the cells at the beginning of the fractionation experiments, it is conceivable that I may have caught a large percentage of OPCs in different phases of the cell cycle. It is therefore possible that the cleaved form of β-dystroglycan is also differentially expressed throughout the cell cycle and may account for the differences I have observed. It would be interesting to block OPCs in each phase of the cell cycle and determine if this is the case.

Throughout this chapter I have repeatedly referred to the 30 kDa form of β-dystroglycan as the "cleaved" form of β-dystroglycan. While matrix metalloproteinase (MMP) -2 and -9 have been reported to cleave β-dystroglycan (Yamada *et al.* 2001), I cannot confirm whether this is the case in oligodendroglia. Work done in our lab suggests that regulated cleavage of β-dystroglycan does occur during normal oligodendrocyte development *in vitro* and *in vivo* (Cindy Leiton and Holly Colognato, unpublished observations); however, the exact mechanism by which this occurs remains unclear. It would, however, be interesting to assess whether regulated

cleavage of β-dystroglycan occurs, for example, throughout the cell cycle as described above. I was also interested to learn whether the cleaved form of β-dystroglycan was present in different glial cells, and showed one example from a cell fractionation experiment performed on astrocytes. Interestingly, the cleaved form and the full length forms of β-dystroglycan are present in the nuclear fraction of astrocytes at what seem to be comparable levels. This is in contrast to OPCs and iOLs in which the cleaved form of β-dystroglycan is almost exclusively expressed in the nuclear fraction. This may suggest that regulated cleavage of β-dystroglycan is differs between glial cell types, and suggests different functional requirements for β-dystroglycan in the nucleus.

Finally, I also demonstrated the expression of endogenous β-dystroglycan in OPCs and iOLs by indirect fluorescence microscopy. I showed that β-dystroglycan is expression throughout the cytosol in alternately diffuse and punctate staining patterns with a strong presence in the cell body. I also demonstrated that β-dystroglycan is found in or near the nucleus in both OPCs and iOLs. I showed one example of particularly concentrated β-dystroglycan expression in the nucleus of an OPC possibly prior to dividing. While I can confirm from this analysis that endogenous β-dystroglycan expression can be detected in OPCs and iOLs, an obvious pitfall in this analysis is that nuclear localization of β-dystroglycan cannot be confirmed with a great deal of certainty without confocal imaging. It would also be interesting to visualize (α/β) dystroglycan expression together in order to assess whether there are different expression patterns in different cell compartments (i.e. the nucleus). These experiments will be carried out in the immediate future.

Cytosolic β-dystroglycan overexpression

In the final three figures of this chapter, I performed preliminary experiments in OPCs overexpressing a cytosolic β-dystroglycan (Cyto-BDG-GFP) construct to examine the subcellular location (Fig. 4-3), trafficking (Fig. 4-4), and functional significance of the cytosolic domain of β-dystroglycan (Fig. 4-5). I first demonstrated that Cyto-BDG-GFP was found prominently expressed in the nucleus of OPCs. Cyto-BDG-GFP was also found in punctate staining throughout the cell body consistent with my findings in Fig. 4-2. These results were obtained using confocal imaging showing one slice through the middle of the nucleus. The question arises as to how the Cyto-BDG-GFP construct is being translocated into the nucleus. Two recent studies have shown that the cytosolic domain of β-dystroglycan contains a functional bipartite NLS that is required either for direct entry into the nucleus, or facilitated entry via α-importin and β-importin (Oppizzi *et al.* 2008; Lara-Chacon *et al.* 2010). One way to confirm this would be to mutate the NLS in our Cyto-BDG-GFP construct and determine whether entry into the nucleus is restricted. I also showed that β-dystroglycan co-localizes with dystrophin in the cytosol in vector control (Ctl-GFP) transfected OPCs. I also demonstrated that dystrophin expression significantly redistributed into the nucleus of OPCs transfected with the Cyto-BDG-GFP construct. This finding is not unexpected as several recent studies have shown that β-dystroglycan exists in a complex with the dystrophin isoform Dp71 in the nucleus and nuclear envelope (Fuentes-Mera *et al.* 2006; Gonzalez-Ramirez *et al.* 2008; Villarreal-Silva *et al.* 2010, 2011). However, the anti-dystrophin antibody that I used in this experiment (MANDRA-1) recognizes all six isoforms of dystrophin (Dp427, Dp260, Dp140, Dp116, Dp71, Dp40). The most abundant isoform in the brain is Dp71, so it is likely that this is the isoform that I am detecting in this experiment. However, this should be confirmed via immunoprecipitation and/or

isoform specific antibodies. I should note that in our lab, there is preliminary RT-PCR data suggesting that oligodendrocytes express the Dp71 transcript (Azeez Aranmolante, unpublished observations).

I also found, albeit in a very preliminary experiment, that microtubule disruption in OPCs overexpressing the Cyto-BDG-GFP construct, redistributes Cyto-BDG-GFP out of the nucleus. While nuclear localization of β-dystroglycan has been shown, it is currently unknown how β-dystroglycan is trafficked to the nucleus. However, dystroglycan internalization into vesicles at the cell membrane upon tyrosine phosphorylation has been shown (Sotgia *et al.* 2003). Whether or not these vesicles are transported along microtubules to the nucleus upon β-dystroglycan phosphorylation is also unknown. However, in my observations of OPCs transfected with a full length (DG-GFP) dystroglycan construct, I have noted strong GFP expression along what appeared to be microtubules. In that instance, however, I cannot corfirm whether these were microtubules since I did not co-stain with tubulin antibodies. Since the Cyto-BDG-GFP construct localizes so prominently in the nucleus, I hypothesized that disrupting microtubules might also disrupt trafficking of Cyto-BDG-GFP to the nucleus. Several pitfalls are inherent in this experiment. First, this was an initial qualitative analysis of the redistribution of Cyto-BDG-GFP in response to microtubule disruption. I also noted many Cyto-BDG-GFP transfected cells in the nocodazole treated cells that retained a strong nuclear GFP signal. The significance of this experiment would certainly be more meaningful if the pixel intensities in the nucleus were measured in a number of cells over the course of several experiments. The second pitfall is that nocodazole treatment is eventually cytotoxic to cells. Based on an earlier study done in oligodendrocytes, I used nocodazole at a concentration of 10 μg/ml for 2 hours (Song *et al.* 2001). Those experiments were performed in differentiating oligodendrocytes, and it is therefore

possible that the nocodozole conditions were too harsh for more fragile OPCs. Indeed, I did notice apoptotic nuclei in many cells treated with nocodazole. In this case, breakdown of the nuclear envelope may also contribute to decreased GFP signal in the nucleus. These experiments need to be optimized and repeated using confocal imaging and pixel intensity measurement to determine whether the initial observations I have shown are indeed representative of functional trafficking of β-dystroglycan to the nucleus.

In the final figure of this chapter (Fig. 4-5) I identified a functional role for cleaved β-dystroglycan using Cyto-BDG-GFP overexpression followed by BrdU incorporation in experiments designed to measure OPC proliferation in response to increasing amounts of the soluble growth factor PDGF. Here I have shown that in high growth factor conditions (10 ng/ml and 20 ng/ml PDGF) there is no significant difference in the number of BrdU-positive OPCs expressing either Cyto-BDG-GFP or Ctl-GFP. I was surprised, however, to find that in the absence of growth factor, or in growth factor limiting conditions (1 ng/ml PDGF), there was a significant increase in the number of BrdU-positive OPCs expressing Cyto-BDG-GFP over OPCs expressing Ctl-GFP. This suggests that in conditions that normally promote cell cycle exit, Cyto-BDG-GFP overexpressing cells are delayed in exiting the cell cycle. Dystroglycan depletion in Swiss 3T3 cells, on the other hand, has been reported to cause the accumulation of cells in G1-phase during cell cycle progression assays (Higginson *et al.* 2007). In another study, Dp71 depletion in PC12 cells was reported to decrease nuclear β-dystroglycan levels, and cause a delay in the G0/G1 transition (Villarreal-Silva *et al.* 2011). In Fig. 4-3, I demonstrated that Cyto-BDG-GFP and dystrophin are prominently co-localized in the nucleus. Taken together, my results and the previous two studies suggest that Cyto-BDG-GFP and dystrophin, possibly in a complex, facilitate cell cycle progression in OPCs. It is unclear how this might occur in OPCs;

however, accumulation of the cyclin-dependent kinase inhibitor 1B ($p27^{Kip1}$) in oligodendrocyte precursors is correlated with their differentiation (Cassacia-Bonnefil *et al.* 1997). I have not determined whether $p27^{Kip1}$ levels are decreased in OPCs expressing Cyto-BDG-GFP, but this is a potential mechanism to explain the delay in cell cycle exit and should be addressed.

Figure 4-1

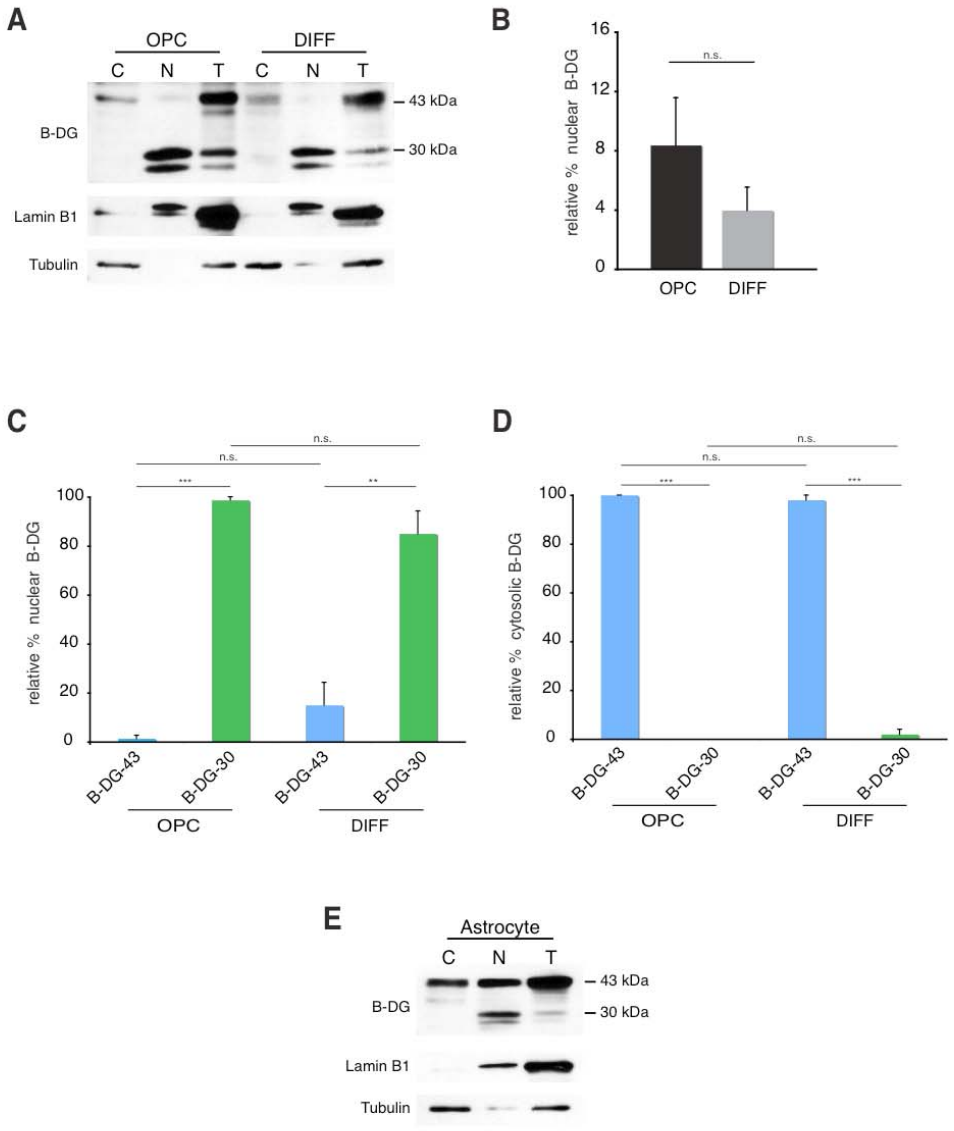
A
OPC
DIFF
C
N
T
C
N
T
B-DG
43 kDa
30 kDa
Lamin B1
Tubulin
B
relative % nuclear B-DG
n.s.
16
12
8
4
0
OPC
DIFF
C
relative % nuclear B-DG
n.s.
n.s.
***
**
100
80
60
40
20
0
B-DG-43
B-DG-30
B-DG-43
B-DG-30
OPC
DIFF
D
relative % cytosolic B-DG
n.s.
n.s.
***
***
100
80
60
40
20
0
B-DG-43
B-DG-30
B-DG-43
B-DG-30
OPC
DIFF
E
Astrocyte
C
N
T
B-DG
43 kDa
30 kDa
Lamin B1
Tubulin

Figure 4-1. Subcellular distribution of β-dystroglycan in oligodendrocytes and progenitor cells. Subcellular fractionation was performed on lysates obtained from oligodendrocyte progenitor cells (OPCs) maintained in proliferation media (Sato's medium supplemented with 20 ng/ml PDGF and 20 ng/ml FGF), and from oligodendrocytes grown for 3 days on poly-D-lysine (PDL) coated dishes in differentiation media. **A)** Representative immunoblot showing the subcellular distribution of full length (43 kDa) or cleaved (30 kDa) β-dystroglycan in cytosolic (C), nuclear (N), and total (T) cell lysates obtained from oligodendrocyte progenitors (OPC) and differentiated oligodendrocytes (DIFF). Loading controls for the nuclear fractions (lamin B1), and the cytosolic fractions (α-tubulin), are shown in the blots below. **B)** Bar graph depicting the relative percent (±SEM) distribution of total β-dystroglycan (full length, 43 kDa + cleaved, 30 kDa) in the nuclear fraction of OPCs and differentiated oligodendrocytes (DIFF) as determined by densitometry in 3 independent fractionation experiments. **C)** Bar graph depicting the relative percent distribution (±SEM) of full length (B-DG-43) and cleaved (B-DG-30) β-dystroglycan in the nuclear fractions of OPC and oligodendrocyte lysates (**P<0.01). **D)** Bar graph depicting the relative percent distribution (±SEM) of full length (B-DG-43) and cleaved (B-DG-30) β-dystroglycan in the cytosolic fractions of OPC and oligodendrocyte lysates (***P<0.001). **E)** Representative immunoblot showing the subcellular distribution of full length or cleaved β-dystroglycan in astrocytes cultured on PDL for 2 days in OPC maintenance medium. Both the full length and cleaved forms of β-dystroglycan are found in the nuclear fraction of astrocytes (n=1). n.s., not significant.

Figure 4-2

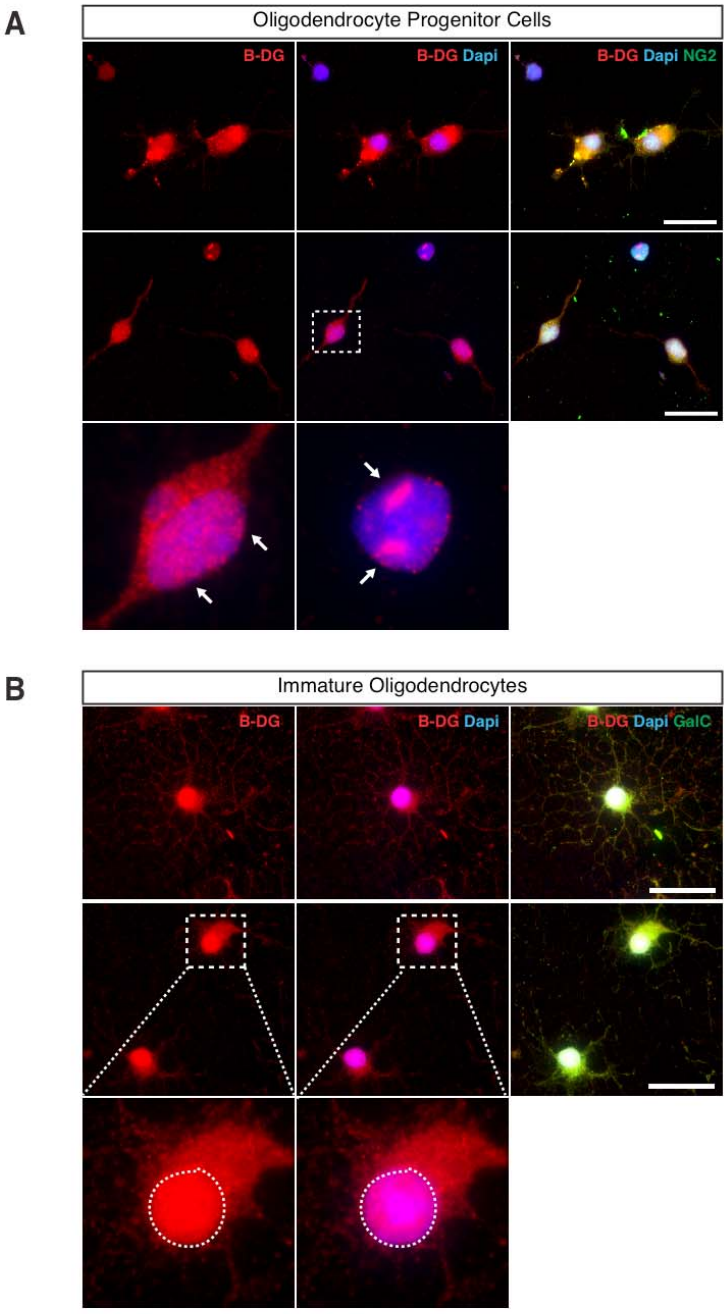
A
Oligodendrocyte Progenitor Cells
B-DG
B-DG Dapi
B-DG Dapi NG2
B
Immature Oligodendrocytes
B-DG
B-DG Dapi
B-DG Dapi GalC

Figure 4-2. Endogenous β-dystroglycan expression in oligodendrocytes and progenitor cells. A) Representative fluorescence micrographs of oligodendrocyte progenitor cells (OPCs) showing immunoreactivity for β-dystroglycan (red), and a marker for OPCs, NG2 (green), in combination with DAPI for nuclei (blue). Top two panels show β-dystroglycan distribution in OPCs throughout the cytoplasm and extending into processes. β-dystroglycan immunoreactivity is also found in closely associated with the nucleus (see insets, bottom two panels). Arrows in lower left panel point out diffuse and punctate β-dystroglycan immunoreactivity in the cytoplasm and around the nucleus. Arrows in lower right panel show two strong concentrations of β-dystroglycan immunoreactivity in the nucleus of a rounded OPC, possibly prior to dividing. Scale bars = 25 μm. **B)** Representative fluorescence micrographs of oligodendrocyte progenitor cells (OPCs) showing immunoreactivity for β-dystroglycan (red), and the oligodendrocyte marker GalC (green), in combination with DAPI for nuclei (blue). Top two panels show β-dystroglycan distribution in oligodendrocytes throughout the cytoplasm and extending into processes and branches. β-dystroglycan immunoreactivity also strongly co-localizes with the nucleus (see inset, bottom two panels). Bottom left panel shows strong β-dystroglycan immunoreactivity associated with the nucleus (outlined). Bottom right panel shows β-dystroglycan and DAPI co-localization in the same cell as shown in the bottom left panel. Scale bars = 25 μm.

Figure 4-3

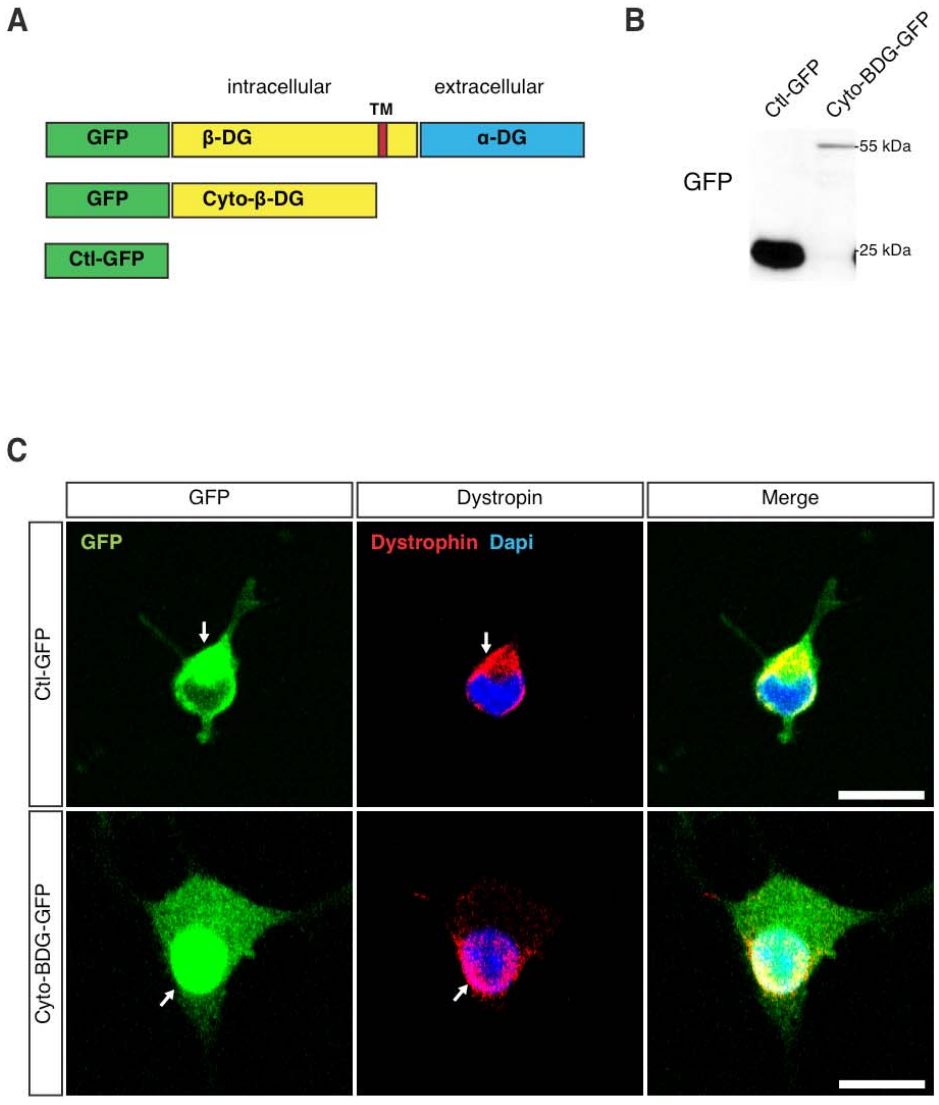
A
intracellular
extracellular
TM
GFP
β-DG
α-DG
GFP
Cyto-β-DG
Ctl-GFP
B
Ctl-GFP
Cyto-BDG-GFP
GFP
55 kDa
25 kDa
C
GFP
Dystropin
Merge
Ctl-GFP
Cyto-BDG-GFP
GFP
Dystrophin Dapi

Figure 4-3. Overexpression of cytosolic β-dystroglycan shows preferential localization in the nucleus of oligodendrocyte progenitor cells. Oligodendrocyte progenitor cells (OPCs) were transfected with a construct containing the cytosolic domain of β-dystroglycan fused to GFP, maintained in proliferation media (Sato's medium supplemented with 20 ng/ml PDGF and 20 ng/ml FGF) for an additional day, and fixed for visualization by confocal microscopy or lysed to determine transfection efficiency. **A)** A schematic of the cytosolic β-dystroglycan-GFP fusion construct in comparison to full length dystroglycan and the control GFP vector. The cytosolic construct consists of the entire C-terminal tail of β-dystroglycan on the intracellular side of the transmembrane (TM) domain. **B)** Representative immunoblot showing the transfection efficiency of the cytosolic β-dystroglycan-GFP fusion construct (Cyto-BDG-GFP) and the control vector (Ctl-GFP). A band in the Ctl-GFP tranfected cells is detected at 25 kDa, while a band at 55 kDa is detected in Cyto-BDG-GFP transfected OPCs. **C)** Representative confocal images showing GFP (green) and dystrophin (red) immunoreactivity, co-stained with DAPI (blue) for nuclei, in OPCs transfected with the cytosolic β-dystroglycan construct (Cyto-BDG-GFP) or control vector (Ctl-GFP). GFP immunoreactivity is prominent in the nucleus of Cyto-BDG-GFP transfected cells, while in Ctl-GFP transfected cells, GFP immunoreactivity is predominantly cytosolic (see arrows in left panels). Strong GFP immunoreactivity in the nucleus of OPCs transfected with Cyto-BDG-GFP is associated with a redistribution of dystrophin from the cytoplasm to the nucleus (see arrows in middle panels). Scale bars = 10μm.

Figure 4-4

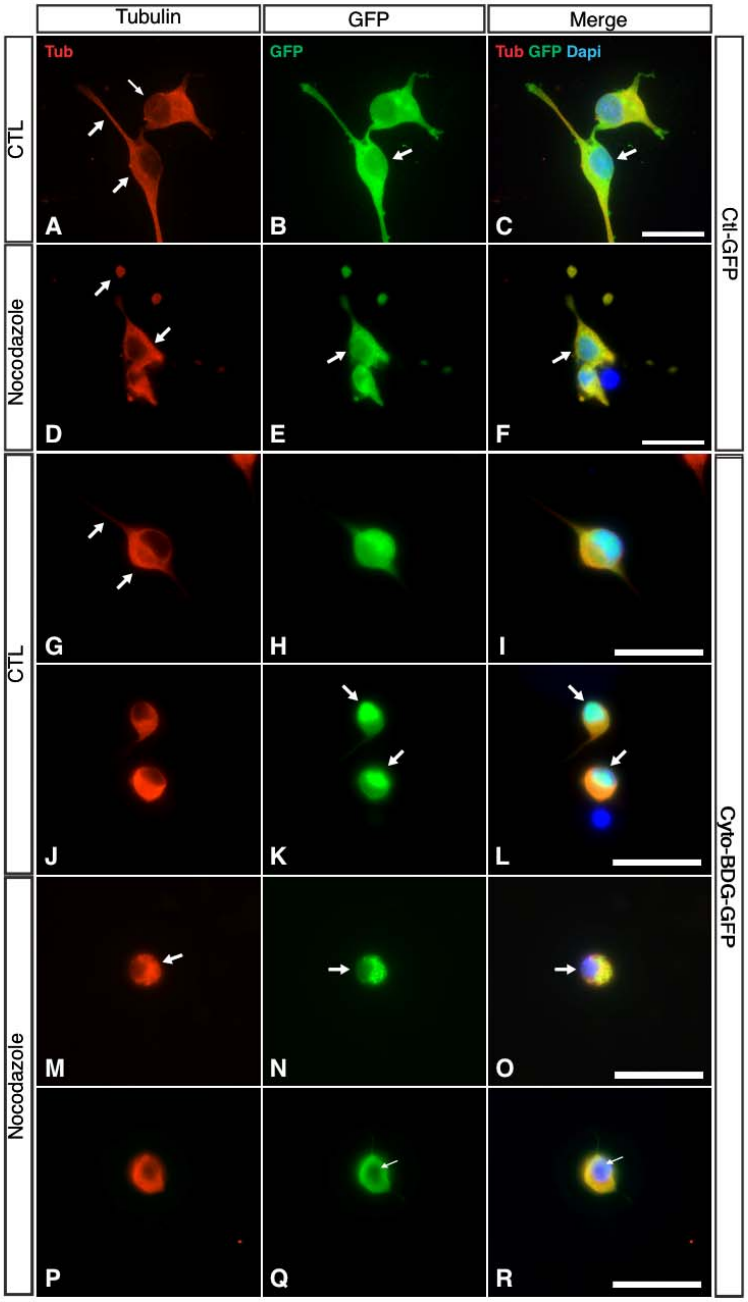
Tubulin
GFP
Merge
CTL
Nocodazole
CTL
Nocodazole
Tub
GFP
Tub GFP Dapi
A
B
C
D
E
F
G
H
I
J
K
L
M
N
O
P
Q
R
Ctl-GFP
Cyto-BDG-GFP

Figure 4-4. Cytosolic β-dystroglycan is redistributed out of the nucleus following microtubule disruption. (A-R) Oligodendrocyte progenitor cells (OPCs) were transfected with a construct containing the cytosolic domain of β-dystroglycan (Cyto-BDG-GFP) **(G-R)**, or control vector (Ctl-GFP) **(A-F)**, and subsequently treated for 2 hours with the microtubule depolymerizing agent nocodazole, or vehicle control, DMSO (CTL). Treated cells were fixed and immunolabeled with antibodies to detect α-tubulin (red) and GFP (green), in conjunction with DAPI (blue) to label nuclei, for visualization via fluorescence microscopy. α-Tubulin immunoreactivity shows that microtubule organization is evenly distributed in a mesh like framework throughout the cell body, around the nucleus, and in parallel bundles extending into processes in CTL treated OPCs transfected with either Cyto-BDG-GFP or Ctl-GFP **(see arrows: A,G)**. In nocodazole-treated cells, microtubules depolymerize and condense while processes retract **(see arrows: D,M)**. In Ctl-GFP transfected cells, GFP staining is distributed evenly throughout the cytoplasm in both CTL and nocodazole treated cells **(B,E)**. Strong nuclear GFP staining is prominent in CTL treated Cyto-BDG-GFP transfected OPCs **(H,I, arrows in K,L)**. Cyto-BDG-GFP transfected OPCs treated with nocodazole show a redistribution of GFP staining from the nucleus to the cytosol **(see arrows: N,O,Q,R)**. In contrast, Ctl-GFP transfected OPCs treated with nocodazole retain GFP immunoreactivity around the nucleus similar to untreated controls **(see arrows: B,C,E,F)**. Scale bars = 25 μm.

Figure 4-5

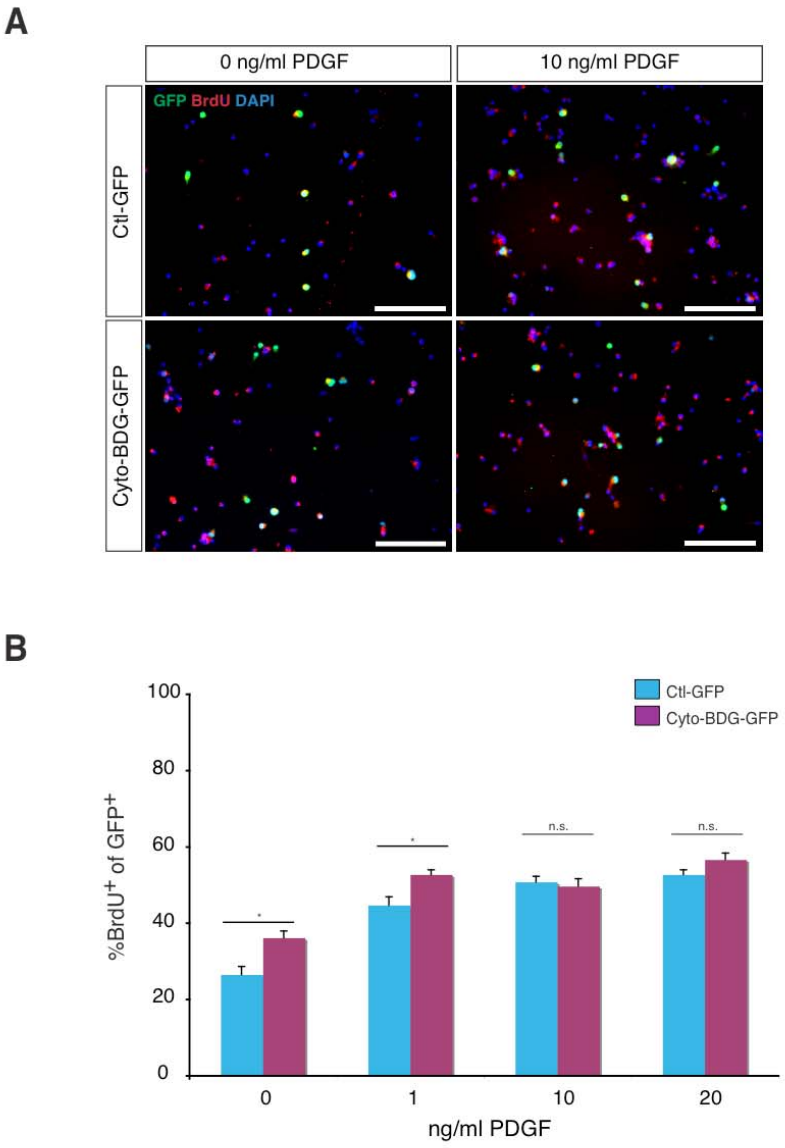
A
0 ng/ml PDGF
10 ng/ml PDGF
Ctl-GFP
Cyto-BDG-GFP
GFP BrdU DAPI
B
Ctl-GFP
Cyto-BDG-GFP
%BrdU+ of GFP+
100
80
60
40
20
0
n.s.
n.s.
0
1
10
20
ng/ml PDGF

Figure 4-5. Delayed cell cycle exit in oligodendrocyte progenitor cells overexpressing cytosolic β-dystroglycan. Oligodendrocyte progenitor cells (OPCs) were transfected with a construct containing the cytosolic domain of β-dystroglycan (Cyto-BDG-GFP), or control vector (Ctl-GFP), and subsequently treated with increasing amounts of the soluble growth factor PDGF. After BrdU incorporation for 8 hours, OPCs were fixed and stained for indirect immunoflourescence microscopy. **A)** Representative micrograph of OPCs immunolabeled with antibodies to detect GFP (green) and BrdU (red), in conjunction with DAPI (blue) to visualize nuclei. More GPF/BrdU double-positive cells are present in the absence of growth factor (0 ng/ml PDGF) in OPCs transfected with Cyto-BDG-GFP versus Ctl-GFP transfected cells. In the presence of 10 ng/ml PDGF, there is no difference in the number of GPF/BrdU double-positive cells in OPCs transfected with either Cyto-BDG-GFP or Ctl-GFP. Scale bars = 100 μm. **B)** Bar graph depicting the percent BrdU and GFP double-positive population (±SEM) of OPCs transfected with either Cyto-BDG-GFP or Ctl-GFP and treated with increasing amounts of PDGF for 8 hours. OPCs transfected with Cyto-BDG-GFP showed a significant increase over Ctl-GFP transfected cells in the percentage of BrdU positive cells in the absence of growth factor, or in the presence of 1 ng/ml PDGF suggesting delayed cell cycle exit in growth factor-limiting conditions (n=3; *$P<0.04$).

Chapter 5

GENERAL DISCUSSION

The studies contained within this dissertation have been designed to elucidate the functional role of dystroglycan in normal oligodendrocyte development. Here I have demonstrated that dystroglycan has a role in promoting filopodia formation, process outgrowth, and process branching in newly-formed premyelinating oligodendrocytes. Dystroglycan is found in filopodia, processes, and process branch points where it is positioned to affect local cytoskeletal reorganization. Laminin mediates the effects of dystroglycan on cytoskeletal remodeling, as disrupting dystroglycan interactions does not affect filopodia formation, process extension, or process branching in oligodendrocytes differentiated on poly-D-lysine substrate. In addition, dystroglycan is found in a complex with focal adhesion kinase (FAK), previously implicated in regulating process outgrowth and branching downstream of the Src family kinase Fyn (Hoshina *et al.* 2007). Taken together, these findings suggest that dystroglycan-laminin interactions promote cytoskeletal reorganization, and thus, may influence the morphological differentiation of pre-myelinating oligodendrocytes.

In addition, I have examined a novel role for β-dystroglycan in the nucleus of oligodendrocyte progenitor cells and pre-myelinating oligodendrocytes. Here I have demonstrated that a significant fraction of β-dystroglycan localizes in the nucleus of both oligodendrocyte progenitor cells and pre-myelinating oligodendrocytes. I have further shown

that cleaved β-dystroglycan is the predominant form of dystroglycan present within the nucleus of oligodendrocyte progenitor cells and pre-myelinating oligodendrocytes. Finally, I have demonstrated that the cytosolic domain of β-dystroglycan, when overexpressed in oligodendrocyte progenitor cells, preferentially localizes in the nucleus and delays cell cycle exit in conditions that promote cell cycle exit. These findings suggest that there may be a previously unknown functional role for dystroglycan in the nucleus during oligodendroglial development.

The two studies contained within this dissertation represent fundamentally different functional roles for dystroglycan during oligodendroglial development. On the one hand, dystroglycan mediates interactions with laminin in the extracellular matrix and promotes cytoskeletal reorganization facilitating the morphological differentiation of newly-formed oligodendrocytes. On the other hand, β-dystroglycan translocates into the nucleus of oligodendrocyte progenitors and influences the cell cycle. These two distinct functions suggest that dystroglycan itself is regulated during oligodendrocyte development. While this possiblity has yet to be examined, I propose a model in which the regulated cleavage of β-dystroglycan is required during oligodendrocyte progenitor proliferation for normal cell cycle progression. Upon cell cycle exit and the initial phase of process outgrowth, α/β-dystroglycan are positioned within the cell membrane and stabilized to coordinate cytoskeletal skeletal reorganization. A flaw in this model is that cleaved β-dystroglycan is also in found within the nucleus of pre-myelinating oligodendrocytes. However, it has been reported that the proteolytic activity of matrix metalloproteinase (MMP)-9 regulates oligodendroglial process outgrowth by remodeling the extracellular matrix (ECM) (Oh *et al.* 1999). Additionally, MMP2-9 are known to cleave β-dystroglycan (Yamada *et al.* 2001). Thus, regulated cleavage of β-dystroglycan may not only be

neccessary for remodeling the ECM, but may represent a feedback mechanism that disengages β-dystroglycan from the cell membrane, and allows for nuclear translocation.

Dystroglycan regulation of the oligodendroglial cytoskeleton

In order to examine the role of dystroglycan in filopodia formation, process outgrowth and process branching, I used an *in vitro* cell culture system utilizing primary rat oligodendrocyte progenitor cells. Two techniques were used to either disrupt dystroglycan-laminin interactions, or, to deplete cells of dystroglycan. Oligodendrocytes were either cultured in the presence or absence of α-dystroglycan blocking antibodies (clone IIH6), or depleted of dystroglycan using small interfering (si) RNAs. IIH6 antibodies recocognize the carbohydrate epitopes on α-dystroglycan and interfere with laminin-dystroglycan interactions. I demonstrated that when grown on laminin coated chamber slides in the presence of IIH6, oligodendrocytes form fewer filopodia, extend shorter processes, and exhibit decreased branching complexity. Oligodendrocytes also express the the laminin receptor α6β1 integrin (Milner and ffrench-Constant 1994; Buttery and ffrench-Constant 1999). Since oligodendrocytes derived from mice lacking the β1 subunit of integrin also extend shorter processes when differentiated in culture, I also examined process outgrowth and branching in the presence of both IIH6 and the β1 integrin blocking antibody (Ha2/5) in order to assess the functional contribution of each receptor. To my surprise, while I saw a decrease in process outgrowth and process branching complexity, it was not as substantial as expected. This may suggest either the presence of another unidentified laminin receptor expressed by oligodendrocytes, or competition between dystroglycan and integrin for binding laminin. Additionally, I showed that when cultured on laminin coated plates,

oligodendrocytes depleted of dystroglycan via siRNA extended significantly shorter processes, and exhibited a pronounced reduction in process complexity, as compared to oligodendrocytes incubated with the dystroglycan-blocking antibody. In this experiment, however, I cannot rule out the possibility that the transfection procedure itself was damaging to many of the cells that were analyzed in this experiment, thus contributing the effects I observed. However, transfection of a control siRNA as the comparing factor, as was done, should have minimized such an effect.

While cell culture is a powerful tool to dissect mechanisms that otherwise would not be possible *in vivo*, to truly understand the functional contribution of dystroglycan in normal oligodendrocyte development, an *in vivo* approach is necessary. I have been undertaking preliminary studies using a conditional oligodendrocyte specific dystroglycan mouse line, in which dystroglycan was excised via cre recombinase under the 2',3'-cyclic nucleotide 3'-phosphodiesterase (CNP) promoter, active in pre-myelinating oligodendrocytes (although this promoter has been reported to be active in a subset of OPCs as well). Initial observations of these mice suggest that oligodendrocyte differentiation is delayed in P21 animals. Myelin basic protein (MBP) levels are decreased in cortical lysates, and the number of CC1 (a marker for mature oligodendrocytes)-positive cells in the corpus callosum is also decreased compared to WT mice. However, in aged adults (16+ months) MBP expression is similar to WT mice in cortical, cerebellar, and spinal cord lysates. Additionally, the number of CC1-positive cells in the corpus callosum appears normal in older dystroglycan knockout mice. It is unclear if there are any myelination defects in these mice; however, these experiments are planned in the near future.

To extend the process outgrowth study, the same cortical dissection technique used to obtain rat primary oligodendrocyte progenitor cells, can also be used to obtain oligodendrocyte progenitors from the conditional oligodendrocyte-specific knockout mouse. Manipulation of

these cells would be minimized; however, a drawback is that the cell yield from primary mouse oligodendrocyte precursor preparations is low in comparison to the yield obtained from rats. While morphometric analysis could be performed, biochemical studies may be limited. Morphometric analysis may also be accomplished *in vivo*. For example, a transgenic mouse line has been created that expresses membrane-associated EGFP (maEGFP) under control of the MBP enhancer in limited numbers of oligodendrocytes thereby allowing the visualization of individual oligodendrocytes (Chong *et al.* 2012). This mouse can be used for morphometric anaylsis and 3D rendering of processes using thick sections and confocal microscopy. A drawback of this approach is that in order to observe dystroglycan loss-of-function, lentiviral-mediated delivery of dystroglycan targeting siRNAs would need to be performed, or extensive backcrossing to obtain triple transgenic mice in which CNP-Cre: DAG flox/flox mutants can be obtained on the MBP-EGFP line.

Another interesting aspect that remains to be explored in terms of dystroglycan regulation of process outgrowth and branching, is the downstream signaling mechanism. For example, in REF52 and Swiss 3T3 cells, dystroglycan can recruit a complex containing the ezrin-radixin-moesin adapter protein, ezrin (Spence *et al.* 2004). Ezrin, a cytoskeletal adapter protein, then recruits the Rho GTP/GDP exchange factor Dbl to the cell membrane, thereby localizing activation of the RhoGTPase Cdc42 which drives filopodia fomation (Batchelor *et al.* 2007). I have shown that filopodia formation is decreased in α-dystroglycan blocking experiments, however, it remains unknown whether a similar mechanism is found in oligodendrocytes. These experiments can be performed via immunoprecipitation, GST pull-down assays, or by Cdc42 activation assys. Finally, since dystroglycan is often found in process branch points, it would be of interest to determine whether or not dystroglycan is in a complex with proteins involved in F-

actin assembly. Wiskott-Aldrich syndrome protein family verprolin homologous (WASP), is a molecular scaffold that links the Rho GTPases Rho, Cdc42, and Rac1, to the activation of actin-related protein 2/3 (Arp2/3) (Etienne-Manneville and Hall 2002). WAVE1, similar to dystroglycan, is upregulated during oligodendrocyte differentiation, and localized along the edge of processes and branches (Kim *et al.* 2006). Arp2/3 is involved in actin nucleation, and is likely enriched branch points in oligodendrocyte processes. It would be informative to know whether dystroglycan and WAVE1 localize together, and whether disrupting dystroglycan function alters WAVE1-mediated F-actin assembly.

Nuclear β-dystroglycan: functional implications

Nuclear localization of β-dystroglycan has only recently been reported in a number of transformed or cancer cell lines including Hela, C2C12 muscle, PC12 neuronal, Swiss 3T3, and mammary epithelial (MepG-C7, MEpL, MEpG, MEpE, EpH4) (Fuentes-Mera *et al.* 2006; Gonzalez-Ramirez *et al.* 2008; Oppizzi *et al.* 2008; Lara-Chacon *et al.* 2010; Villarreal-Silva *et al.* 2010; Villarreal-Silva *et al.* 2011). The only study to report the cleaved 30 kDa isoform in the nuclear fraction has been in a study that included C2C12 muscle cells, where the cleaved form was only a minor fraction of the total nuclear β-dystroglycan (Lara-Chacon *et al.* 2010). A functional bipartite nuclear localization sequence has been indentified in the cytosolic domain of β-dystroglycan in two separate studies (Oppizzi *et al.* 2008; Lara-Chacon *et al.* 2010). NLS-mediated tranlocation of β-dystroglycan into the nucleus of a cell was reported in C2C12 muscle cells. The functional significance of nuclear localized β-dystroglycan is currently unknown.

Here I have reported for the first time, that β-dystroglycan is found in the nuclear fraction of both oligodendrocyte progenitor cells and immature oligodendrocytes. Furthermore, I have shown that the most prominent form of β-dystroglycan found in the nuclear fraction of both oligodendrocyte progenitor cells and immature oligodendrocytes is the cleaved 30 kDa form of β-dystroglycan, which is distinct from the previous studies that have found that intact β-dystroglycan is found in the nucleus. I have demonstrated via indirect immunoflourescence microscopy that endogenous β-dystroglycan is expressed throughout the cytoplasm and in the nucleus of both oligodendrocyte progenitor cells and immature oligodendrocytes. Using confocal imaging, I have shown that a construct containing the cytosolic domain of β-dystroglycan is preferentially found in the nucleus of oligodendrocyte progenitor cells. Additionally, the cytoskletal adaptor protein dystrophin is redistributed from the cytosol to the nucleus in oligodendrocyte precursor cells expressing the cytosolic domain of β-dystroglycan. Furthermore, I found that nuclear localization of the cytosolic β-dystroglycan construct is redistributed out of the nucleus following disruption of microtubules in oligodendrocyte progenitors. Finally, I have reported that oligodendrocyte progenitor cells expressing the cytosolic domain of β-dystroglycan are delayed in exiting the cell cycle in conditions that promote cell cycle exit. Taken together, these results suggest that nuclear localized β-dystroglycan influences oligodendrocyte progenitor cell cycle exit, and potentially plays a role in regulating the timing and progression oligodendroglial development.

The role of nuclear localized β-dystroglycan remains largely unexplored, in any cell type. However, several studies have identified a dystrophin-associated protein complex (DAPC) containing the short Dp71 isoform of dystrophin, as well as several other components of the

dystrophin glycoprotein complex (DGC), in the nucleus of several cell types. β-dystroglycan has been shown, for example, to form a complex in Hela cells with the following components of the DGC: Dp71, β-dystroglycan β-sarcoglycan, α- and β- syntrophin; α1- and β-dystrobrevin and neuronal nitric oxide synthase (nNOS) (Fuentes-Mera *et al.* 2006). Additional, using nuclear fractionation assays performed in Hela cells, Fuentes-Mera *et al.* also reported that Dp71, β-dystroglycan, β-dystrobrevin, actin, and the nuclear matrix protein lamin B1 co-purified together in the nuclear matrix fraction. Most of these proteins have been similarly identified in the nucleus of C2C12 muscle, and PC12 neuronal cells (Gonzalez-Ramirez *et al.* 2008; Villarreal-Silva *et al.* 2010). The previous three reports have speculated that the role of the DAPC in the nucleus is to stabilize and organinze the the nuclear matrix. Indeed, deletion of Dp71 in PC12 cells has been shown to decrease the nuclear expression of most all of the previously mentioned DAPC components above, including β-dystroglycan (Villarreal-Silva *et al.* 2010). The link between β-dystroglycan and Dp71 in the nuclear envelope was further investigated in PC12 cells during mitosis and cytokinesis (Villareal-Silva *et al.* 2011). In this study, Villarreal-Silva *et al.* demonstrated that Dp71, β-dystroglycan, and lamin B1 co-localize at the mitotic spindle, midbody, and cleavage furrow in PC12 cells during mitosis and cytokinesis respectively. In the absence of Dp71, Villarreal-Silva *et al.* note a drastic reduction in β-dystroglycan expression in these structures, commensurate with significant reduction in lamin B1 immunoreactivity and partial breakdown of the nuclear envelope. Additionally the authors found that BrdU incorporation is significantly reduced in Dp71-depleted PC12 cells which show a delay in G0/G1 transition. Another independent study previously reported that β-dystroglycan is also localized to the mitotic spindle, midbody, and cleavage furrow (Higginson *et al.* 2008). In this study, Higginson *et al.* deplete Swiss 3T3 cells of β-dystroglycan and report an accumulation of cells in

G1 phase of the cell cycle. When viewed together, it is clear that in PC12 and Swiss 3T3 cells, β-dystroglycan and Dp71 are central components of several complexes found in the nucleus, nuclear matrix, the mitotic spindle, midbody, and cleavage furrow.

How can my results be interpreted in view of theses findings? First, I've found strong co-localization between a construct containing the cytosolic domain of β-dystroglycan and dystrophin in the nucleus of oligodendrocyte progenitors. This is consistent with the studies above in PC12 cells. Second, while depletion of Dp71 results in a decrease in BrdU incorporation and β-dystroglycan expression in the nucleus of PC12 cells, I have conversely found that BrdU incorporation is *increased* in oligodendrocyte progenitor cells *overexpressing* the cytosolic domain of β-dystroglycan. This too seems to correlate with the two studies mentioned above. Interestingly, I have also observed endogenous β-dystroglycan localized to the cleavage furrow of dividing oligodendrocyte progenitors (not shown). Additionally, I also quite frequently observe multinucleated oligodendrocytes following overexpression of the cytosolic β-dystroglycan construct. This point is interesting in light of the finding above that Dp71 knockdown decreases expression of the nuclear envelope protein lamin B1 causing breakdown of the nuclear lamina. Overexpression of the cytosolic domain of β-dystroglycan may dysregulate the nuclear complex that resides within the nuclear lamina or the cleavage furrow, thus delaying or perturbing final progression through the cell cycle.

To address these possibilities, I first need to ascertain the dystrophin isoform present in oligodendrocyte progenitors. In addition, I should identify the other members of the DAPC that are localized in the nucleus, and whether they are consistent with those found, for example, in PC12 cells as shown above. β-dystroglycan interactions can be determined via

immunoprecipitation and co-localization studies using immunocytochemical techniques followed by confocal microscopy. I can utilize the cytosolic β-dystroglycan construct in functional assays by mutating the dystrophin binding site to determine the spatial-temporal requirement for β-dystroglycan-dystrophin interactions throughout the cell cycle and during oligodendrocyte differentiation. These initial steps should provide a greater understanding of the role of nuclear localized β-dystroglycan in oligodendroglial development.

Chapter 6

EXPERIMENTAL METHODS

Cell Culture

Oligodendrocyte progenitor cells (OPCs) were dissociated from P0-P2 rat cortices and cultured at 37°C, 7.5% CO_2 on poly-D-lysine (PDL)-coated flasks with high-glucose Dulbecco's modified Eagle's medium (DMEM) containing 10% fetal calf serum (FCS) (OPC maintenance media). Media was changed every 3-4 days for 10-14 days to obtain mixed glial cultures containing OPCs and microglia on astrocyte monolayers. Purified OPCs were obtained by physical agitation on an orbital shaker, and subsequent differential adhesion (McCarthy and de Vellis, 1980). For morphometric assays, OPCs were resuspended in a modified Sato's medium containing 0.5% FCS (differentiation media) and grown in 8-well chamber slides (Nunclon) coated with 10 μg/ml PDL or laminin-2 (Purified Human Merosin, Millipore). For laminin coating, slides were pre-coated with PDL for 1 hour, washed, and then coated with laminin for 4 hours at 37°C. After coating, slides were blocked with heat-inactivated bovine serum albumin (BSA) for 30 minutes at 37°C, and then washed twice with phosphate buffered saline (PBS). For experiments including dystroglycan blocking antibodies, OPCs were resuspended in differentiation media containing either dystroglycan blocking antibody (IIH6C4) or an isotype control IgM (MOPC 104E; Sigma) immediately prior to seeding cells. For dual antibody blocking experiments using integrin β1 blocking antibody (Ha2/5) and IIH6C4, OPCs were

seeded in laminin-coated chamber slides for 2 hours, to allow for complete attachment prior to the addition of either blocking antibodies or control IgM.

DAG1-GFP expressing Virus-Like Particle (VLP) production

The full length DAG1-GFP ORF was excised from pEGFPN3-DAG-GFP with SalI and NotI; ends were filled in with Klenow polymerase (Chen, 2003). This fragment was ligated to pHAGE, Tat/Rev-dependent HIV1 based lentiviral packaging vector, and screened for correct orientation. pHAGE was modified to contain the human Ubiquitin C promoter, cloning sites (NotI-XbaI), and an EMCV Internal Ribosomal Entry Site (IRES) followed by mCherry with the isoprenylation site from human k-ras (mCherryCAAX). DAG1-GFP VLPs were produced by co-transfection into HEK 293-T cells with Tat, Rev, Gag-pol and VSV-G envelope protein expressing vectors as described (Mostoslavsky, 2006). Virus-containing culture supernatant was harvested on the first, second and third days after transfection; supernatant from first and second day collections were stored on ice until the final collection. Debris was cleared from the virus-containing supernatant at 3000 *g* for 10 minutes, followed by filtration with a 0.4μm PES-syringe filter. VLPs were concentrated by ultracentrifugation at 100,000 *g* for 2 hours. The VLP pellet was resuspended in 1.2 ml of DMEM (no serum), and stored at -80°C in 100μl aliquots. OPCs were seeded into PDL-coated chamber slides and maintained overnight in proliferation media (Sato, 20 ng/ml PDGFa, 20 ng/ml FGF). The next day, media was removed from OPCs and replaced with infection mixture (one 100μl aliquot of VLPs thawed on ice and diluted into 400μl of DMEM with 5μg/ml polybrene) for 2 hours at 37°C, 7.5% CO_2. The infection mixture was removed, replaced with proliferation media, and returned to the incubator overnight. The

following day, proliferation media was replaced with differentiation media, and oligodendrocytes were differentiated for an additional 2-3 days.

Dystroglycan siRNA & Cyto-BDG-GFP Transfection

As previously described (Colognato *et al.* 2007), dystroglycan depletion was achieved using a pool of 4 siRNA duplexes targeting rat dystroglycan mRNA (Dharmacon), while a pool of 4 rat non-targeting siRNA duplexes was used as a control. Fluorescent siGLO siRNA (Dharmacon) was used to determine the percentage of cells with siRNA uptake (~90%). A dystroglycan deletion construct (a generous gift from Dr. Steve Winder) lacking the entire cytosolic domain β-dystroglycan (Cyto-BDG-GFP) was used in overexpression assays and generated as previously described (Chen *et al.* 2003). Purified OPCs were resuspended in proliferation media, plated onto Petri dishes, and maintained overnight at 37°C, 7.5% CO_2. The following day OPCs were collected by brief trypsinization with 0.5X Trypsin-EDTA (Sigma) in PBS. Trypsinization was stopped using DMEM + 10% FCS and OPCs were gently pelleted and resuspended in proliferation media. Cells were allowed to rest in suspension for 1.5 hours at 37°C after which they were gently repelleted and transfected by electroporation using the Rat Oligodendrocyte Nucleofector Kit (Amaxa). For dystroglycan siRNA transfections, OPCs were seeded into PDL-coated Nunclon tissue culture plates and maintained for two days at 37°C in proliferation media (with one media change on day 1) to ensure time for adequate dystroglycan knockdown. For morphometric assays, the cells were gently trypsinized, resuspended in differentiation media, and grown in 8-well chamber slides coated with either PDL or laminin. For Cyto-BDG-GFP overexpression experiments, OPCs were seeded into PDL-coated Nunclon tissue culture plates, or acid-washed glass coverslips, and maintained 12-14 hours at 37°C in

proliferation media. For proliferation assays, OPCs were then incubated with Sato's medium supplemented with 5-bromo-2'-deoxyuridine (BrdU) and increasing amounts of PDGF (0,1,10,20 ng/ml) for 8 hours. Proliferation was detected via indirect immunocytochemistry to visualize BrdU incorporation in GFP expressing cells. A minimum of 100 GFP-positive cells per condition condition were counted in 3 independent experiments. For microtubule disruption assays, OPCs were treated with 10 μg/ml nocodazole (Sigma) for two hours, fixed, and incubated with antibodies to detect α-tubulin and GFP via indirect fluorescence microscopy.

Subcellular Fractionation

Purified OPCs were seeded into PDL-coated dishes and either 1) expanded for 3 days in Sato's medium +0.5% FCS supplemented with 20ng/ml PDGF and 20 ng/ml FGF, or 2) grown for 3 days in differentiation medium. Cells were collected by brief trypsinization with 0.5X Trypsin-EDTA (Sigma) in PBS. Trypsinization was stopped using DMEM + 10% FCS and cells were gently pelleted. The pellets were resuspended in ice cold PBS, re-pelleted at 4°C, and resuspended in ice-cold PBS. A portion was removed for total cell lysates. The remaining cells were gently centrifuged and resuspended in lysis buffer 1 (LB1) containing 20mM HEPES pH 7.9, 1.5 mM $MgCl_2$, 10 mM KCl, 0.5 mM DTT, Protease Inhibitor III-EDTA free (Calbiochem), and Phosphatase Inhibitor II (Calbiochem). Cells were incubated on ice for 20 minutes, passed 10X through a 25 gauge needle, and centrifuged for 5 minutes at 5,000 rpm. The supernantant containing the cytosolic fraction was removed to a new tube. The pellet (nuclear fraction) was washed in LB1, re-centrifuged, and resuspended in lysis buffer 2 (LB2) containing 20mM HEPES pH 7.9, 1.5 mM $MgCl_2$, 0.2 mM EDTA, 20% glycerol, 0.42M NaCl, 0.5 mM DTT, Protease Inhibitor III-EDTA free (Calbiochem), and Phosphatase Inhibitor II (Calbiochem). The

nuclear fraction was placed on a rotating wheel at 4°C for 30 minutes and then centrifuged for 5 minutes at 13,200 rpm. The supernatant containing the nuclear fraction was removed to a new tube. The nuclear, cytosolic, and total fractions were assayed for protein concentration, boiled in SDS-PAGE sample buffer, and resolved on a 10% SDS-PAGE gel as described below.

Protein Analysis

Cells were lysed for 15 minutes at 0°C in radioimmunoprecipitation (RIPA) buffer containing 50 mM Tris-HCL (pH 7.4), 150 mM NaCl, 1 mM EDTA, 1% Triton X-100, 0.5% sodium deoxycholate, 0.1% SDS, Protease Inhibitor III-EDTA free (Calbiochem), and Phosphatase Inhibitor II (Calbiochem). Lysates were centrifuged to remove insoluble material, and a detergent compatible protein assay (BioRad) was used to determine protein concentration. Lysates were boiled for 10 minutes in SDS-PAGE sample buffer (NuPAGE, Invitrogen) containing 12% β-Mercaptoethanol, and proteins were resolved on 8% SDS-PAGE gels. Proteins were transferred to nitrocellulose membranes, which were blocked in Tris buffered saline containing 0.1% Tween20 (TBS-T) and 4% BSA. β-dystroglycan, however, required blocking in TBS-T containing 1% non-fat milk. Membranes were incubated overnight at 4°C with primary antibodies, washed with TBS-T, and incubated at room temperature for 1 hour with either biotinylated secondary antibodies (1:10,000), or HRP-conjugated secondary antibodies (1:2000). Biotinylated antibodies were washed and incubated with Peroxidase-conjugated Streptavidin (1:10,000) for 1 hour at room temperature. Detection of immunoreactive proteins on film was performed using enhanced chemiluminescence (ECL) (GE Healthcare).

Immunoprecipitation

Oligodendrocytes were differentiated on PDL-coated NUNC dishes for 4 days and lysed in ice-cold RIPA buffer. Lysates were incubated on ice for 15 minutes, and then clarified at 4°C to remove insoluble material. 250 ug of pre-cleared lysates were incubated with Protein A/G beads (Pierce) and either 5 ug/ml mouse IgG anti-β-DG (Novocastra), 5 ug/ml mouse IgG anti-FAK (BD Transduction), or 5 ug/ml control mouse IgG (Jackson) on a rotating wheel at 4°C overnight. Next, beads were pelleted and washed 3 times with RIPA buffer with protease and phosphatase inhibitors. Immunoprecipitated proteins were eluted from beads by boiling in SDS-PAGE sample buffer for 10 minutes and separated on an 8% SDS-PAGE gel.

Antibodies

Mouse IgM α-dystroglycan antibody (clone IIH6C4; Millipore) was used for immunocytochemistry, or, following dialysis to remove sodium azide, used in dystroglycan blocking experiments at 10 ug/ml. Hamster IgM against integrin β1 (clone Ha2/5, Pharmingen) was used at 10 μg/ml in blocking experiments. The following antibodies were used for immunocytochemistry: rabbit anti-FAK (phospho Y397), rabbit anti-NG2 Chondroitin Sulfate Proteoglycan (Chemicon), whole antiserum produced in rabbit against Galactocerebroside (GalC - Sigma), and mouse anti- 2',3'-cyclic nucleotide 3'-phosphodiesterase (CNPase - Sigma). Mouse anti-α-tubulin (Upstate) was used for immunobloting and immunocytochemistry. The following antibodies were used for immunoblot analysis: mouse anti-β-dystroglycan (Novocastra), rabbit IgG anti-lamin B1 (Abcam), mouse anti-Focal Adhesion Kinase (FAK - BD Transduction), mouse anti-β-actin (Sigma), biotinylated anti-mouse IgG (Vector Labs), and horseradish peroxidase linked sheep anti-mouse IgG (GE Healthcare). The following secondary antibodies

were used for immunocytochemistry: fluorescein (FITC)-conjugated donkey anti-rabbit IgG or DyLight488 donkey anti-rabbit IgG (Jackson) were used to detect GFP, NG2, GalC, and FAK pY397; Cy3-conjugated donkey anti-mouse IgG (Jackson) was used to detect CNP and β-dystroglycan; biotin-SP-conjugated $F(ab')_2$ donkey anti-mouse IgM (μ chain specific) and Cy3-conjugated streptavidin (Jackson) were used to detect α-dystroglycan; Cy5-conjugated donkey anti-rabbit IgG (Jackson) was used to detect FAK pY397 during coimmunocytochemistry.

Immunocytochemistry

Cells grown in chamber slides for morphological analysis were fixed with 4% paraformaldehyde (PFA) for 10 minutes, washed with PBS, permeabilized with 0.1% Triton X-100 in PBS for 5 minutes, and blocked for 1 hour in blocking buffer (1% BSA in PBS). Primary antibodies were incubated overnight at 4°C in blocking buffer, washed with PBS, and incubated for 1-2 hours at room temperature with secondary antibodies diluted in blocking buffer. Subsequent labeling of F-actin was accomplished using either Texas Red-X-phalloidin or Alexa488 phalloidin (Invitrogen) diluted in blocking buffer for 20 minutes at room temperature. Cell nuclei were labeled with 4',6-diamidino-2-phenylindole (DAPI) for 10 minutes at room temperature, and slides were then coverslipped with Fluoromount G (Southern Biotech). A live labeling technique was used to visualize α-dystroglycan. Briefly, cells were differentiated on acid washed coverslips coated with 25 μg/ml PDL in Boric Acid Buffer (50 mM boric acid, 12.5 mM sodium tetraborate, pH 8.5). At the required time of labeling, differentiation media was removed and replaced with fresh OPC culture media containing IIH6 anti α-dystroglycan and incubated for 20 minutes at room temperature. Following 3 quick washes in OPC media, cells were incubated with biotinylated anti-mouse IgM diluted in OPC media for 20 minutes at room

temperature. After 3 more quick washes with OPC media, cells were incubated with Cy3-conjugated streptavidin diluted in OPC media for 10 minutes at room temperature. Cells were briefly washed 3 more times, fixed with 4% PFA, and co-stained with primary antibodies or phalloidin.

Microscopy and Image Acquisition

Images for morphological analysis were captured with a Zeiss Axiocam MRM digital camera controlled by Zeiss Axiovision software (Rel. 4.8) using an inverted Zeiss Axioplan epifluorescence microscope fitted with a 10X eyepiece and either 20x (0.5 N.A.), 40x (0.75 N.A.), or 63x oil immersion objectives. High resolution α-dystroglycan localization and filopodia images were captured by a Cool Snap HQ2 digital camera controlled by Nikon Elements NES software using a Nikon Eclipse Ti inverted microscope fitted with a 10x eyepiece and either 60x or 100x Plan Apo oil immersion objectives. FAK pY397 and α-dystroglycan confocal images were acquired using a Zeiss LSM 510 Meta confocal microscope running Zeiss LSM software and fitted with a 10x eyepiece and either 100x or 63x Plan Apo oil immersion objectives.

Morphological Analysis

Oligodendrocytes identified by appropriate oligodendrocyte lineage protein antibodies were analyzed, and a minimum of 100 cells per experimental condition were measured (minimum 3 independent experiments). The length of the longest process was visualized by phalloidin labeling of F-actin and measured using ImageJ analysis software (NIH). A process was measured if the length of the process from the cell body to the leading distal edge was equal

to or greater than the diameter of the cell body. Additionally, where distinguishing the base of wide processes from the cell body was difficult, length was measured from the point where process width was equal to or less than half the width of the cell body diameter. Data is reported as the mean process length (μm).

The mean numbers of primary processes per cell were counted only in cells also measured for process length. Similarly, the numbers of secondary processes were counted only in cells also measured for process length (see Fig. 2A). Process complexity was measured using a Sholl analysis plug-in for ImageJ (see Fig. 3A). The following parameters were used for all Sholl analyses: 10 μm starting radius, 50 μm ending radius, 10 μm step size, and 0.1 μm span. Data is reported as the mean number of intersections per radius. A minimum of 30 randomly chosen cells per condition with at least one process ≥ 50 μm were analyzed (n=3 independent experiments).

The total length and number of filopodia formed by immature oligodendrocytes was measured using Zeiss Axiovision software (Rel. 4.8). OPCs were differentiated for 12 hours on PDL- or laminin-coated chamber slides in the presence or absence of dystroglycan blocking antibodies. A minimum of 30 randomly chosen oligodendrocytes per condition were analyzed and total number of filopodia per cell and filopodia length was measured (n=3 independent experiments). Data is reported as the mean number of filopodia per cell, or as mean filopodia length (μm). Additionally, to normalize filopodial measurements with respect to overall cell size, the total number of filopodia per cell was divided by the perimeter of the cell, and expressed as filopodia per micron of cell perimeter.

Statistical Analysis

Statistical analysis was performed using SigmaPlot 11 data analysis software. The Mann-Whitney Rank Sum Test was used to assess statistical significance in all experiments. Results were deemed significant if $P < 0.05$. All error bars represent Standard Error of the Mean (s.e.m.).

BIBLIOGRAPHY

Aguirre, A., and V. Gallo. 2004. Postnatal neurogenesis and gliogenesis in the olfactory bulb from NG2-expressing progenitors of the subventricular zone. J Neurosci. 24:10530-41.

Akhavan, A., S.N. Crivelli, M. Singh, V.R. Lingappa, and J.L. Muschler. 2008. SEA domain proteolysis determines the functional composition of dystroglycan. Faseb J. 22:612-21.

Armstrong, R.C., L. Harvath, and M.E. Dubois-Dalcq. 1990. Type 1 astrocytes and oligodendrocyte-type 2 astrocyte glial progenitors migrate toward distinct molecules. J Neurosci Res. 27:400-7.

Bansal, R., M. Kumar, K. Murray, R.S. Morrison, and S.E. Pfeiffer. 1996. Regulation of FGF receptors in the oligodendrocyte lineage. Mol Cell Neurosci. 7:263-75.

Barkhof, F., M. Filippi, D.H. Miller, P. Scheltens, A. Campi, C.H. Polman, G. Comi, H.J. Ader, N. Losseff, and J. Valk. 1997. Comparison of MRI criteria at first presentation to predict conversion to clinically definite multiple sclerosis. Brain. 120 (Pt 11):2059-69.

Barnett, M.H., and J.W. Prineas. 2004. Relapsing and remitting multiple sclerosis: pathology of the newly forming lesion. Ann Neurol. 55:458-68.

Barres, B.A., I.K. Hart, H.S. Coles, J.F. Burne, J.T. Voyvodic, W.D. Richardson, and M.C. Raff. 1992. Cell death and control of cell survival in the oligodendrocyte lineage. Cell. 70:31-46.

Barres, B.A., M.A. Lazar, and M.C. Raff. 1994b. A novel role for thyroid hormone, glucocorticoids and retinoic acid in timing oligodendrocyte development. Development. 120:1097-108.

Barres, B.A., M.C. Raff, F. Gaese, I. Bartke, G. Dechant, and Y.A. Barde. 1994a. A crucial role for neurotrophin-3 in oligodendrocyte development. Nature. 367:371-5.

Barres, B.A., R. Schmid, M. Sendnter, and M.C. Raff. 1993a. Multiple extracellular signals are required for long-term oligodendrocyte survival. Development. 118:283-95.

Barresi, R., and K.P. Campbell. 2006. Dystroglycan: from biosynthesis to pathogenesis of human disease. J Cell Sci. 119:199-207.

Barresi, R., D.E. Michele, M. Kanagawa, H.A. Harper, S.A. Dovico, J.S. Satz, S.A. Moore, W. Zhang, H. Schachter, J.P. Dumanski, R.D. Cohn, I. Nishino, and K.P. Campbell. 2004. LARGE can functionally bypass alpha-dystroglycan glycosylation defects in distinct congenital muscular dystrophies. Nat Med. 10:696-703.

Barros, C.S., T. Nguyen, K.S. Spencer, A. Nishiyama, H. Colognato, and U. Muller. 2009. Beta1 integrins are required for normal CNS myelination and promote AKT-dependent myelin outgrowth. Development. 136:2717-24.

Batchelor, C.L., J.R. Higginson, Y.J. Chen, C. Vanni, A. Eva, and S.J. Winder. 2007. Recruitment of Dbl by ezrin and dystroglycan drives membrane proximal Cdc42 activation and filopodia formation. Cell Cycle. 6:353-63.

Bauer, N.G., C. Richter-Landsberg, and C. Ffrench-Constant. 2009. Role of the oligodendroglial cytoskeleton in differentiation and myelination. Glia. 57:1691-705.

Beggs, H.E., D. Schahin-Reed, K. Zang, S. Goebbels, K.A. Nave, J. Gorski, K.R. Jones, D. Sretavan, and L.F. Reichardt. 2003. FAK deficiency in cells contributing to the basal lamina results in cortical abnormalities resembling congenital muscular dystrophies. Neuron. 40:501-14.

Benninger, Y., H. Colognato, T. Thurnherr, R.J. Franklin, D.P. Leone, S. Atanasoski, K.A. Nave, C. Ffrench-Constant, U. Suter, and J.B. Relvas. 2006. Beta1-integrin signaling mediates premyelinating oligodendrocyte survival but is not required for CNS myelination and remyelination. J Neurosci. 26:7665-73.

Berti, C., L. Bartesaghi, M. Ghidinelli, D. Zambroni, G. Figlia, Z.L. Chen, A. Quattrini, L. Wrabetz, and M.L. Feltri. 2011. Non-redundant function of dystroglycan and beta1 integrins in radial sorting of axons. Development. 138:4025-37.

Bogler, O., and M. Noble. 1994. Measurement of time in oligodendrocyte-type-2 astrocyte (O-2A) progenitors is a cellular process distinct from differentiation or division. Dev Biol. 162:525-38.

Bogler, O., D. Wren, S.C. Barnett, H. Land, and M. Noble. 1990. Cooperation between two growth factors promotes extended self-renewal and inhibits differentiation of oligodendrocyte-type-2 astrocyte (O-2A) progenitor cells. Proc Natl Acad Sci U S A. 87:6368-72.

Bottenstein, J.E., and G.H. Sato. 1979. Growth of a rat neuroblastoma cell line in serum-free supplemented medium. Proc Natl Acad Sci U S A. 76:514-7.

Bray, G.M., S. Perkins, A.C. Peterson, and A.J. Aguayo. 1977. Schwann cell multiplication deficit in nerve roots of newborn dystrophic mice. A radioautographic and ultrastructural study. J Neurol Sci. 32:203-12.

Buttery, P.C., and C. ffrench-Constant. 1999. Laminin-2/integrin interactions enhance myelin membrane formation by oligodendrocytes. Mol Cell Neurosci. 14:199-212.

Camara, J., Z. Wang, C. Nunes-Fonseca, H.C. Friedman, M. Grove, D.L. Sherman, N.H. Komiyama, S.G. Grant, P.J. Brophy, A. Peterson, and C. ffrench-Constant. 2009. Integrin-mediated axoglial interactions initiate myelination in the central nervous system. J Cell Biol. 185:699-712.

Caro, P.A., M. Scavina, E. Hoffman, E. Pegoraro, and H.G. Marks. 1999. MR imaging findings in children with merosin-deficient congenital muscular dystrophy. AJNR Am J Neuroradiol. 20:324-6.

Carson, M.J., R.R. Behringer, R.L. Brinster, and F.A. McMorris. 1993. Insulin-like growth factor I increases brain growth and central nervous system myelination in transgenic mice. Neuron. 10:729-40.

Casaccia-Bonnefil, P., R. Tikoo, H. Kiyokawa, V. Friedrich, Jr., M.V. Chao, and A. Koff. 1997. Oligodendrocyte precursor differentiation is perturbed in the absence of the cyclin-dependent kinase inhibitor p27Kip1. Genes Dev. 11:2335-46.

Cavaldesi, M., G. Macchia, S. Barca, P. Defilippi, G. Tarone, and T.C. Petrucci. 1999. Association of the dystroglycan complex isolated from bovine brain synaptosomes with proteins involved in signal transduction. J Neurochem. 72:1648-55.

Charles, P., M.P. Hernandez, B. Stankoff, M.S. Aigrot, C. Colin, G. Rougon, B. Zalc, and C. Lubetzki. 2000. Negative regulation of central nervous system myelination by polysialylated-neural cell adhesion molecule. Proc Natl Acad Sci U S A. 97:7585-90.

Chen, Y.J., H.J. Spence, J.M. Cameron, T. Jess, J.L. Ilsley, and S.J. Winder. 2003. Direct interaction of beta-dystroglycan with F-actin. Biochem J. 375:329-37.

Chong, S.Y., S.S. Rosenberg, S.P. Fancy, C. Zhao, Y.A. Shen, A.T. Hahn, A.W. McGee, X. Xu, B. Zheng, L.I. Zhang, D.H. Rowitch, R.J. Franklin, Q.R. Lu, and J.R. Chan. 2012. Neurite outgrowth inhibitor Nogo-A establishes spatial segregation and extent of oligodendrocyte myelination. Proc Natl Acad Sci U S A. 109:1299-304.

Chrast, R., G. Saher, K.A. Nave, and M.H. Verheijen. 2011. Lipid metabolism in myelinating glial cells: lessons from human inherited disorders and mouse models. J Lipid Res. 52:419-34.

Chun, S.J., M.N. Rasband, R.L. Sidman, A.A. Habib, and T. Vartanian. 2003. Integrin-linked kinase is required for laminin-2-induced oligodendrocyte cell spreading and CNS myelination. J Cell Biol. 163:397-408.

Clement, E., E. Mercuri, C. Godfrey, J. Smith, S. Robb, M. Kinali, V. Straub, K. Bushby, A. Manzur, B. Talim, F. Cowan, R. Quinlivan, A. Klein, C. Longman, R. McWilliam, H. Topaloglu, R. Mein, S. Abbs, K. North, A.J. Barkovich, M. Rutherford, and F. Muntoni. 2008. Brain involvement in muscular dystrophies with defective dystroglycan glycosylation. Ann Neurol. 64:573-82.

Colognato, H., W. Baron, V. Avellana-Adalid, J.B. Relvas, A. Baron-Van Evercooren, E. Georges-Labouesse, and C. ffrench-Constant. 2002. CNS integrins switch growth factor signalling to promote target-dependent survival. Nat Cell Biol. 4:833-41.

Colognato, H., C. ffrench-Constant, and M.L. Feltri. 2005. Human diseases reveal novel roles for neural laminins. Trends Neurosci. 28:480-6.

Colognato, H., J. Galvin, Z. Wang, J. Relucio, T. Nguyen, D. Harrison, P.D. Yurchenco, and C. Ffrench-Constant. 2007. Identification of dystroglycan as a second laminin receptor in oligodendrocytes, with a role in myelination. Development. 134:1723-36.

Colognato, H., D.A. Winkelmann, and P.D. Yurchenco. 1999. Laminin polymerization induces a receptor-cytoskeleton network. J Cell Biol. 145:619-31.

Cormand, B., H. Pihko, M. Bayes, L. Valanne, P. Santavuori, B. Talim, R. Gershoni-Baruch, A. Ahmad, H. van Bokhoven, H.G. Brunner, T. Voit, H. Topaloglu, W.B. Dobyns, and A.E. Lehesjoki. 2001. Clinical and genetic distinction between Walker-Warburg syndrome and muscle-eye-brain disease. Neurology. 56:1059-69.

Court, F.A., J.E. Hewitt, K. Davies, B.L. Patton, A. Uncini, L. Wrabetz, and M.L. Feltri. 2009. A laminin-2, dystroglycan, utrophin axis is required for compartmentalization and elongation of myelin segments. J Neurosci. 29:3908-19.

Court, F.A., D. Zambroni, E. Pavoni, C. Colombelli, C. Baragli, G. Figlia, L. Sorokin, W. Ching, J.L. Salzer, L. Wrabetz, and M.L. Feltri. 2011. MMP2-9 cleavage of dystroglycan alters the size and molecular composition of Schwann cell domains. J Neurosci. 31:12208-17.

Dale, R.C., C. de Sousa, W.K. Chong, T.C. Cox, B. Harding, and B.G. Neville. 2000. Acute disseminated encephalomyelitis, multiphasic disseminated encephalomyelitis and multiple sclerosis in children. Brain. 123 Pt 12:2407-22.

Dent, E.W., A.V. Kwiatkowski, L.M. Mebane, U. Philippar, M. Barzik, D.A. Rubinson, S. Gupton, J.E. Van Veen, C. Furman, J. Zhang, A.S. Alberts, S. Mori, and F.B. Gertler. 2007. Filopodia are required for cortical neurite initiation. Nat Cell Biol. 9:1347-59.

Di Muzio, A., M.V. De Angelis, P. Di Fulvio, A. Ratti, A. Pizzuti, L. Stuppia, D. Gambi, and A. Uncini. 2003. Dysmyelinating sensory-motor neuropathy in merosin-deficient congenital muscular dystrophy. Muscle Nerve. 27:500-6.

Dincer, P., B. Balci, Y. Yuva, B. Talim, M. Brockington, D. Dincel, S. Torelli, S. Brown, G. Kale, G. Haliloglu, F.O. Gerceker, R.C. Atalay, C. Yakicier, C. Longman, F. Muntoni, and H. Topaloglu. 2003. A novel form of recessive limb girdle muscular dystrophy with mental retardation and abnormal expression of alpha-dystroglycan. Neuromuscul Disord. 13:771-8.

Driss, A., L. Charrier, Y. Yan, V. Nduati, S. Sitaraman, and D. Merlin. 2006. Dystroglycan receptor is involved in integrin activation in intestinal epithelia. Am J Physiol Gastrointest Liver Physiol. 290:G1228-42.

Dugas, J.C., A. Ibrahim, and B.A. Barres. 2007. A crucial role for p57(Kip2) in the intracellular timer that controls oligodendrocyte differentiation. J Neurosci. 27:6185-96.

Emery, B., D. Agalliu, J.D. Cahoy, T.A. Watkins, J.C. Dugas, S.B. Mulinyawe, A. Ibrahim, K.L. Ligon, D.H. Rowitch, and B.A. Barres. 2009. Myelin gene regulatory factor is a critical transcriptional regulator required for CNS myelination. Cell. 138:172-85.

Ervasti, J.M., and K.P. Campbell. 1991. Membrane organization of the dystrophin-glycoprotein complex. Cell. 66:1121-31.

Ervasti, J.M., and K.P. Campbell. 1993. A role for the dystrophin-glycoprotein complex as a transmembrane linker between laminin and actin. J Cell Biol. 122:809-23.

Espinosa de los Monteros, A., M. Zhang, and J. De Vellis. 1993. O2A progenitor cells transplanted into the neonatal rat brain develop into oligodendrocytes but not astrocytes. Proc Natl Acad Sci U S A. 90:50-4.

Etienne-Manneville, S., and A. Hall. 2002. Rho GTPases in cell biology. Nature. 420:629-35.

Eugster, H.P., K. Frei, R. Bachmann, H. Bluethmann, H. Lassmann, and A. Fontana. 1999. Severity of symptoms and demyelination in MOG-induced EAE depends on TNFR1. Eur J Immunol. 29:626-32.

Eyermann, C., K. Czaplinski, and H. Colognato. 2012. Dystroglycan promotes filopodial formation and process branching in differentiating oligodendroglia. J Neurochem. 120:928-47.

Fancy, S.P., S.E. Baranzini, C. Zhao, D.I. Yuk, K.A. Irvine, S. Kaing, N. Sanai, R.J. Franklin, and D.H. Rowitch. 2009. Dysregulation of the Wnt pathway inhibits timely myelination and remyelination in the mammalian CNS. Genes Dev. 23:1571-85.

Feltri, M.L., D. Graus Porta, S.C. Previtali, A. Nodari, B. Migliavacca, A. Cassetti, A. Littlewood-Evans, L.F. Reichardt, A. Messing, A. Quattrini, U. Mueller, and L. Wrabetz. 2002. Conditional disruption of beta 1 integrin in Schwann cells impedes interactions with axons. J Cell Biol. 156:199-209.

Feltri, M.L., and L. Wrabetz. 2005. Laminins and their receptors in Schwann cells and hereditary neuropathies. J Peripher Nerv Syst. 10:128-43.

Ferletta, M., Y. Kikkawa, H. Yu, J.F. Talts, M. Durbeej, A. Sonnenberg, R. Timpl, K.P. Campbell, P. Ekblom, and E. Genersch. 2003. Opposing roles of integrin alpha6Abeta1 and dystroglycan in laminin-mediated extracellular signal-regulated kinase activation. Mol Biol Cell. 14:2088-103.

Fewou, S.N., H. Ramakrishnan, H. Bussow, V. Gieselmann, and M. Eckhardt. 2007. Down-regulation of polysialic acid is required for efficient myelin formation. J Biol Chem. 282:16700-11.

Forrest, A.D., H.E. Beggs, L.F. Reichardt, J.L. Dupree, R.J. Colello, and B. Fuss. 2009. Focal adhesion kinase (FAK): A regulator of CNS myelination. J Neurosci Res. 87:3456-64.

Frost, A.R., S.V. Bohm, R.N. Sewduth, D. Josifova, C.M. Ogilvie, L. Izatt, and R.G. Roberts. 2010. Heterozygous deletion of a 2-Mb region including the dystroglycan gene in a patient with mild myopathy, facial hypotonia, oral-motor dyspraxia and white matter abnormalities. Eur J Hum Genet. 18:852-5.

Fuentes-Mera, L., R. Rodriguez-Munoz, R. Gonzalez-Ramirez, F. Garcia-Sierra, E. Gonzalez, D. Mornet, and B. Cisneros. 2006. Characterization of a novel Dp71 dystrophin-associated protein complex (DAPC) present in the nucleus of HeLa cells: members of the nuclear DAPC associate with the nuclear matrix. Exp Cell Res. 312:3023-35.

Fujimoto, I., J.L. Bruses, and U. Rutishauser. 2001. Regulation of cell adhesion by polysialic acid. Effects on cadherin, immunoglobulin cell adhesion molecule, and integrin function and independence from neural cell adhesion molecule binding or signaling activity. J Biol Chem. 276:31745-51.

Furtado, G.C., M.C. Marcondes, J.A. Latkowski, J. Tsai, A. Wensky, and J.J. Lafaille. 2008. Swift entry of myelin-specific T lymphocytes into the central nervous system in spontaneous autoimmune encephalomyelitis. J Immunol. 181:4648-55.

Furusho, M., J.L. Dupree, K.A. Nave, and R. Bansal. 2012. Fibroblast growth factor receptor signaling in oligodendrocytes regulates myelin sheath thickness. J Neurosci. 32:6631-41.

Gee, S.H., R.W. Blacher, P.J. Douville, P.R. Provost, P.D. Yurchenco, and S. Carbonetto. 1993. Laminin-binding protein 120 from brain is closely related to the dystrophin-associated glycoprotein, dystroglycan, and binds with high affinity to the major heparin binding domain of laminin. J Biol Chem. 268:14972-80.

Gee, S.H., F. Montanaro, M.H. Lindenbaum, and S. Carbonetto. 1994. Dystroglycan-alpha, a dystrophin-associated glycoprotein, is a functional agrin receptor. Cell. 77:675-86.

Givogri, M.I., R.M. Costa, V. Schonmann, A.J. Silva, A.T. Campagnoni, and E.R. Bongarzone. 2002. Central nervous system myelination in mice with deficient expression of Notch1 receptor. J Neurosci Res. 67:309-20.

Godfrey, C., E. Clement, R. Mein, M. Brockington, J. Smith, B. Talim, V. Straub, S. Robb, R. Quinlivan, L. Feng, C. Jimenez-Mallebrera, E. Mercuri, A.Y. Manzur, M. Kinali, S. Torelli, S.C. Brown, C.A. Sewry, K. Bushby, H. Topaloglu, K. North, S. Abbs, and F. Muntoni. 2007. Refining genotype phenotype correlations in muscular dystrophies with defective glycosylation of dystroglycan. Brain. 130:2725-35.

Gonye, G.E., A.E. Warrington, J.A. DeVito, and S.E. Pfeiffer. 1994. Oligodendrocyte precursor quantitation and localization in perinatal brain using a retrospective bioassay. J Neurosci. 14:5365-72.

Gonzalez-Ramirez, R., S.L. Morales-Lazaro, V. Tapia-Ramirez, D. Mornet, and B. Cisneros. 2008. Nuclear and nuclear envelope localization of dystrophin Dp71 and dystrophin-associated proteins (DAPs) in the C2C12 muscle cells: DAPs nuclear localization is modulated during myogenesis. J Cell Biochem. 105:735-45.

Grandbarbe, L., J. Bouissac, M. Rand, M. Hrabe de Angelis, S. Artavanis-Tsakonas, and E. Mohier. 2003. Delta-Notch signaling controls the generation of neurons/glia from neural stem cells in a stepwise process. Development. 130:1391-402.

Guglieri, M., V. Straub, K. Bushby, and H. Lochmuller. 2008. Limb-girdle muscular dystrophies. Curr Opin Neurol. 21:576-84.

Hara, Y., B. Balci-Hayta, T. Yoshida-Moriguchi, M. Kanagawa, D. Beltran-Valero de Bernabe, H. Gundesli, T. Willer, J.S. Satz, R.W. Crawford, S.J. Burden, S. Kunz, M.B. Oldstone, A. Accardi, B. Talim, F. Muntoni, H. Topaloglu, P. Dincer, and K.P. Campbell. 2011. A dystroglycan mutation associated with limb-girdle muscular dystrophy. N Engl J Med. 364:939-46.

He, Y., J. Sandoval, and P. Casaccia-Bonnefil. 2007. Events at the transition between cell cycle exit and oligodendrocyte progenitor differentiation: the role of HDAC and YY1. Neuron Glia Biol. 3:221-31.

Hess, J., P. Angel, and M. Schorpp-Kistner. 2004. AP-1 subunits: quarrel and harmony among siblings. J Cell Sci. 117:5965-73.

Holzfeind, P.J., P.K. Grewal, H.A. Reitsamer, J. Kechvar, H. Lassmann, H. Hoeger, J.E. Hewitt, and R.E. Bittner. 2002. Skeletal, cardiac and tongue muscle pathology, defective retinal transmission, and neuronal migration defects in the Large(myd) mouse defines a natural model for glycosylation-deficient muscle - eye - brain disorders. Hum Mol Genet. 11:2673-87.

Hoshina, N., T. Tezuka, K. Yokoyama, H. Kozuka-Hata, M. Oyama, and T. Yamamoto. 2007. Focal adhesion kinase regulates laminin-induced oligodendroglial process outgrowth. Genes Cells. 12:1245-54.

Hosokawa, H., H. Ninomiya, Y. Kitamura, K. Fujiwara, and T. Masaki. 2002. Vascular endothelial cells that express dystroglycan are involved in angiogenesis. J Cell Sci. 115:1487-96.

Hsieh, J., J.B. Aimone, B.K. Kaspar, T. Kuwabara, K. Nakashima, and F.H. Gage. 2004. IGF-I instructs multipotent adult neural progenitor cells to become oligodendrocytes. J Cell Biol. 164:111-22.

Hu, Q.D., B.T. Ang, M. Karsak, W.P. Hu, X.Y. Cui, T. Duka, Y. Takeda, W. Chia, N. Sankar, Y.K. Ng, E.A. Ling, T. Maciag, D. Small, R. Trifonova, R. Kopan, H. Okano, M. Nakafuku, S. Chiba, H. Hirai, J.C. Aster, M. Schachner, C.J. Pallen, K. Watanabe, and Z.C. Xiao. 2003. F3/contactin acts as a functional ligand for Notch during oligodendrocyte maturation. Cell. 115:163-75.

Ibraghimov-Beskrovnaya, O., J.M. Ervasti, C.J. Leveille, C.A. Slaughter, S.W. Sernett, and K.P. Campbell. 1992. Primary structure of dystrophin-associated glycoproteins linking dystrophin to the extracellular matrix. Nature. 355:696-702.

Ilsley, J.L., M. Sudol, and S.J. Winder. 2001. The interaction of dystrophin with beta-dystroglycan is regulated by tyrosine phosphorylation. Cell Signal. 13:625-32.

Jackman, N., A. Ishii, and R. Bansal. 2009. Oligodendrocyte development and myelin biogenesis: parsing out the roles of glycosphingolipids. Physiology (Bethesda). 24:290-7.

Jang, K.J., M.S. Kim, D. Feltrin, N.L. Jeon, K.Y. Suh, and O. Pertz. 2010. Two distinct filopodia populations at the growth cone allow to sense nanotopographical extracellular matrix cues to guide neurite outgrowth. PLoS One. 5:e15966.

Jiang, F., T.J. Frederick, and T.L. Wood. 2001. IGF-I synergizes with FGF-2 to stimulate oligodendrocyte progenitor entry into the cell cycle. Dev Biol. 232:414-23.

Johnson, C.P., I. Fujimoto, U. Rutishauser, and D.E. Leckband. 2005. Direct evidence that neural cell adhesion molecule (NCAM) polysialylation increases intermembrane repulsion and abrogates adhesion. J Biol Chem. 280:137-45.

Jones, K.J., G. Morgan, H. Johnston, V. Tobias, R.A. Ouvrier, I. Wilkinson, and K.N. North. 2001. The expanding phenotype of laminin alpha2 chain (merosin) abnormalities: case series and review. J Med Genet. 38:649-57.

Kim, H.J., A.B. DiBernardo, J.A. Sloane, M.N. Rasband, D. Solomon, B. Kosaras, S.P. Kwak, and T.K. Vartanian. 2006. WAVE1 is required for oligodendrocyte morphogenesis and normal CNS myelination. J Neurosci. 26:5849-59.

Kondo, T., and M. Raff. 2000. Oligodendrocyte precursor cells reprogrammed to become multipotential CNS stem cells. Science. 289:1754-7.

Kondo-Iida, E., K. Kobayashi, M. Watanabe, J. Sasaki, T. Kumagai, H. Koide, K. Saito, M. Osawa, Y. Nakamura, and T. Toda. 1999. Novel mutations and genotype-phenotype relationships in 107 families with Fukuyama-type congenital muscular dystrophy (FCMD). Hum Mol Genet. 8:2303-9.

Lachapelle, F., M. Gumpel, M. Baulac, C. Jacque, P. Duc, and N. Baumann. 1983. Transplantation of CNS fragments into the brain of shiverer mutant mice: extensive myelination by implanted oligodendrocytes. I. Immunohistochemical studies. Dev Neurosci. 6:325-34.

Lafrenaye, A.D., and B. Fuss. 2010. Focal adhesion kinase can play unique and opposing roles in regulating the morphology of differentiating oligodendrocytes. J Neurochem. 115:269-82.

Lappe-Siefke, C., S. Goebbels, M. Gravel, E. Nicksch, J. Lee, P.E. Braun, I.R. Griffiths, and K.A. Nave. 2003. Disruption of Cnp1 uncouples oligodendroglial functions in axonal support and myelination. Nat Genet. 33:366-74.

Lara-Chacon, B., M.B. de Leon, D. Leocadio, P. Gomez, L. Fuentes-Mera, I. Martinez-Vieyra, A. Ortega, D.A. Jans, and B. Cisneros. 2010. Characterization of an Importin alpha/beta-recognized nuclear localization signal in beta-dystroglycan. J Cell Biochem. 110:706-17.

Larsen, P.H., A.G. DaSilva, K. Conant, and V.W. Yong. 2006. Myelin formation during development of the CNS is delayed in matrix metalloproteinase-9 and -12 null mice. J Neurosci. 26:2207-14.

Liu, Y., and M.S. Rao. 2004. Glial progenitors in the CNS and possible lineage relationships among them. Biol Cell. 96:279-90.

Liu, Z., X. Hu, J. Cai, B. Liu, X. Peng, M. Wegner, and M. Qiu. 2007. Induction of oligodendrocyte differentiation by Olig2 and Sox10: evidence for reciprocal interactions and dosage-dependent mechanisms. Dev Biol. 302:683-93.

Losasso, C., F. Di Tommaso, A. Sgambato, R. Ardito, A. Cittadini, B. Giardina, T.C. Petrucci, and A. Brancaccio. 2000. Anomalous dystroglycan in carcinoma cell lines. FEBS Lett. 484:194-8.

Lu, Q.R., T. Sun, Z. Zhu, N. Ma, M. Garcia, C.D. Stiles, and D.H. Rowitch. 2002. Common developmental requirement for Olig function indicates a motor neuron/oligodendrocyte connection. Cell. 109:75-86.

Lunn, K.F., P.W. Baas, and I.D. Duncan. 1997. Microtubule organization and stability in the oligodendrocyte. J Neurosci. 17:4921-32.

Mabie, P.C., M.F. Mehler, R. Marmur, A. Papavasiliou, Q. Song, and J.A. Kessler. 1997. Bone morphogenetic proteins induce astroglial differentiation of oligodendroglial-astroglial progenitor cells. J Neurosci. 17:4112-20.

Mason, J.L., P. Ye, K. Suzuki, A.J. D'Ercole, and G.K. Matsushima. 2000. Insulin-like growth factor-1 inhibits mature oligodendrocyte apoptosis during primary demyelination. J Neurosci. 20:5703-8.

Matsumura, K., H. Yamada, F. Saito, Y. Sunada, and T. Shimizu. 1997. Peripheral nerve involvement in merosin-deficient congenital muscular dystrophy and dy mouse. Neuromuscul Disord. 7:7-12.

Mattila, P.K., and P. Lappalainen. 2008. Filopodia: molecular architecture and cellular functions. Nat Rev Mol Cell Biol. 9:446-54.

Mattson, M.P. 2003. Excitotoxic and excitoprotective mechanisms: abundant targets for the prevention and treatment of neurodegenerative disorders. Neuromolecular Med. 3:65-94.

McCarthy, K.D., and J. de Vellis. 1980. Preparation of separate astroglial and oligodendroglial cell cultures from rat cerebral tissue. J Cell Biol. 85:890-902.

McKinnon, R.D., T. Matsui, M. Aranda, and M. Dubois-Dalcq. 1991. A role for fibroblast growth factor in oligodendrocyte development. Ann N Y Acad Sci. 638:378-86.

McMorris, F.A., T.M. Smith, S. DeSalvo, and R.W. Furlanetto. 1986. Insulin-like growth factor I/somatomedin C: a potent inducer of oligodendrocyte development. Proc Natl Acad Sci U S A. 83:822-6.

McTigue, D.M., and R.B. Tripathi. 2008. The life, death, and replacement of oligodendrocytes in the adult CNS. J Neurochem. 107:1-19.

Mehler, M.F., P.C. Mabie, G. Zhu, S. Gokhan, and J.A. Kessler. 2000. Developmental changes in progenitor cell responsiveness to bone morphogenetic proteins differentially modulate progressive CNS lineage fate. Dev Neurosci. 22:74-85.

Michele, D.E., R. Barresi, M. Kanagawa, F. Saito, R.D. Cohn, J.S. Satz, J. Dollar, I. Nishino, R.I. Kelley, H. Somer, V. Straub, K.D. Mathews, S.A. Moore, and K.P. Campbell. 2002. Post-translational disruption of dystroglycan-ligand interactions in congenital muscular dystrophies. Nature. 418:417-22.

Miller, R.H. 2002. Regulation of oligodendrocyte development in the vertebrate CNS. Prog Neurobiol. 67:451-67.

Miller, R.H., J. Payne, L. Milner, H. Zhang, and D.M. Orentas. 1997. Spinal cord oligodendrocytes develop from a limited number of migratory highly proliferative precursors. J Neurosci Res. 50:157-68.

Milner, R., and C. Ffrench-Constant. 1994. A developmental analysis of oligodendroglial integrins in primary cells: changes in alpha v-associated beta subunits during differentiation. Development. 120:3497-506.

Miner, J.H., and P.D. Yurchenco. 2004. Laminin functions in tissue morphogenesis. Annu Rev Cell Dev Biol. 20:255-84.

Mirsky, R., and K.R. Jessen. 1999. The neurobiology of Schwann cells. Brain Pathol. 9:293-311.

Mitra, S.K., D.A. Hanson, and D.D. Schlaepfer. 2005. Focal adhesion kinase: in command and control of cell motility. Nat Rev Mol Cell Biol. 6:56-68.

Miyagoe-Suzuki, Y., M. Nakagawa, and S. Takeda. 2000. Merosin and congenital muscular dystrophy. Microsc Res Tech. 48:181-91.

Montanaro, F., M. Lindenbaum, and S. Carbonetto. 1999. alpha-Dystroglycan is a laminin receptor involved in extracellular matrix assembly on myotubes and muscle cell viability. J Cell Biol. 145:1325-40.

Moore, C.J., and S.J. Winder. 2010. Dystroglycan versatility in cell adhesion: a tale of multiple motifs. Cell Commun Signal. 8:3.

Moore, S.A., F. Saito, J. Chen, D.E. Michele, M.D. Henry, A. Messing, R.D. Cohn, S.E. Ross-Barta, S. Westra, R.A. Williamson, T. Hoshi, and K.P. Campbell. 2002. Deletion of brain dystroglycan recapitulates aspects of congenital muscular dystrophy. Nature. 418:422-5.

Mostoslavsky, G., A.J. Fabian, S. Rooney, F.W. Alt, and R.C. Mulligan. 2006. Complete correction of murine Artemis immunodeficiency by lentiviral vector-mediated gene transfer. Proc Natl Acad Sci U S A. 103:16406-11.

Nakahara, J., S. Aiso, and N. Suzuki. 2010. Autoimmune versus oligodendrogliopathy: the pathogenesis of multiple sclerosis. Arch Immunol Ther Exp (Warsz). 58:325-33.

Nishiyama, A., M. Komitova, R. Suzuki, and X. Zhu. 2009. Polydendrocytes (NG2 cells): multifunctional cells with lineage plasticity. Nat Rev Neurosci. 10:9-22.

Noble, M., K. Murray, P. Stroobant, M.D. Waterfield, and P. Riddle. 1988. Platelet-derived growth factor promotes division and motility and inhibits premature differentiation of the oligodendrocyte/type-2 astrocyte progenitor cell. Nature. 333:560-2.

Nodari, A., S.C. Previtali, G. Dati, S. Occhi, F.A. Court, C. Colombelli, D. Zambroni, G. Dina, U. Del Carro, K.P. Campbell, A. Quattrini, L. Wrabetz, and M.L. Feltri. 2008. Alpha6beta4 integrin and dystroglycan cooperate to stabilize the myelin sheath. J Neurosci. 28:6714-9.

O'Meara, R.W., J.P. Michalski, and R. Kothary. 2010. Integrin signaling in oligodendrocytes and its importance in CNS myelination. J Signal Transduct. 2011:354091.

Occhi, S., D. Zambroni, U. Del Carro, S. Amadio, E.E. Sirkowski, S.S. Scherer, K.P. Campbell, S.A. Moore, Z.L. Chen, S. Strickland, A. Di Muzio, A. Uncini, L. Wrabetz, and M.L. Feltri. 2005. Both laminin and Schwann cell dystroglycan are necessary for proper clustering of sodium channels at nodes of Ranvier. J Neurosci. 25:9418-27.

Oh, L.Y., P.H. Larsen, C.A. Krekoski, D.R. Edwards, F. Donovan, Z. Werb, and V.W. Yong. 1999. Matrix metalloproteinase-9/gelatinase B is required for process outgrowth by oligodendrocytes. J Neurosci. 19:8464-75.

Oppizzi, M.L., A. Akhavan, M. Singh, J.E. Fata, and J.L. Muschler. 2008. Nuclear translocation of beta-dystroglycan reveals a distinctive trafficking pattern of autoproteolyzed mucins. Traffic. 9:2063-72.

Orentas, D.M., J.E. Hayes, K.L. Dyer, and R.H. Miller. 1999. Sonic hedgehog signaling is required during the appearance of spinal cord oligodendrocyte precursors. Development. 126:2419-29.

Park, H.C., and B. Appel. 2003. Delta-Notch signaling regulates oligodendrocyte specification. Development. 130:3747-55.

Peng, H.B., A.A. Ali, D.F. Daggett, H. Rauvala, J.R. Hassell, and N.R. Smalheiser. 1998. The relationship between perlecan and dystroglycan and its implication in the formation of the neuromuscular junction. Cell Adhes Commun. 5:475-89.

Philpot, J., F. Cowan, J. Pennock, C. Sewry, V. Dubowitz, G. Bydder, and F. Muntoni. 1999. Merosin-deficient congenital muscular dystrophy: the spectrum of brain involvement on magnetic resonance imaging. Neuromuscul Disord. 9:81-5.

Polito, A., and R. Reynolds. 2005. NG2-expressing cells as oligodendrocyte progenitors in the normal and demyelinated adult central nervous system. J Anat. 207:707-16.

Previtali, S.C., A. Nodari, C. Taveggia, C. Pardini, G. Dina, A. Villa, L. Wrabetz, A. Quattrini, and M.L. Feltri. 2003. Expression of laminin receptors in schwann cell differentiation: evidence for distinct roles. J Neurosci. 23:5520-30.

Pringle, N.P., H.S. Mudhar, E.J. Collarini, and W.D. Richardson. 1992. PDGF receptors in the rat CNS: during late neurogenesis, PDGF alpha-receptor expression appears to be restricted to glial cells of the oligodendrocyte lineage. Development. 115:535-51.

Privat, A., C. Jacque, J.M. Bourre, P. Dupouey, and N. Baumann. 1979. Absence of the major dense line in myelin of the mutant mouse "shiverer". Neurosci Lett. 12:107-12.

Qian, X., A.A. Davis, S.K. Goderie, and S. Temple. 1997. FGF2 concentration regulates the generation of neurons and glia from multipotent cortical stem cells. Neuron. 18:81-93.

Quijano-Roy, S., F. Renault, N. Romero, P. Guicheney, M. Fardeau, and B. Estournet. 2004. EMG and nerve conduction studies in children with congenital muscular dystrophy. Muscle Nerve. 29:292-9.

Reboldi, A., C. Coisne, D. Baumjohann, F. Benvenuto, D. Bottinelli, S. Lira, A. Uccelli, A. Lanzavecchia, B. Engelhardt, and F. Sallusto. 2009. C-C chemokine receptor 6-regulated entry of TH-17 cells into the CNS through the choroid plexus is required for the initiation of EAE. Nat Immunol. 10:514-23.

Relucio, J., M.J. Menezes, Y. Miyagoe-Suzuki, S. Takeda, and H. Colognato. 2012. Laminin regulates postnatal oligodendrocyte production by promoting oligodendrocyte progenitor survival in the subventricular zone. Glia.

Relucio, J., I.D. Tzvetanova, W. Ao, S. Lindquist, and H. Colognato. 2009. Laminin alters fyn regulatory mechanisms and promotes oligodendrocyte development. J Neurosci. 29:11794-806.

Renaud, D.L. 2012. Inherited leukoencephalopathies. Semin Neurol. 32:3-8.

Richardson, W.D., N. Kessaris, and N. Pringle. 2006. Oligodendrocyte wars. Nat Rev Neurosci. 7:11-8.

Richardson, W.D., N. Pringle, M.J. Mosley, B. Westermark, and M. Dubois-Dalcq. 1988. A role for platelet-derived growth factor in normal gliogenesis in the central nervous system. Cell. 53:309-19.

Richter-Landsberg, C. 2008. The cytoskeleton in oligodendrocytes. Microtubule dynamics in health and disease. J Mol Neurosci. 35:55-63.

Rosenberg, S.S., and J.R. Chan. 2009. Modulating myelination: knowing when to say Wnt. Genes Dev. 23:1487-93.

Rumsby, M., F. Afsari, M. Stark, and E. Hughson. 2003. Microfilament and microtubule organization and dynamics in process extension by central glia-4 oligodendrocytes: evidence for a microtubule organizing center. Glia. 42:118-29.

Russo, K., E. Di Stasio, G. Macchia, G. Rosa, A. Brancaccio, and T.C. Petrucci. 2000. Characterization of the beta-dystroglycan-growth factor receptor 2 (Grb2) interaction. Biochem Biophys Res Commun. 274:93-8.

Saito, F., S.A. Moore, R. Barresi, M.D. Henry, A. Messing, S.E. Ross-Barta, R.D. Cohn, R.A. Williamson, K.A. Sluka, D.L. Sherman, P.J. Brophy, J.D. Schmelzer, P.A. Low, L. Wrabetz, M.L. Feltri, and K.P. Campbell. 2003. Unique role of dystroglycan in peripheral nerve myelination, nodal structure, and sodium channel stabilization. Neuron. 38:747-58.

Sato, S., Y. Omori, K. Katoh, M. Kondo, M. Kanagawa, K. Miyata, K. Funabiki, T. Koyasu, N. Kajimura, T. Miyoshi, H. Sawai, K. Kobayashi, A. Tani, T. Toda, J. Usukura, Y. Tano, T. Fujikado, and T. Furukawa. 2008. Pikachurin, a dystroglycan ligand, is essential for photoreceptor ribbon synapse formation. Nat Neurosci. 11:923-31.

Satz, J.S., R. Barresi, M. Durbeej, T. Willer, A. Turner, S.A. Moore, and K.P. Campbell. 2008. Brain and eye malformations resembling Walker-Warburg syndrome are recapitulated in mice by dystroglycan deletion in the epiblast. J Neurosci. 28:10567-75.

Satz, J.S., A.P. Ostendorf, S. Hou, A. Turner, H. Kusano, J.C. Lee, R. Turk, H. Nguyen, S.E. Ross-Barta, S. Westra, T. Hoshi, S.A. Moore, and K.P. Campbell. 2010. Distinct functions of glial and neuronal dystroglycan in the developing and adult mouse brain. J Neurosci. 30:14560-72.

Scherer, S.S., P.E. Braun, J. Grinspan, E. Collarini, D.Y. Wang, and J. Kamholz. 1994. Differential regulation of the 2',3'-cyclic nucleotide 3'-phosphodiesterase gene during oligodendrocyte development. Neuron. 12:1363-75.

Schroder, J.E., M.R. Tegeler, U. Grosshans, E. Porten, M. Blank, J. Lee, C. Esapa, D.J. Blake, and S. Kroger. 2007. Dystroglycan regulates structure, proliferation and differentiation of neuroepithelial cells in the developing vertebrate CNS. Dev Biol. 307:62-78.

Sgambato, A., and A. Brancaccio. 2005. The dystroglycan complex: from biology to cancer. J Cell Physiol. 205:163-9.

Sgambato, A., M.A. Di Salvatore, B. De Paola, A. Rettino, B. Faraglia, A. Boninsegna, C. Graziani, A. Camerini, G. Proietti, and A. Cittadini. 2006. Analysis of dystroglycan regulation and functions in mouse mammary epithelial cells and implications for mammary tumorigenesis. J Cell Physiol. 207:520-9.

Shang, Z.J., M. Ethunandan, D.C. Gorecki, and P.A. Brennan. 2008. Aberrant expression of beta-dystroglycan may be due to processing by matrix metalloproteinases-2 and -9 in oral squamous cell carcinoma. Oral Oncol. 44:1139-46.

Shen, S., J. Li, and P. Casaccia-Bonnefil. 2005. Histone modifications affect timing of oligodendrocyte progenitor differentiation in the developing rat brain. J Cell Biol. 169:577-89.

Sherman, D.L., and P.J. Brophy. 2005. Mechanisms of axon ensheathment and myelin growth. Nat Rev Neurosci. 6:683-90.

Sherman, D.L., C. Fabrizi, C.S. Gillespie, and P.J. Brophy. 2001. Specific disruption of a schwann cell dystrophin-related protein complex in a demyelinating neuropathy. Neuron. 30:677-87.

Shimizu, T., T. Kagawa, T. Wada, Y. Muroyama, S. Takada, and K. Ikenaka. 2005. Wnt signaling controls the timing of oligodendrocyte development in the spinal cord. Dev Biol. 282:397-410.

Shorer, Z., J. Philpot, F. Muntoni, C. Sewry, and V. Dubowitz. 1995. Demyelinating peripheral neuropathy in merosin-deficient congenital muscular dystrophy. J Child Neurol. 10:472-5.

Singh, J., Y. Itahana, S. Knight-Krajewski, M. Kanagawa, K.P. Campbell, M.J. Bissell, and J. Muschler. 2004. Proteolytic enzymes and altered glycosylation modulate dystroglycan function in carcinoma cells. Cancer Res. 64:6152-9.

Smalheiser, N.R., and E. Kim. 1995. Purification of cranin, a laminin binding membrane protein. Identity with dystroglycan and reassessment of its carbohydrate moieties. J Biol Chem. 270:15425-33.

Smalheiser, N.R., and N.B. Schwartz. 1987. Cranin: a laminin-binding protein of cell membranes. Proc Natl Acad Sci U S A. 84:6457-61.

Song, J., B.D. Goetz, P.W. Baas, and I.D. Duncan. 2001. Cytoskeletal reorganization during the formation of oligodendrocyte processes and branches. Mol Cell Neurosci. 17:624-36.

Sotgia, F., G. Bonuccelli, M. Bedford, A. Brancaccio, U. Mayer, M.T. Wilson, R. Campos-Gonzalez, J.W. Brooks, M. Sudol, and M.P. Lisanti. 2003. Localization of phospho-beta-dystroglycan (pY892) to an intracellular vesicular compartment in cultured cells and skeletal muscle fibers in vivo. Biochemistry. 42:7110-23.

Sotgia, F., H. Lee, M.T. Bedford, T. Petrucci, M. Sudol, and M.P. Lisanti. 2001. Tyrosine phosphorylation of beta-dystroglycan at its WW domain binding motif, PPxY, recruits SH2 domain containing proteins. Biochemistry. 40:14585-92.

Spassky, N., F. de Castro, B. Le Bras, K. Heydon, F. Queraud-LeSaux, E. Bloch-Gallego, A. Chedotal, B. Zalc, and J.L. Thomas. 2002. Directional guidance of oligodendroglial migration by class 3 semaphorins and netrin-1. J Neurosci. 22:5992-6004.

Spence, H.J., Y.J. Chen, C.L. Batchelor, J.R. Higginson, H. Suila, O. Carpen, and S.J. Winder. 2004. Ezrin-dependent regulation of the actin cytoskeleton by beta-dystroglycan. Hum Mol Genet. 13:1657-68.

Sperber, B.R., E.A. Boyle-Walsh, M.J. Engleka, P. Gadue, A.C. Peterson, P.L. Stein, S.S. Scherer, and F.A. McMorris. 2001. A unique role for Fyn in CNS myelination. J Neurosci. 21:2039-47.

Sperber, B.R., and F.A. McMorris. 2001. Fyn tyrosine kinase regulates oligodendroglial cell development but is not required for morphological differentiation of oligodendrocytes. J Neurosci Res. 63:303-12.

Stolt, C.C., S. Rehberg, M. Ader, P. Lommes, D. Riethmacher, M. Schachner, U. Bartsch, and M. Wegner. 2002. Terminal differentiation of myelin-forming oligodendrocytes depends on the transcription factor Sox10. Genes Dev. 16:165-70.

Sugita, S., F. Saito, J. Tang, J. Satz, K. Campbell, and T.C. Sudhof. 2001. A stoichiometric complex of neurexins and dystroglycan in brain. J Cell Biol. 154:435-45.

Sun, T., N.P. Pringle, A.P. Hardy, W.D. Richardson, and H.K. Smith. 1998. Pax6 influences the time and site of origin of glial precursors in the ventral neural tube. Mol Cell Neurosci. 12:228-39.

Talts, J.F., Z. Andac, W. Gohring, A. Brancaccio, and R. Timpl. 1999. Binding of the G domains of laminin alpha1 and alpha2 chains and perlecan to heparin, sulfatides, alpha-dystroglycan and several extracellular matrix proteins. Embo J. 18:863-70.

Taveggia, C., M.L. Feltri, and L. Wrabetz. 2010. Signals to promote myelin formation and repair. Nat Rev Neurol. 6:276-87.

Temple, S., and M.C. Raff. 1986. Clonal analysis of oligodendrocyte development in culture: evidence for a developmental clock that counts cell divisions. Cell. 44:773-9.

Thompson, O., I. Kleino, L. Crimaldi, M. Gimona, K. Saksela, and S.J. Winder. 2008. Dystroglycan, Tks5 and Src mediated assembly of podosomes in myoblasts. PLoS One. 3:e3638.

Thompson, O., C.J. Moore, S.A. Hussain, I. Kleino, M. Peckham, E. Hohenester, K.R. Ayscough, K. Saksela, and S.J. Winder. 2009. Modulation of cell spreading and cell-substrate adhesion dynamics by dystroglycan. J Cell Sci. 123:118-27.

Thompson, O., C.J. Moore, S.A. Hussain, I. Kleino, M. Peckham, E. Hohenester, K.R. Ayscough, K. Saksela, and S.J. Winder. 2010. Modulation of cell spreading and cell-substrate adhesion dynamics by dystroglycan. J Cell Sci. 123:118-27.

Tsai, H.H., E. Frost, V. To, S. Robinson, C. Ffrench-Constant, R. Geertman, R.M. Ransohoff, and R.H. Miller. 2002. The chemokine receptor CXCR2 controls positioning of oligodendrocyte precursors in developing spinal cord by arresting their migration. Cell. 110:373-83.

Vartanian, T., G. Fischbach, and R. Miller. 1999. Failure of spinal cord oligodendrocyte development in mice lacking neuregulin. Proc Natl Acad Sci U S A. 96:731-5.

Villarreal-Silva, M., F. Centeno-Cruz, R. Suarez-Sanchez, E. Garrido, and B. Cisneros. 2011. Knockdown of dystrophin Dp71 impairs PC12 cells cycle: localization in the spindle and cytokinesis structures implies a role for Dp71 in cell division. PLoS One. 6:e23504.

Villarreal-Silva, M., R. Suarez-Sanchez, R. Rodriguez-Munoz, D. Mornet, and B. Cisneros. 2010. Dystrophin Dp71 is critical for stability of the DAPs in the nucleus of PC12 cells. Neurochem Res. 35:366-73.

Volpe, J.J., H.C. Kinney, F.E. Jensen, and P.A. Rosenberg. 2011. Reprint of "The developing oligodendrocyte: key cellular target in brain injury in the premature infant". Int J Dev Neurosci. 29:565-82.

Waite, A., C.L. Tinsley, M. Locke, and D.J. Blake. 2009. The neurobiology of the dystrophin-associated glycoprotein complex. Ann Med. 41:344-59.

Wang, C., G. Rougon, and J.Z. Kiss. 1994. Requirement of polysialic acid for the migration of the O-2A glial progenitor cell from neurohypophyseal explants. J Neurosci. 14:4446-57.

Wang, S., A.D. Sdrulla, G. diSibio, G. Bush, D. Nofziger, C. Hicks, G. Weinmaster, and B.A. Barres. 1998. Notch receptor activation inhibits oligodendrocyte differentiation. Neuron. 21:63-75.

Warrington, A.E., and S.E. Pfeiffer. 1992. Proliferation and differentiation of O4+ oligodendrocytes in postnatal rat cerebellum: analysis in unfixed tissue slices using anti-glycolipid antibodies. J Neurosci Res. 33:338-53.

Welker, K.M., and A. Patton. 2012. Assessment of normal myelination with magnetic resonance imaging. Semin Neurol. 32:15-28.

Williamson, R.A., M.D. Henry, K.J. Daniels, R.F. Hrstka, J.C. Lee, Y. Sunada, O. Ibraghimov-Beskrovnaya, and K.P. Campbell. 1997. Dystroglycan is essential for early embryonic development: disruption of Reichert's membrane in Dag1-null mice. Hum Mol Genet. 6:831-41.

Yamada, H., A.J. Denzer, H. Hori, T. Tanaka, L.V. Anderson, S. Fujita, H. Fukuta-Ohi, T. Shimizu, M.A. Ruegg, and K. Matsumura. 1996. Dystroglycan is a dual receptor for agrin and laminin-2 in Schwann cell membrane. J Biol Chem. 271:23418-23.

Yamada, H., F. Saito, H. Fukuta-Ohi, D. Zhong, A. Hase, K. Arai, A. Okuyama, R. Maekawa, T. Shimizu, and K. Matsumura. 2001. Processing of beta-dystroglycan by matrix metalloproteinase disrupts the link between the extracellular matrix and cell membrane via the dystroglycan complex. Hum Mol Genet. 10:1563-9.

Yamada, H., T. Shimizu, T. Tanaka, K.P. Campbell, and K. Matsumura. 1994. Dystroglycan is a binding protein of laminin and merosin in peripheral nerve. FEBS Lett. 352:49-53.

Yang, B., D. Jung, D. Motto, J. Meyer, G. Koretzky, and K.P. Campbell. 1995. SH3 domain-mediated interaction of dystroglycan and Grb2. J Biol Chem. 270:11711-4.

Ye, P., J. Carson, and A.J. D'Ercole. 1995a. In vivo actions of insulin-like growth factor-I (IGF-I) on brain myelination: studies of IGF-I and IGF binding protein-1 (IGFBP-1) transgenic mice. J Neurosci. 15:7344-56.

Ye, P., J. Carson, and A.J. D'Ercole. 1995b. Insulin-like growth factor-I influences the initiation of myelination: studies of the anterior commissure of transgenic mice. Neurosci Lett. 201:235-8.

Yeh, H.J., K.G. Ruit, Y.X. Wang, W.C. Parks, W.D. Snider, and T.F. Deuel. 1991. PDGF A-chain gene is expressed by mammalian neurons during development and in maturity. Cell. 64:209-16.

Zeller, N.K., M.J. Hunkeler, A.T. Campagnoni, J. Sprague, and R.A. Lazzarini. 1984. Characterization of mouse myelin basic protein messenger RNAs with a myelin basic protein cDNA clone. Proc Natl Acad Sci U S A. 81:18-22.

Zezula, J., P. Casaccia-Bonnefil, S.A. Ezhevsky, D.J. Osterhout, J.M. Levine, S.F. Dowdy, M.V. Chao, and A. Koff. 2001. p21cip1 is required for the differentiation of oligodendrocytes independently of cell cycle withdrawal. EMBO Rep. 2:27-34.

Zhong, D., F. Saito, Y. Saito, A. Nakamura, T. Shimizu, and K. Matsumura. 2006. Characterization of the protease activity that cleaves the extracellular domain of beta-dystroglycan. Biochem Biophys Res Commun. 345:867-71.

Zhou, Q., and D.J. Anderson. 2002. The bHLH transcription factors OLIG2 and OLIG1 couple neuronal and glial subtype specification. Cell. 109:61-73.

Zhu, X., D.E. Bergles, and A. Nishiyama. 2008. NG2 cells generate both oligodendrocytes and gray matter astrocytes. Development. 135:145-57.